

**Temporal Changes in the Microbial Nitrogen Cycling Communities in Intertidal
Estuarine Seagrass Ecosystems**

J. J. Hardy

A thesis submitted for the degree of Master's by Dissertation (MSD) in
Environmental Biology

School of Life Sciences

University of Essex

30.09.2024

Temporal Changes in the Microbial Nitrogen Cycling Communities in Intertidal Estuarine Seagrass Ecosystems

Research Statement

All fieldwork sampling was performed in conjunction with a PhD student (Alice Malcolm-McKay). All sediment, leaf and root biomass, and DNA extraction samples were performed together and the corresponding raw data on sediment dry weights, nutrients, and qPCR data for the taxonomic genes (i.e. Bacterial and Archaeal 16S rRNA genes). Anion/cation processing of extracted nutrients was conducted by John Green. All other functional gene analysis (e.g. N-cycle genes), N₂O measurements and subsequent data analysis including statistical analysis was conducted independently.

List of Abbreviations

AMO: Ammonia monooxygenase

Anammox: Anaerobic ammonia oxidation

AOA: Ammonia-oxidising archaea

AOB: Ammonia-oxidising bacteria

C: Carbon

CC: Climate change

CLT: Central limit theorem

Comammox: Complete ammonia oxidation

DIN: Dissolved inorganic nitrogen

DIRAMMOX- Dissimilatory reduction of ammonium

DON: Dissolved organic nitrogen

DNRA: Dissimilatory nitrate reduction to ammonium

GHG: Greenhouse gas

GLM: Generalised linear model

HZO: Hydrazine oxidoreductase

HZS: Hydrazine synthase

IN: Inorganic nitrogen

LM: Linear model

LME: Linear mixed effect

N: Nitrogen

NOB: Nitrite-oxidizing bacteria

NOR: Nitric oxide reductase

NXR: Nitrite oxidoreductase

OC: Organic carbon

ODZ: Oxygen depleted zones

OMZs: Oxygen minimum zones

ON: Organic nitrogen

RT: Retention time

UK: United Kingdom

CONTENTS

Abstract

1.0. Introduction

- 1.1. The Importance of the Nitrogen Cycle
- 1.2. Nitrogen Fixation
- 1.3. Nitrification
- 1.4. COMMAMOX
- 1.5. ANAMMOX
- 1.6. DNRA
- 1.7. Dirammox
- 1.8. Denitrification
- 1.9. Seagrass and the nitrogen cycle
- 1.10. Rationale

1.11. Aims, Objectives and Hypotheses

2.0. Methods

- 2.1. Sample Sites and Sampling
- 2.2. N₂O Gas Flux Sampling
- 2.3. Bulk Sediment and Rhizosphere Sampling
- 2.4. Leaf and Root Biomass
- 2.5. Nutrient Analysis
- 2.6. DNA Extraction and qPCR Analysis of Taxonomic and Functional Genes
- 2.7. Statistical Analysis

3.0. Results

- 3.1. Analysis of Leaf and Root Biomass

- 3.2. Sediment Nutrient Analysis
- 3.3. N₂O Production
- 3.4. qPCR Analysis of Bacterial and Archaeal 16S rRNA Gene Abundance
- 3.5. qPCR Analysis of Ammonia-Oxidising Bacteria (AOB) and Archaea (AOA) *amoA* Gene Abundance
- 3.6. qPCR Analysis of Denitrifier Gene Abundance
- 3.7. Relationships between N₂O Production, Leaf and Root Biomass, Nutrient Availability, and Microbial Abundance

4.0. Discussion

5.0. Future work

6.0. References

7.0. Appendix

Abstract

Coastal vegetated habitats have recently begun to gain attention for their potential to act as greenhouse gas sinks. However, so far, this research has largely focused on the microbial driven carbon dioxide (CO₂) flux in saltmarshes, whilst the more potent greenhouse gas (GHG) nitrous oxide (N₂O) has often been overlooked. The overarching aim of this study was to measure the temporal changes in the microbial communities driving the cycling of nitrogen (N) in estuarine seagrass (*Zostera nolte*) meadows on the coast of East Anglia, United Kingdom, and relate to sediment nutrient concentrations and N₂O flux. This study found that seagrass meadows harboured higher abundances of archaeal and bacterial 16S rRNA genes compared to non-vegetated sediments. Ammonia-oxidation was largely dominated by ammonia-oxidising bacteria (AOB) rather than archaea (AOA) throughout the year. Specifically, greater AOA abundance was found in the rhizosphere in spring, whereas greater AOB abundance occurred in non-vegetated anoxic sediments in winter. Nitrite (NO₂⁻) reduction was potentially being driven by *nirS* rather than *nirK* gene associated communities. Additionally, the *nosZ* gene was significantly higher than either *nirS* or *nirK* regardless of seagrass presence, but significantly lower than the two genes combined. N₂O concentration was negligible in winter, but drastically increased in the spring. Furthermore, non-vegetated habitats sunk N₂O at a higher rate than seagrass habitats. However, more importantly, there was a decrease in N₂O in both habitats over time. Eutrophication nutrients (e.g. nitrates, ammonium) were also found at higher concentrations in the seagrass sediments. These findings suggest that *Zostera nolte* seagrass meadows can act as a sink for N₂O due to the overall reduction in N₂O emissions and may work as a nature-based solution to reduce GHG emissions and estuarine eutrophication as part of the wider estuarine ecosystem function.

Chapter 1.0: Introduction

Coastal ecosystems are changing rapidly, enhanced by climate change, and as a result there has been increased interest in coastal vegetated habitats and their ability to mitigate climate change, either by reducing erosion or sequestering greenhouse gases (GHGs) (Burden *et al.* 2020). Seagrasses and saltmarshes are two key habitats that have been the focus of many recent studies regarding their restoration and their uses as nature-based solutions to mitigate the impacts of climate change (Ramesh *et al.* 2019; Duarte *et al.* 2013; Shafiqul Islam *et al.* 2021). There has been some attention on saltmarshes and their role in GHG flux, but less so for temperate seagrasses, with very few studies on intertidal seagrasses and next to none focussed on the United Kingdom (UK).

Seagrass habitats have a number of very important roles within the larger seascape. They act as nursery grounds for many species of fish, thus supporting mature fisheries, provide hunting grounds for protected coastal birds at low tide, act as a storm barrier to reduce erosion, and improve water quality of the surrounding area (Unsworth *et al.* 2018; Unsworth and Butterworth, 2021; Valdez *et al.* 2020).

Seagrass habitats are distributed globally (**Fig. 1.1**) with the largest meadows found in Australia (~40,000km²) and the Bahamas (up to ~92,500km²) (Gallagher *et al.* 2022). However, due to a lack of spatial assessments, there may be far more extensive meadows that have not yet been detected; there is no globally complete database (Unsworth *et al.* 2019). In the UK, for example, the literature is especially incomplete, preventing any accurate assessments as to where seagrasses are thriving or, alternatively, in particularly poor condition. (Green *et al.* 2021). There are two species of seagrass in the UK: *Zostera marina*, which is largely found in sheltered subtidal areas though can extend to the low intertidal zone, and *Zostera noltei*, which

is commonly located in the mid-upper intertidal zone in low energy bays and estuaries (Tubbs and Tubbs, 1983; d'Avack *et al.* 2024).

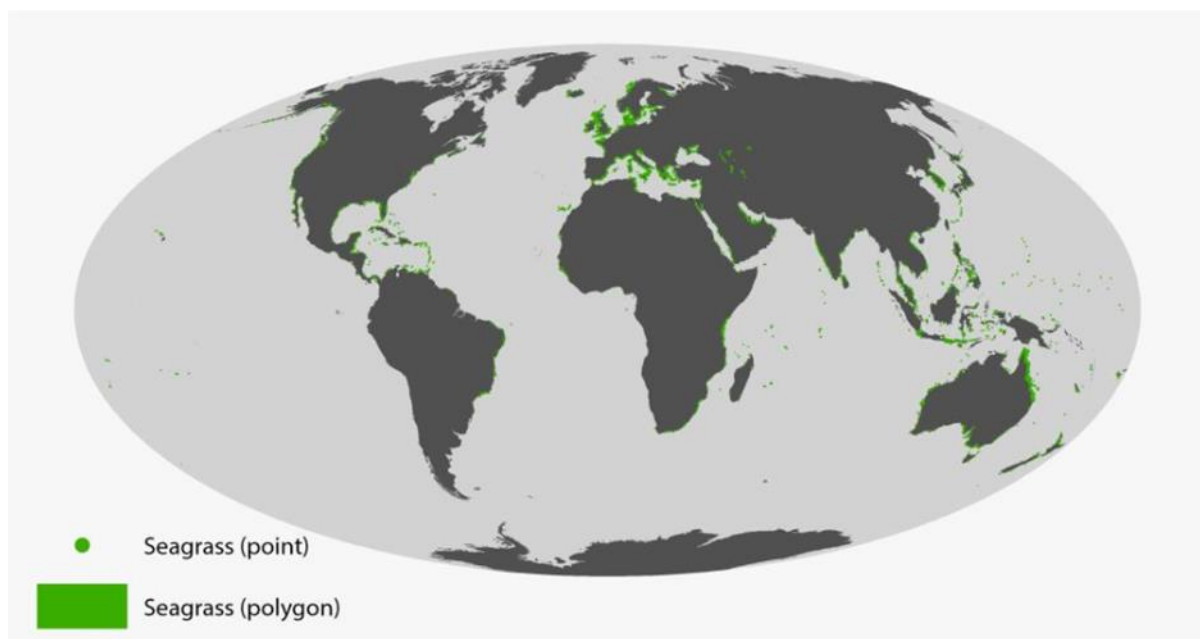


Fig 1.1. Global distribution of seagrasses (compiled by UNEP World Conservation Monitoring Centre) (UN Environment Programme, 2020).

In the UK, seagrass ecosystems have declined; with losses of ~84% reported since the 1980s (Green *et al.* 2021). Most research conducted on global GHG sequestration by seagrass meadows focussed primarily on carbon dioxide (CO₂) (Serrano *et al.* 2021; Miyajima & Hamaguchi, 2018; Duarte, Sintes, & Marba, 2013); and to a lesser extent, methane (CH₄) (Ollivier *et al.* 2022; Al-Haj *et al.*, 2022). There is currently a large knowledge gap on the effect of seagrasses on nitrous oxide (N₂O) flux, a GHG with 298 times more global warming potential than CO₂, though there are existing theories that seagrass meadows could be N₂O sinks (1000; He *et al.* 2024). There is also very little known about N-cycling and N-cycling communities within seagrass meadows, especially regarding species such as *Zostera noltei*, which are under-studied in comparison to the more commonly researched *Posidonia spp.* or

Thalassima spp. Furthermore, coastal ecosystems are also subjected to large anthropogenic inputs of both ammonia and nitrates in coastal waters from wastewater and agricultural run-off (Withers *et al.* 2014). It is known that seagrasses in the UK are highly stressed, with N levels up to 75% higher than the global average; little is known, however, about the effect of N pollution on these meadows (Jones and Unsworth, 2016). The question that is now being asked is whether seagrasses, such as *Zostera noltei*, can turnover N and potentially reduce N levels in these coastal ecosystems; it is not yet known whether *Zostera noltei* is associated with a net loss or a net gain in N.

Seagrasses can influence the microbial diversity within coastal sediments, fostering a more complex and diverse microbial community compared to non-vegetated sediments or open ocean environments (Detcharon *et al.*, 2024). The rhizosphere of seagrasses (i.e. the soil adhering to the roots) provides a nutrient-rich environment for microbial colonisation, supporting a diverse array of bacteria, archaea, and fungi with specialised metabolic capacities (Cúcio *et al.* 2020). In addition to physical changes to coastal sediments, it is the hosting of these different microbial communities that could alter the role of vegetated habitats in recycling N compared to bare sediments (Garcias-Bonet *et al.* 2020).

For example, the presence of seagrasses promote symbiotic relationships between plants and dinitrogen (N₂)-fixing microbes, further enriching microbial diversity and metabolic activity within coastal sediments (Cúcio *et al.* 2020). Seagrasses are therefore key foundation species in coastal environments, providing habitat, oxygenation, and stabilising sediment; they often inhabit nutrient-poor waters, relying on efficient nutrient cycling mechanisms for growth and survival (Duffy, 2006). Symbiotic relationships between seagrasses and N₂-fixing microorganisms, such as

diazotrophic bacteria, are pivotal in this regard. Diazotrophs, including genera like *Azospirillum*, *Azobacter*, and *Rhizobium*, colonise seagrass roots and establish nodules where they convert atmospheric N₂ into biologically available forms like ammonia, enhancing N availability for seagrass uptake (Welsh, 2000). In return, seagrasses provide organic carbon (OC) within their root systems, creating a conducive microenvironment for microbial colonisation and growth. This symbiotic association not only aids seagrass productivity but also contributes significantly to N-cycling within the ecosystem. Understanding the intricacies of these symbiotic relationships is vital for effective conservation and management strategies aimed at preserving seagrass ecosystems in the face of environmental stressors. Studies by Cúcio *et al.* (2020) shed light on the diversity and distribution of N₂-fixing bacteria associated with seagrasses, providing valuable insights into the interactions sustaining these critical coastal habitats.

However, climate change poses significant challenges to seagrass ecosystems and their role in the N-cycle. Rising sea temperatures, ocean acidification, and changes in precipitation patterns can impact seagrass growth and productivity, altering N inputs and outputs within these habitats (Short & Wylie-Echeverria, 1996). Climate-induced disturbances such as extreme weather events and coastal erosion can disrupt seagrass beds, leading to changes in sediment biogeochemistry and microbial community composition. Additionally, climate change-related stressors may affect the symbiotic relationships between seagrasses and N₂-fixing microbes, potentially influencing nitrogen cycling dynamics within coastal ecosystems. Although, seagrasses have the potential to enhance N removal, there is currently a paucity of information on the role of seagrass and the microbial communities associated with them in the cycling of N.

1.1. The Importance of the Nitrogen Cycle

N is one of the most essential elements on the planet; it is a key component of nucleic acid and tissue protein synthesis for growth, repair, and reproduction; thus, the cycling of N is essential to all life on Earth (Cécile and Daniel, 2000). The N- and Carbon (C)- cycle are tightly coupled; the fine balance between them is incredibly important for all life as we know it (Shibata *et al.* 2015). For example, photosynthetic autotrophs need N for photosynthetic pigments such as chlorophyll and the proteins involved in the Calvin cycle (Evans, 1989). As a result, many plants have evolved to have a symbiotic relationship with N₂-fixing microorganisms, either growing within the root tissue as legumes, or colonising the rhizosphere (Mus *et al.* 2016). A shift in this C/N balance could result in reduced crop yields, increased eutrophication of rivers, estuaries, and oceans, and increased climate change (Zaehle and Dalmonech, 2011). However, anthropogenic impacts such as some agricultural practices, are disrupting the N-/C-cycle balance. For example, N-based fertilisers (usually in the form of nitrate (NO₃⁻) which is accessible to plants) may result in an influx of N into the environment, which may enter aquatic ecosystems, and in extreme cases, can lead to hypoxic dead zones (Stein and Klotz, 2016).

The N-cycle and the N transformation processes that occur therein are carried out exclusively by microorganisms. The N-cycle consists of both oxic (e.g. aerobic oxidation of ammonium) and anoxic processes (e.g. denitrification, anaerobic ammonium oxidation, anammox, dissimilatory nitrate reduction to ammonium (DNRA)) (**Fig. 1.2**). The biological processes that contribute to the production of N₂O are denitrification, nitrification, and DNRA (**Fig. 1.2**), though there are also some abiotic processes that produce trace amounts of N₂O (Coyne *et al.* 2024)

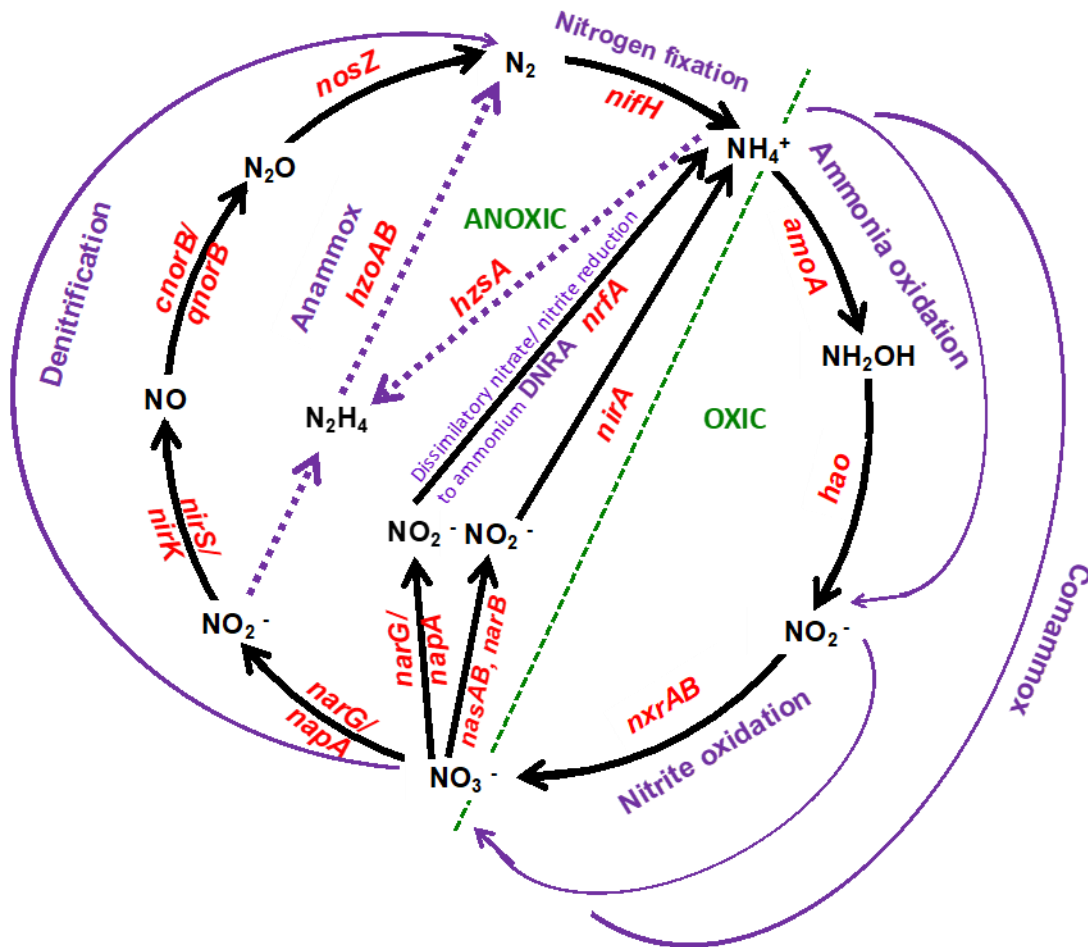


Fig 1.2. The nitrogen cycle associated genes (Underwood *et al.* 2022)

1.2. Nitrogen Fixation

Dinitrogen (N_2) gas is abundant within our atmosphere, contributing to about 78% of the total composition (Fields, 2004). However, N_2 is inaccessible to all eukaryotes and most prokaryotes and archaea; only N_2 -fixing microorganisms can fix inorganic nitrogen (IN) into organic nitrogen (ON) (Kneip *et al.* 2007). N_2 fixation converts inorganic atmospheric N_2 into ammonium (NH_4^+) (Fig. 1.2), which can then be assimilated into biomass by a diverse range of microorganisms known as diazotrophs, as well as into plant biomass (Stein and Klotz, 2016; Zehr and Capone, 2020; von Wirén *et al.* 2001).

Traditionally, diazotrophs included cyanobacteria such as *Trichodesmium* and *Cyanothece* and archaea, though more recently there have been other groups discovered, such as alga symbiotic cyanobacteria and diatom symbiotic cyanobacteria, as well as heterotrophic and photoheterotrophic bacteria (Pajares and Ramos, 2019; Zehr and Capone, 2020). Diazotrophs possess the enzyme nitrogenase (encoded by the *nif* genes), which is the only enzyme known to catalyse the conversion of N₂ to ammonia and is inhibited by oxygen (Threatt and Rees, 2022). The *nifH* gene encodes for two identical subunits of the iron (Fe) protein of the nitrogenase complex; though *nifD* and *nifK* (which are structural genes for the α subunit of dinitrogenase) (Gaby *et al.* 2018; Lammers and Haselkorn, 1983; Turk-Kubo *et al.* 2022). Different groups of diazotrophs have alternative mechanisms to prevent O₂ inhibition; for example, cyanobacteria use either temporal separation or spatial separation such as specialised cells (heterocysts) that create their own anoxic environment (Fay, 1992).

In marine ecosystems, the ecology, diversity, and distribution of diazotrophs varies greatly depending on a range of environmental factors, including O₂, light, inorganic N, phosphorus, Iron, organic matter and DIN (Fay, 1992; Pajares and Ramos, 2019). The vast majority of studies focus on the non-heterocystous cyanobacteria, *Trichodesmium*, which is a large, filamentous species often associated with colonies forming on the open ocean surface in the tropics (Monteiro, Follows, and Dutkiewicz, 2010). In tropical and subtropical regions N₂-fixation rates tend to be higher due to higher temperatures and increased light availability (Monteiro, Follows, and Dutkiewicz, 2010). In these regions, diazotroph diversity is often dominated by cyanobacteria, which thrive in warm, oligotrophic waters, where nitrogen fixation may be more constant throughout the year but can still exhibit fluctuations linked to seasonal changes in nutrient inputs and oceanographic processes (Monteiro, Follows,

and Dutkiewicz, 2010). Conversely, in colder regions, N₂-fixation rates are generally lower, with diazotroph communities comprising of heterotrophic bacteria and archaea, though N₂-fixation rates fluctuate seasonally in response to changes in temperature, light, nutrient availability, and biological factors such as phytoplankton blooms (Pajares and Ramos, 2019). In the UK specifically, nitrogen fixation rates fall at about 0.35mmol N m⁻² d⁻¹ (Rees, Gilbert & Kelly-Gerreyn, 2009).

In environments where light is not limiting, such as unvegetated shallow water and intertidal sediments, photoautotrophic cyanobacteria thrive when compared with other types of diazotrophs which may be limited by C availability (Herbert, 1999). Regardless of this, the highest rates of N₂-fixation are still observed where there are high levels of organic carbon availability; this is likely due to a lack of suitable carbon compounds available for C-fixation in unvegetated coastal habitats in comparison to vegetated sediments (Herbert, 1999).

1.3. Nitrification

Nitrification is crucial in global nitrogen cycling and involves the oxidation of ammonium (NH₄⁺) to nitrite (NO₂⁻) which is further oxidised to nitrate (NO₃⁻) (**Fig. 1.2**) (Pajares and Ramos, 2019). The first stage of nitrification is the oxidation of ammonia to nitrite *via* hydroxylamine and is mediated by ammonia-oxidising bacteria (AOB) and archaea (AOA), which possess the enzyme ammonia monooxygenase (encoded by the *amoA* gene) (Ward, 2011). The second stage is the oxidation nitrite to nitrate and is carried out by nitrite-oxidizing bacteria (NOB), primarily belonging to the genus *Nitrosospira*, which utilise nitrite oxidoreductase (NXR) (Ward, 2011).

The AOB include the taxa *Betaproteobacteria* and *Gammaproteobacteria*, which include members of the genera *Nitrosomonas* and *Nitrosospira* (Taylor and

Kurtz, 2020). The AOA, however, are grouped into five main clusters (*Nitrososphaera*, *Nitrosocosmicus*, *Nitrosotalea* and *Nitrosopumilus*), with *Nitrosopumilus* spp. commonly found among the AOA (Beman & Francis, 2006; Lehtovirta-Morley, 2018). Marine environments typically have lower ammonia concentrations, but higher oxygen levels compared to terrestrial and freshwater systems. This influences the distribution and activity of nitrifiers, with marine nitrification often occurring at lower rates but over larger spatial scales (Ward, 2011). Additionally, marine nitrifiers may exhibit unique adaptations to saline conditions, including halotolerance and osmoregulation mechanisms (Ward, 2011). In marine environments, AOA often outnumber AOB and may dominate ammonia oxidation, especially in oligotrophic regions (Beman & Francis, 2006). Similarly, various NOB, such as *Nitrosospira* spp., contribute to nitrite oxidation, exhibiting niche specialisation to different environmental conditions (Daims *et al.* 2015; Wuchter *et al.* 2006). Both the AOA and the AOB appear to produce N₂O differently, with the yield of N₂O produced by the AOA being lower than that produced by the AOB; this suggests that if the relative abundance of AOB is higher than the AOA, N₂O emissions may increase (Hink *et al.* 2018). Seasonal and geographical variations in microbial communities associated with nitrification are influenced by factors such as temperature, salinity, nutrient availability, and organic matter inputs. For instance, coastal upwelling regions may harbour distinct nitrifying communities compared to nutrient-rich estuaries or open ocean environments (Pajares and Ramos, 2019).

Microbial nitrification plays a pivotal role in supporting the growth and productivity of marine plants. Specifically, in vegetated coastal areas, such as seagrass meadows, nitrification contributes to nitrate availability (5.99 g N m⁻² year⁻¹ in vegetated habitats in England as opposed to 0.14 g N m⁻² year⁻¹ in uncolonized

sediment) is critical for primary producers (Herbert, 1999; Zakem *et al.* 2018). Furthermore, nitrification may indirectly benefit seagrasses by reducing ammonia toxicity in sediments, which in turn could inhibit their growth and reproduction (di Biase *et al.* 2022; Li *et al.* 2019). In contrast, non-vegetated coastal ecosystems may have lower nitrification rates due to reduced organic matter inputs and microbial activity in the absence of plant-symbiotic nitrifiers (Welsh, 2000). However, nutrient dynamics in these environments can still influence primary productivity and ecosystem functioning (Caffrey & Kemp, 1990). Understanding the differences in nitrification between vegetated and non-vegetated coastal ecosystems, particularly in the context of seagrass habitats, is crucial for effective coastal management and conservation efforts for the rapidly declining habitat (Jones and Unsworth, 2016).

1.4. COMMAMOX

Complete ammonia oxidation (comammox) stands as a groundbreaking discovery in microbial N-cycling, challenging well-established beliefs of ammonia oxidation (van Kessel *et al.* 2017). Discovered in 2015 by van Kessel *et al.*, comammox revolutionised our understanding by revealing that a single microorganism can catalyse the entire conversion of ammonia (NH_3) to nitrate (NO_3^-), in one enzymatic step (**Fig. 1.2**). This process contradicts the conventional idea that ammonia oxidation requires the cooperation of two distinct groups of microorganisms, namely the ammonia oxidisers and nitrite oxidisers. Specifically, comammox relies on the presence of both ammonia monooxygenase (AMO) and nitrite oxidoreductase (NXR) enzymes within the same organism, facilitating the complete oxidation of ammonia to nitrate. The pivotal genes associated with comammox include *amoA*, encoding the subunit of ammonia monooxygenase responsible for ammonia oxidation, and *nxrAB*,

responsible for nitrite oxidation (van Kessel *et al.* 2017). Understanding comammox has expanded our knowledge of microbial N metabolism and its implications for ecosystem functioning and biogeochemical cycles.

The organisms involved in comammox primarily belong to the *Nitrosospira* genus, particularly the *Nitrosospira inopinata* clade, although other lineages within *Nitrosospira* may also exhibit comammox capabilities (Pjevac *et al.* 2017). They are often found co-existing in the same sediment with AOB or AOA, possibly occupying different niches due to the low levels of competition they appear to exhibit (Tianlin *et al.* 2019). Comammox bacteria have been found across diverse habitats, including freshwater, marine, and soil ecosystems (Bartelme, McLellan & Newton, 2017). However, their abundance and diversity can vary significantly depending on habitat and seasonal factors. For instance, in aquatic environments, comammox bacteria have been detected in both surface waters and deep-sea sediments, with studies suggesting that their distribution may be influenced by environmental factors such as nutrient availability, temperature, and oxygen levels (Liu *et al.* 2020). In soil ecosystems, comammox bacteria have been found in various terrestrial environments, including agricultural soils and forest soils, where their abundance may fluctuate in response to factors such as soil pH, moisture content, and organic matter inputs (Pjevac *et al.* 2017). Furthermore, comammox bacteria have been observed in engineered systems, including wastewater treatment plants and drinking water distribution systems, where they play a role in nitrogen removal processes (Pinto *et al.* 2016). Additionally, seasonal variations in comammox bacterial populations have been observed, with studies indicating changes in their relative abundance and activity levels in different seasons, possibly driven by shifts in environmental conditions and microbial community dynamics (Liu *et al.* 2020).

In coastal environments such as seagrass meadows, where macrophytes provide habitat complexity and organic matter inputs, higher rates of comammox gene abundance and microbial diversity have been documented compared to the open ocean (Underwood *et al.* 2022). The presence of seagrasses greatly alters nutrient cycling processes across the entire colonised sediment, as opposed to bare mud (Seymour *et al.* 2018). Additionally, the rhizosphere of seagrasses harbours a diverse microbial community, including comammox bacteria (Ling *et al.* 2021). Conversely, in non-vegetated coastal ecosystems such as sandy beaches or rocky shores, lower rates of comammox and altered microbial diversity may be observed due to reduced organic matter inputs and microbial habitat complexity (Underwood *et al.* 2022). Environmental factors such as temperature, salinity, and nutrient availability further modulate the distribution and activity of comammox bacteria in these coastal vegetated and non-vegetated environments (Underwood *et al.* 2022). The discovery of comammox has enhanced our understanding of the ecosystem dynamics driving nitrogen cycling and ecosystem dynamics in these ecologically important habitats.

1.5. ANAMMOX

Anaerobic ammonia oxidation (anammox) is a crucial microbial driven process in the nitrogen cycle, which occurs under anaerobic conditions (**Fig. 1.2**) and involves the oxidation of ammonia (NH_3) to dinitrogen gas (N_2) using nitrite (NO_2^-) as the electron acceptor (Pajares & Ramos, 2019). Discovered in the 1990s, anammox has since been recognized as a key pathway for nitrogen removal in various environments, including marine sediments, wastewater treatment plants, and oxygen-depleted zones in aquatic ecosystems (Pajares & Ramos, 2019). The process is mediated by specialised bacteria belonging to the phylum Planctomycetes, particularly within the

genera *Candidatus Kuenenia*, *Candidatus Scalindua*, and *Candidatus Brocadia* (Kuypers *et al.* 2003). *Candidatus Brocadia* is known to catalyse the reduction of nitrite to nitric oxide (NO), whereas *Candidatus Kuenenia* and *Candidatus Scalindua* are responsible for the conversion of ammonia to hydrazine (N₂H₄) (Kuypers *et al.* 2003). These reactions are facilitated by enzymes such as hydrazine synthase (HZS), hydrazine oxidoreductase (HZO) and nitric oxide reductase (NOR), which are essential for the efficient conversion of ammonia and nitrite to dinitrogen gas (Kuypers *et al.* 2003). These microorganisms possess unique cellular structures, including intracellular compartments known as anammoxosomes, where the anammox reaction takes place (van Niftrik *et al.* 2004). Anammox has garnered significant attention for its ecological significance and potential applications in nitrogen removal technologies.

Anammox bacteria have been found in various geographical regions, including marine, freshwater, and terrestrial environments, where they contribute to N removal. Anammox rates may vary depending on factors such as temperature, nutrient availability, and organic matter inputs; additionally, microbial diversity and anammox rates may vary seasonally, with higher rates observed in warmer months and in regions with higher nutrient inputs (Pajares & Ramos, 2019). In vegetated coastal ecosystems such as seagrass meadows, anammox rates and microbial diversity may change between non-vegetated coastal environments due to differences in organic matter inputs and microbial habitat complexity (Underwood *et al.* 2022). Seagrass meadows provide organic matter and create anaerobic microsites favourable for anammox bacteria, potentially leading to higher rates of nitrogen removal compared to non-vegetated coastal habitats.

1.6. DNRA

Dissimilatory nitrate reduction to ammonium (DNRA) is a key microbial process in coastal ecosystems, influencing nitrogen cycling by retaining bioavailable nitrogen in the system rather than removing it via denitrification (Burgin and Hamilton, 2007). DNRA occurs under anoxic or suboxic conditions where bacteria use NO_3^- or NO_2^- as electron acceptors, reducing them to NH_4^+ instead of N_2 gas (Kraft et al., 2014). This process is particularly significant in organic-rich sediments, where labile C availability and sulphide concentrations favour DNRA over denitrification (Giblin *et al.* 2013). The competition between these pathways determines whether N is recycled within the ecosystem or permanently removed, influencing primary productivity and eutrophication dynamics (Rütting *et al.* 2011).

Coastal environments provide ideal conditions for DNRA due to fluctuating O_2 levels, high organic matter deposition, and variable redox states (Rutting *et al.* 2021). Studies show that DNRA rates increase under sulphate-reducing conditions, where sulphide inhibits denitrification but enhances DNRA by providing electrons for NO_3^- reduction (Tiedje, 1988). Additionally, anthropogenic influences such as nutrient runoff and wastewater discharge elevate N loads, potentially enhancing DNRA activity in estuaries and coastal sediments (An and Gardner, 2002). However, increased DNRA may lead to higher NH_4^+ concentrations, fuelling algal blooms and altering the N balance in these ecosystems (Roberts *et al.* 2014).

Understanding DNRA's role in N retention has important implications for managing coastal eutrophication and ecosystem health. While denitrification is often viewed as the primary N removal pathway, DNRA can dominate under certain environmental conditions, especially in sediments rich in organic C and S (Hardison *et al.* 2015). Management strategies focusing on reducing anthropogenic nitrogen inputs and enhancing conditions favouring denitrification over DNRA could mitigate

excess N retention and its ecological consequences (Burgin and Hamilton, 2007). However, future research is required further explore the environmental controls on DNRA and its interaction with other N transformation processes in dynamic coastal systems, such as within seagrass meadows (Kraft *et al.* 2014).

1.7. DIRAMMOX

Dissimilatory reduction of ammonium coupled to anaerobic oxidation of methane (DIRAMMOX) is an emerging pathway in N-cycling that can influence N dynamics in coastal ecosystems, particularly in seagrass meadows. This process involves the microbial oxidation of methane (CH_4) using NH_4^+ as an electron acceptor, leading to N removal in the form of N_2 gas (Haroon *et al.*, 2013). Seagrass beds create organic-rich sediments that enhance CH_4 production via methanogenesis, providing a potential substrate for DIRAMMOX (Ettwig *et al.* 2016). The presence of sulphate-reducing bacteria and anaerobic methanotrophs in seagrass sediments suggests that DIRAMMOX could act as an alternative N loss pathway alongside denitrification and anammox, particularly in environments with fluctuating O_2 levels and high organic matter input (Asplund *et al.* 2022).

Seagrass meadows play a critical role in modulating sediment biogeochemistry, potentially enhancing DIRAMMOX activity through rhizosphere- O_2 dynamics and organic matter deposition. The O_2 released by seagrass roots creates microaerophilic conditions that can support diverse microbial communities, including those involved in CH_4 oxidation and N transformations (Nielsen *et al.* 2001). Additionally, the decomposition of seagrass litter fuels anaerobic microbial processes, contributing to CH_4 and NH_4^+ availability, which are key substrates for DIRAMMOX (Treusch *et al.* 2005). While the relative importance of DIRAMMOX in seagrass sediments remains

underexplored, its potential to reduce N retention and CH₄ emissions highlights its significance in coastal N budgets and GHG dynamics (Zhao *et al.* 2024).

The role of DIRAMMOX in seagrass ecosystems has important implications for coastal management and conservation; seagrass beds are vital blue carbon sinks, and their ability to influence N- and CH₄-cycling could impact efforts to mitigate eutrophication and GHG emissions (Duarte *et al.* 2010). Further research is needed to quantify DIRAMMOX rates in seagrass sediments and identify the environmental conditions that promote this process over alternative N transformation pathways (Bodelier *et al.* 2014).

1.8. Denitrification

Denitrification involves the stepwise reduction of nitrate, to nitrite, nitric and nitrous oxide and finally to dinitrogen gas, and occurs predominantly in anaerobic environments where oxygen is limited or absent, such as waterlogged soils, wetlands, sediments, and oxygen-depleted zones in aquatic ecosystems (Martinez-Espinosa *et al.* 2021). These environments provide ideal conditions for denitrifying bacteria (Pajares and Ramos, 2019).

Geographically, denitrification rates tend to be highest in regions characterized by high levels of organic matter input, such as agricultural areas with intensive fertilizer use, as well as in coastal zones and estuaries where terrestrial runoff introduces excess nutrients into marine environments (Dong *et al.* 2006; Herbert, 1999). Additionally, tropical and subtropical regions with warm temperatures and high levels of precipitation often exhibit elevated denitrification rates due to enhanced microbial activity and organic matter decomposition. Conversely, denitrification rates may be lower in arid or cold regions with limited organic matter inputs and lower microbial

activity (Pajares and Ramos, 2019). In coastal environments, such as mudflats, seagrass meadows, and saltmarshes, denitrification rates are often elevated due to high inputs of organic matter, nutrients, and reactive nitrogen from terrestrial sources, leading to anaerobic conditions favourable for denitrifying microorganisms (Underwood *et al.* 2022).

In marine ecosystems, denitrification occurs primarily in oxygen-depleted zones such as oxygen minimum zones (OMZs) and sediments, where microbial communities are adapted to low-oxygen conditions (Pajares and Ramos, 2019). Denitrification also occurs in a wide variety of freshwater ecosystems, including rivers, lakes, and wetlands, where anaerobic conditions and nutrient inputs drive denitrification processes (Martinez-Espinosa *et al.* 2021). In terrestrial environments, denitrification rates can vary widely depending on factors such as soil moisture, temperature, and organic matter content, with higher rates typically observed in wetland soils and riparian zones (Wang *et al.* 2009). In vegetated ecosystems such as wetlands and riparian zones, denitrifier communities may be influenced by the presence of plant roots and the associated rhizosphere communities, which provide organic matter inputs and create anaerobic microsites favourable for denitrification (Pajares and Ramos, 2019). Consequently, vegetated ecosystems may harbour a greater diversity of denitrifying microorganisms compared to non-vegetated environments such as sandy beaches or rocky shores, where organic matter input may be limited (Underwood *et al.* 2022). Overall, the spatial and temporal variability of denitrification across different environments is essential for managing N-cycling and its impacts on ecosystem health.

The microbes involved in denitrification are highly diverse and encompass various bacterial and archaeal taxa. Denitrification involves multiple enzymatic stages

mediated by different groups of microorganisms. Firstly, nitrate (NO_3^-) is reduced to nitrite (NO_2^-) by nitrate reductase enzymes, typically encoded by genes such as *narG* or *napA*, which are predominantly found in various bacterial taxa including *Pseudomonas*, *Paracoccus*, and *Bacillus* (Sparacino-Watkins, Stolz & Basu, 2014). Subsequently, nitrite is further reduced to NO by nitrite reductase enzymes, which can be either copper-containing NirK or cytochrome cd1-containing NirS, depending on the organism (Jones *et al.* 2013). These enzymes are typically found in denitrifying bacteria such as *Pseudomonas stutzeri* and *Paracoccus denitrificans* (Jones *et al.* 2013).

Phylogenetic analyses reveal that *nirS* and *nirK* are divided into multiple clades that correspond to different ecological niches and evolutionary trajectories. *nirS* has been shown to have at least three major clades, with variations in substrate affinity and environmental adaptation, particularly in anoxic and suboxic environments such as marine sediments and wastewater treatment plants (Sun and Jiang, 2022). *nirK*, on the other hand, exhibits even greater diversification, with clades adapted to a range of conditions, including terrestrial ecosystems where fluctuating oxygen levels drive microbial community shifts (Heylen *et al.* 2016). These genetic and ecological differences influence the efficiency of NO_2^- reduction and the relative production of NO and N_2O .

Further reduction of NO to N_2O is catalysed by nitric oxide reductase enzymes, encoded by genes such as *norB* and *norZ*, which are present in denitrifiers like *Pseudomonas aeruginosa* and *Paracoccus pantotrophus* (Borreo-de Acuna *et al.* 2016). Finally, nitrous oxide is reduced to nitrogen gas (N_2) by nitrous oxide reductase enzymes, encoded by *nosZ* genes, primarily found in denitrifying bacteria such as *P. denitrificans* and *P. aeruginosa* (Jones *et al.* 2013). The *nosZ* gene exists in two

phylogenetically distinct clades: *nosZ-I*, found in canonical denitrifiers, and *nosZ-II*, present in non-denitrifying microorganisms that lack other denitrification genes but contribute to N₂O reduction (Jones *et al.* 2013). These variations in gene distribution and phylogeny influence denitrification rates and the balance between nitrogen retention and N₂O emissions in different ecosystems (Hallin *et al.* 2018).

Incomplete denitrification occurs when the microbial reduction of NO₃⁻ to N₂ gas halts prematurely, leading to the accumulation and release of N₂O. This process is influenced by factors such as oxygen availability, carbon source, and environmental conditions. For instance, in wastewater-impacted estuaries, incomplete denitrification has been identified as a significant driver of elevated N₂O emissions, with observed rates surpassing those predicted by standard models (Garf *et al.* 2014). Similarly, studies in arid soil crusts have demonstrated that N₂O production predominantly originates from incomplete denitrification within anoxic layers (Abed *et al.* 2013). These findings underscore the role of incomplete denitrification in contributing to atmospheric N₂O and NO levels, thereby exacerbating climate change.

1.9. Seagrass and the Nitrogen Cycle

Seagrass meadows significantly influence the nitrogen cycle in coastal ecosystems through various mechanisms. One primary pathway is the assimilation of DIN, such as NH₄⁺ and NO₃⁻, directly from the water column and sediment porewater (Alexandre *et al.* 2020). This uptake reduces the availability of nitrogen for phytoplankton and algal blooms, thereby maintaining water clarity and supporting overall ecosystem health. Additionally, seagrasses can absorb dissolved inorganic nitrogen (DON), which becomes increasingly important under conditions like ocean warming that elevate nitrogen demand (Alexandre *et al.* 2020).

Beyond direct N uptake, seagrasses facilitate N-fixation by hosting diazotrophic microorganisms in their rhizosphere. These N-fixing bacteria convert atmospheric N₂ into bioavailable forms, supplementing the N pool available to seagrasses and other organisms (Papazachariou *et al.* 2024). For instance, studies have shown that seagrass debris in temperate coastal waters harbours substantial N-fixation activity carried out by cyanobacteria and heterotrophic bacteria (Papazachariou *et al.* 2024).

The release of O₂ from seagrass roots into the rhizosphere profoundly impacts sediment biogeochemistry and N-cycling. This oxygenation creates microenvironments that influence various N transformation processes, such as nitrification and denitrification (Jovanovic *et al.* 2015). By modulating these microbial processes, seagrasses could play a crucial role in regulating N availability and mitigating N-related eutrophication in coastal ecosystems. This study aims to begin to bridge the gap in this understanding.

1.10. Rationale

Seagrass may play a crucial role in the cycling of nitrogen and, more specifically in the mitigation of N₂O produced within coastal ecosystems compared to the open ocean or non-vegetated estuarine sediments, and thereby contribute to the overall functioning of coastal ecosystems. For example, the presence of seagrass may facilitate key processes involved in denitrification within their rhizosphere, where the dense root system of seagrasses creates anaerobic microsites and, therefore, denitrifier microorganisms may thrive, converting nitrate and nitrite into N₂ under oxygen-limited conditions (Chen *et al.* 2020). Such increased microbial activity may in turn contribute to higher N removal rates in seagrass habitats compared to non-vegetated sediments or open ocean environments (Chen *et al.* 2020).

The intricate network of seagrass roots may also trap and retain organic matter and micronutrients, providing additional substrates for microbial processes. Thus, having an increased understanding of the dynamics of N-cycling microorganisms associated with seagrass habitats is pivotal for the preservation and sustainable management of coastal ecosystems worldwide. Moreover, the issue of climate change highlights the importance of conservation and management efforts to preserve and restore these critical coastal ecosystems. The role of temperate seagrasses in N-cycling and could be a valuable justification for investment in seagrass restoration as a nature-based solution under a future changing climate and anthropogenic pollution on coastal ecosystems.

1.11. Aims, Objectives, and Hypotheses

The overarching aim of this thesis is to better understand the sediment microbial communities involved in the N-cycle associated with intertidal seagrass meadows of *Zostera noltei* in three estuarine sites located in Essex and Suffolk: Nacton Shore, Copperas Bay, and Leigh-on-Sea.

Specific Objectives:

1. Characterise changes in the abundance and community structure of microorganisms (with focus on those involved in the N-cycle) in *Zostera noltei* meadows compared to non-vegetated sediments over a seasonal cycle and relate to nutrient concentrations and N₂O production.
2. Evaluate whether *Zostera noltei* presence has an impact on N₂O production compared to non-vegetated sediment and determine whether seagrasses can potentially facilitate the sinking of this potent GHG

It is hypothesised that:

1. Increased seagrass biomass in the spring and summer will lead to an increase in organic matter and NH_4^+ inputs, increasing nitrifier/denitrifier abundances in the rhizosphere compared to the bulk sediment (and non-vegetated sediments) and resulting in reduced N_2O levels in seagrass meadows by favouring complete denitrification over incomplete denitrification.
2. N_2O concentration will increase in the spring in comparison to winter due to warmer temperatures promoting ground thawing and therefore increasing nitrifier/denitrifier abundances and coupled nitrification-denitrification processes, with a higher proportion of incomplete denitrification.

Chapter 2.0: Methods**2.1. Sample Sites and Sampling**

Samples were collected from three sites in Essex and Suffolk: Copperas Bay (Orwell Estuary), Nacton Shore (Stour Estuary), and Leigh-on-Sea (Thames Estuary) (**Fig. 2.1**).

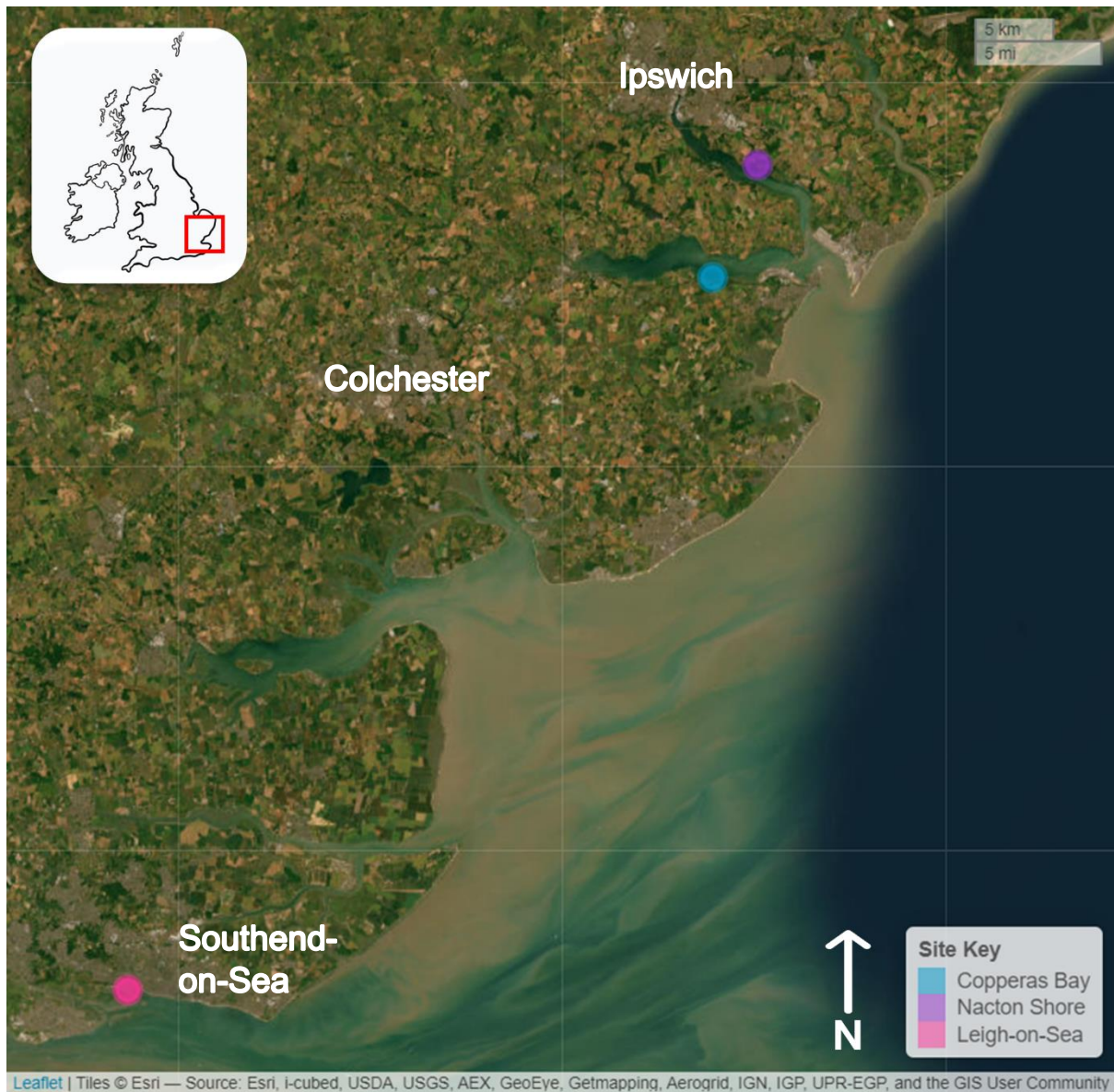


Fig 2.1. Map showing the study sites in the East coast of England.

These sites were selected due to the known presence of seagrass in relatively good health, meaning the beds weren't scarred by trawling or destroyed by other various factors, and weren't decreasing in size. The site in the best condition was Leigh-on-Sea, with incredibly high shoot density and canopy height in comparison to other sites in the UK; it was difficult to find any accessible bare mud flat. Nacton Shore, though still in good condition, was relatively worse than Leigh-on-Sea, likely due to high dog walker presence and minimal distance from the trail. Of the three, Copperas

Bay had the lowest shoot density and canopy height, though it appeared as if the meadow was actively expanding due to rhizome presence in some unvegetated areas. Copperas Bay is a site under the jurisdiction of the RSPB and the public are not permitted to enter. The site is largely shaded by trees, which may be the cause of the perceived lower health due to limited daylight for photosynthesis.

A 'trial' sampling was performed in September 2023, followed by four seasonal sampling periods; Autumn (November 2023 during seagrass dieback), Winter samples (January/ February 2024 when the seagrass was dormant and the detritus leaves had been washed away), Spring (April 2024 when new growth was under way), and Summer (July 2024 during peak biomass). All samples were collected at low tide during daylight hours, on days where there was no more than light precipitation and no ground freezing. Environmental parameters were noted such as cloud cover, water and air temperature, and water pH, and can be found in the appendix (**Table A7**).

2.2. N₂O Gas Flux Sampling

N₂O gas flux measurements were performed using triplicate collars and gas chambers. An example of the apparatus is shown below (**Fig. 2.2**).

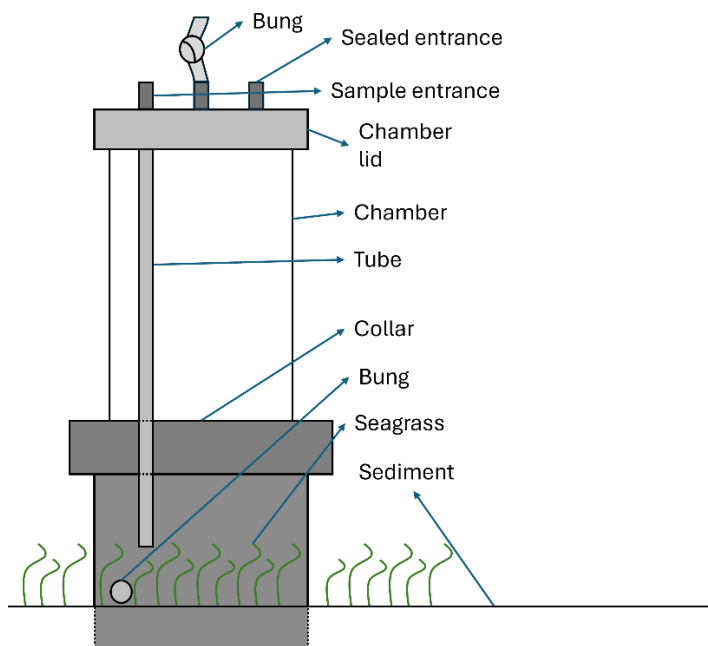


Fig 2.2. Diagram showing the apparatus used to take N_2O gas flux measurements, consisting of three main parts: the collar, the chamber, and the chamber lid. The diagram shows the apparatus as it would be used in the field in a vegetated area at low tide; the only difference in a non-vegetated area would be the absence of seagrass. Seagrass would be laying across the sediment at low tide instead of standing upright.

N_2O measurements were performed in winter, spring, and summer only. At least 24h before sampling, triplicate collars were inserted in the middle of the seagrass meadow (vegetated) and triplicate collars in the mudflat (non-vegetated). Holes were drilled into the collars at sediment level to allow any water brought in by the tide to drain away as it would in a normal tidal cycle; upon arrival to the site, these holes were sealed with bungs immediately to minimise sediment disturbance affecting any results.

To begin sampling, a gas chamber was inserted into the collar and allowed to acclimate for 5 min. The chamber had three sampling ports at the top, two of which were sealed with silica, one of which with a tube positioned ~3cm away from the

sediment surface (**Fig. 2.2**). After acclimation, the open entrance was sealed with a bung and two samples were extracted using a 20mL syringe and needle (flushed three times prior to each sample); the first being inserted into the silica-sealed entrance with the tube attached, and the second taken from outside the chamber for an ambient control. Gas samples (including two ambient gas samples) were injected into 12mL exetainers. Gas samples were collected at five-minute intervals, until 5 samples had been collected from within the chamber. Once the fifth chamber sample was collected, a second ambient sample was collected to account for any environmental changes. This process was repeated for each replicate collar, and all samples stored in a cool, dry, dark box for up to three months.

N₂O gas flux was measured by gas chromatography (GC-2014 gas chromatograph, Shimadzu). Ambient air temperature and pressure on the day of sample processing was noted to account for changes in the compression of the gas sample. A gas-tight needle was flushed three times with synthetic air prior to extracting the sample. A standard of 1000ppm N₂O synthetic air was injected to calculate the retention time (RT) of N₂O. There were two peaks measured: the first being N₂, with a RT of 45sec-1min, and the second being N₂O, with a RT of ~2min. 5 mins were left between each injection. Triplicate samples of the air in the laboratory were also injected. The average peak area was calculated for each sample; any samples without a 2min RT were recorded as having 0ppm N₂O, and below the limits of detection.

2.3. Bulk Sediment and Rhizosphere Sampling

Bulk sediment samples (~10g) and rhizosphere samples (~0.01-0.3g) were taken from within the centre of each collar, paired with the gas flux data. Sterilised 20mL syringes with the ends cut off were used to collect sediment cores. All equipment

was sterilised with 70% (v/v) ethanol. Each sediment core was split into sterile 20mL falcon tubes; one containing ~10g of anoxic sediment (described as incredibly dark and within the bottom 2cm of the core), and another containing ~20g of the oxic sediment (described as light in colour and within the top 2cm of the core). The final falcon tube was filled with 10mL of sterile milli-Q water for the rhizosphere sediments (~2g including rhizome). Sediments were collected from a depth of 0-5cm. Set depths could not be outlined due to extreme variability in oxygen penetration of the sediment in every sample; however, it must be noted that oxygen content was not directly measured, and therefore 'anoxic' and 'oxic' are loosely defined. In the presence of seagrass, there were no rhizosphere samples obtained for summer 2023.

Triplicate rhizosphere samples were collected by pulling the seagrass roots out of the core using tweezers. Excess sediment was removed by tapping the tweezers (while they gripped the root) with a sterile spatula. The entire root with the rhizosphere sediment attached was then placed into a sterile falcon tube containing 10mL of sterile milli-Q water. This process was repeated until as many roots as possible were collected, this varied from ~3-15. Any roots that had no rhizosphere attached (i.e. scraped off the root during extraction) were discarded as the rhizosphere had been disrupted. Anoxic sediment (approximately bottom 2cm of the core, identified by a distinct dark colour) and oxic sediment (approximately the top 1-2cm of the core, identified by its lighter brown colour). Any sediment in the oxic/anoxic interface was discarded. All samples were placed on ice in a cool bag on-site and stored at -20°C.

2.4. Leaf and Root Biomass

Leaf and root biomass samples were collected from inside the collars on vegetated sites. Before collection, the collar height was calculated by placing a ruler

within the collar with the zero being at the sediment surface and repeated three times for an average. Leaf biomass was collected within the collar using sterile scissors to cut the seagrass at the sediment surface. A 20mL syringe with the end cut off was used to extract a sediment core containing the seagrass root biomass and placed in a sterile bag. The leaf and root biomass samples were processed immediately to prevent degradation. For the leaf biomass, each sample was placed into a fine mesh sieve (0.5mm) and any sediment/ non-seagrass biota (such as invertebrates, twigs, and algae) was removed. Seagrass biomass was collected and placed into a 60°C oven overnight or until constant weight. For root biomass, extraction was performed by scraping small amounts of the bulk sediment using a sterile spatula until the roots were exposed. Roots were extracted from the bulk sediment using sterile tweezers, before being washed in a small volume of sterile milli-Q water and incubated in an oven overnight at 60°C until constant weight. The water/sediment mixture was placed into a sterile pre-weighed pot (~5cm deep, ~10cm diameter), left at room temperature overnight to allow for the sediment to settle at the bottom. Excess water was removed, and the remaining sediment dried in a 60°C oven overnight until constant weight.

2.5. Nutrient Analysis

Nutrient (anion/cation) concentrations (e.g. NH_4^+ , NO_3^- , NO_2^-) were measured in bulk sediment (1g wet weight) and rhizosphere (0.01-0.3g) samples using a Dionex ICS-3000 (Thermo Scientific UK) as previously described (Scarlett *et al.* 2021). Dry weights were calculated by drying weighed sediment overnight at room temperature until constant weight.

2.6. DNA Extraction and qPCR Analysis of Taxonomic and Functional Genes

DNA was extracted from 0.25g wet weight sediment using a soil DNeasy PowerMas Soil Kit (Qiagen) following the manufacturers recommendations. Gene abundance was quantified by qPCR with a SensiFAST SYBR No-ROX Kit (Bioline) on a CFX384 Real-Time PCR Detection System (BioRad) using the following primers: Bacterial 16S rRNA (S-D-Bact-0341-b-S-17/S-D-Bact-0785-a-A-21), Archaeal 16S rRNA (344f-16S-Archaea/915r-16S-Archaea), ammonia monooxygenase (*amoA*) genes from archaea (CrenamoA- 23F/CrenamoA-616R), and bacteria (*amoA*-1F/*amoA*-2R), (nitrite reductase) gene *nirS*-Cd3aF/*nirS*-R3cd, *nirK* (nitrite reductase) gene (*nirK*-1F/*nirK*-5R), and *nosZ* (nitrous oxide reductase) gene (*nosZ*2F/*nosZ*2R) (Klindworth *et al.* 2013; Lane *et al.* 1985; Tourna *et al.*, 2008; Rotthauwe, Witzel, & Liesack, 1997; Throbäck *et al.*, 2004; Braker, Fesefeldt, & Witzel, 1998; Henry *et al.*, 2006). Thermocycling involved an initial denaturation at 95°C for 3 mins followed by 30 cycles of 95°C for 5 sec, 60°C for 30 secs, which included a combined annealing and extension time. Product specificity was confirmed by using melting point analysis. R² values for the standards curves were >0.981 with an amplification efficiency of at least 89%. Standards, samples, and non-template controls were run in triplicate.

2.7. Statistical Analysis

Sediment type was included as a factor during every mixed model during analysis, except for N₂O and biomass analysis. This was due to these measurements being a factor of all sediment types simultaneously. All other variables were dependent on sediment type, hence why sediment was not a measured variable itself. When comparing N₂O with variables such as nutrient availability, leaf and root biomass, and microbial community, a mean concentration for each collar was calculated per treatment per season to reduce the complexity of the statistical analysis.

Histograms of the residuals were created for N₂O concentration to determine the distribution to ensure the correct statistical tests were used; this data followed a negative binomial distribution, so the `nbinom2` family was used during analysis via generalised linear mixed effects model (GLMM) with site and collar as random factors. After observing there was a large number of 0-values in winter, the data was tested for zero-inflation in order to ensure the correct analytical approach was used; the `glmmTMB` package was selected for analysis due to its function, `ziformula` (Brooks *et al.* 2017). N₂O concentration was analysed in association with N₂O producing (*nirS*, *nirK*) and N₂O removing (*nosZ*) genes, nutrient concentrations, and leaf and root biomass. For GLMMs and LMEs throughout statistical analysis, autumn was the base season, bare sediment was the base treatment type, and anoxic was the base sediment type.

A histogram of the residuals was created for each nutrient type. Sulphate followed a normal distribution, and a normal LME was used as a result. For nitrite, nitrate, phosphate and ammonia, as with all previous histograms, the data followed a negative binomial distribution, and therefore for each nutrient a generalised linear mixed effects model (GLMM) with a negative binomial distribution (family= `nbinom2`) using the `glmmTMB` (phosphate) or `lme4` (nitrate, nitrite, ammonia) packages in R were selected for analyses of these data (Brooks *et al.* 2017). Zero-inflation was accounted for by using the `glmmTMB` packages feature, `ziformula` (`ziformula = ~1`). To allow for the negative binomial family to be used, nitrate and nitrite had to be multiplied by 100 and rounded to the nearest integer due to low concentrations, while ammonia was solely rounded. The `parameters::p-value` function in the `sjstats` package was used to extract p-values from the LME. Each nutrient was analysed with site as a random factor with sediment type, treatment type, and season. For fully maximised

models, factor * factor was used; for simplified models, factor + factor was utilised instead. The data for every gene conformed to a negative binomial distribution in the histograms, but due to the size of the gene dataset, RStudio could not conduct the analysis while accounting for the distribution with the glmmTMB package without crashing. This may be an issue with computer power, or sensitivities of the most likely distributions for the sample data, or sample size. Therefore, analysis using a normal distribution was undertaken, where given the genomic sample size we should expect the model to appropriately account for the dispersion in the data. The central limit theorem (CLT) shows that for large amounts of data, even when the data is non-normal, the averages or the sums of the datapoints will generally follow normal distribution (Billingsley, 1995). Rather than general mixed effects models, linear mixed effect models were used during any analysis with the gene data with the lmer function in the lme4 package (Bates *et al.* 2015). Each individual gene was first analysed with season, sediment type, and treatment type with site as a random factor in a fully maximised model, before being analysed with nutrient availability in a simplified model (again with site as a random factor) to prevent over-testing.

Analysis for root and leaf biomass was conducted through generalised linear models, with site as a random factor. Histograms were used to determine the distribution; as with the average N₂O concentration, both leaf and root biomass conformed to a negative binomial distribution, with high levels of zero-inflation especially in the root biomass. This meant the glmmTMB package in R was selected for analysis of these data, with a negative binomial family (nbinom2) (Brooks *et al.* 2017). Zero-inflation was accounted for by using the glmmTMB packages feature, ziformula (ziformula = ~1). Each biomass type was analysed with site as a random factor with sediment type, treatment type, and season. For fully maximised models,

factor * factor was used; for simplified models, factor + factor was utilised instead. this was accounted for during analysis. Root and leaf biomass was first compared with each other per season per treatment to understand these relationships, before conducting further analysis for root biomass and leaf biomass singularly. Each biomass was compared with nutrient availability per season per treatment with site as a random factor to understand which (if any) nutrients impacted seagrass growth the most in these sites.

Chapter 3.0: Results

3.1. Analysis of Leaf and Root Biomass

The highest median dry root biomass of all the four seasons was found in spring (~0.007g) (**Fig. 3.1A**), with winter and summer having slightly lower medians. The mean root biomass found in spring, summer and winter were similar (~0.006g). However, autumn had a much lower range of root biomass, while also having lower mean and median root biomass. In contrast, leaf biomass shows almost the opposite pattern (**Fig. 3.1B**). Spring shows one of the lowest leaf biomass ranges, with only winter having a lower mean and median (~10g). Summer has a much higher range of leaf biomass with the highest mean (~90g) and median (~80g) of all seasons, with autumn being the second highest for mean (~40g) and median (~35g).

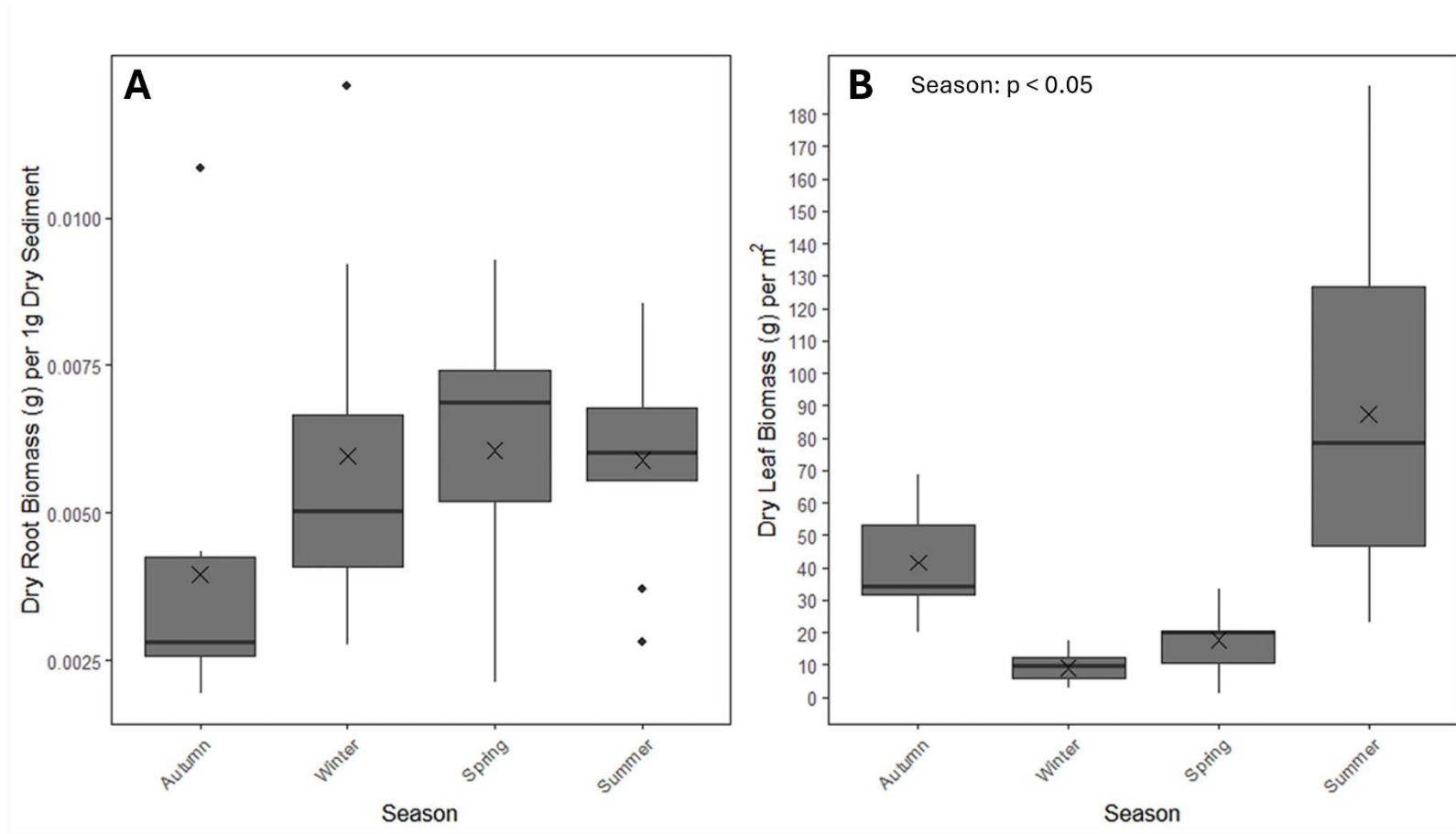


Fig 3.1. Seagrass leaf and root biomass data, shown as root dry weight (g) per 1g of dry sediment (**A**) and leaf dry weight (g) per m^2 of the seagrass meadow (**B**) across four seasons. The edges of the boxes represent the upper and lower quartiles, while the thick black line represents the median and the X marks the mean. The ends of the whiskers represent the range, with outliers represented by black dots.

Autumn was used as the base season by the model. It was determined that leaf biomass was significantly higher in summer than in autumn (GLM: z-value= 3.069, p-value= 0.00215) and significantly lower in spring and winter than in autumn, with winter having a higher level of significance (GLM: Leaf:Spring; z-value= -4.733, p-value= <0.001; Leaf:Winter; z-value= -7.369, p-value= <0.001). There were no significant differences in root biomass regardless of season (GLM: p-value > 0.1).

3.2. Sediment and Nutrient Analysis

Anion and cation concentration in sediments were measured and the data is presented in **Fig. 3.2** (See also Appendix, **Tables A2-A6**).

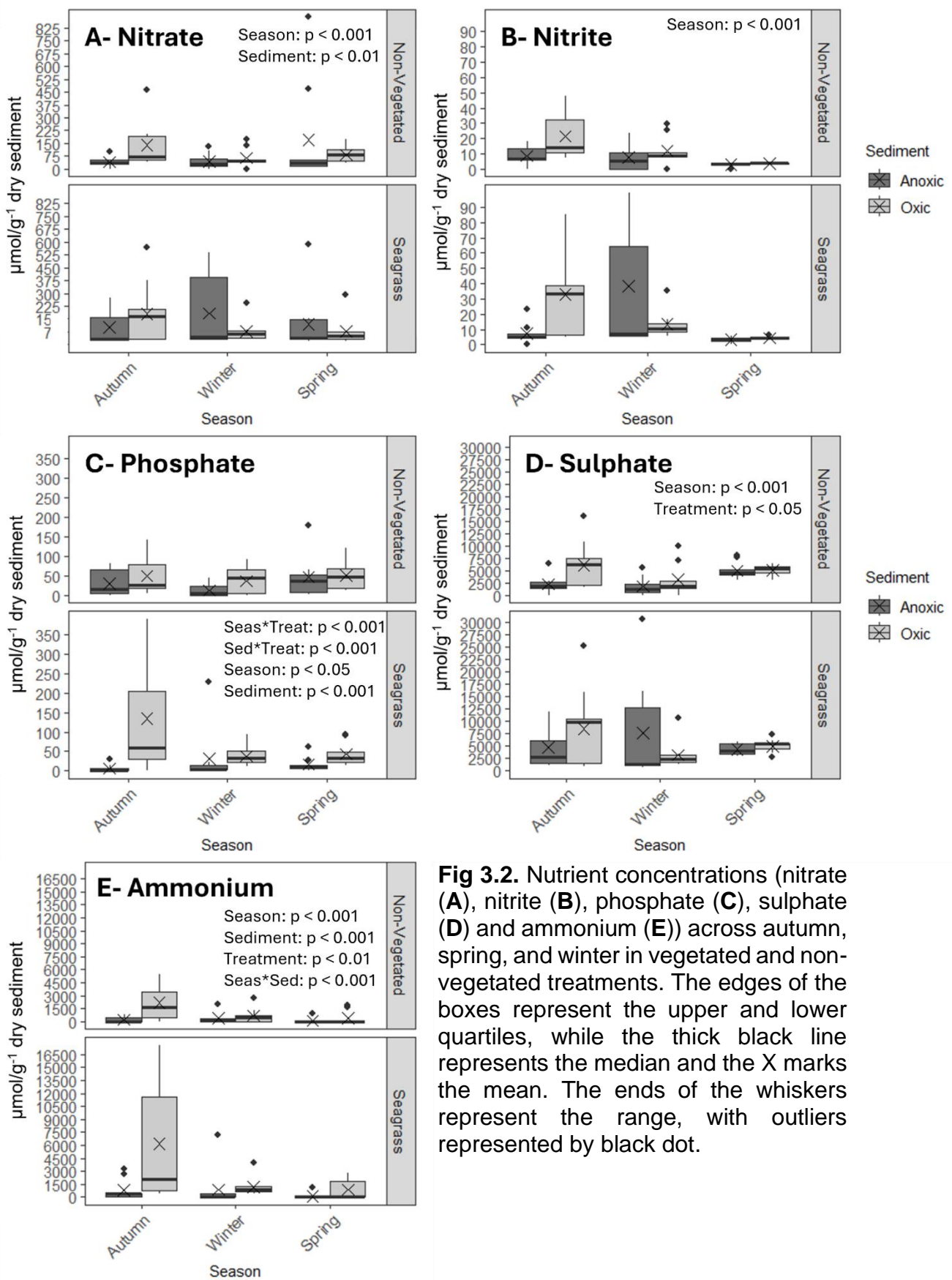


Fig 3.2. Nutrient concentrations (nitrate (A), nitrite (B), phosphate (C), sulphate (D) and ammonium (E)) across autumn, spring, and winter in vegetated and non-vegetated treatments. The edges of the boxes represent the upper and lower quartiles, while the thick black line represents the median and the X marks the mean. The ends of the whiskers represent the range, with outliers represented by black dot.

Mean nitrate concentrations in non-vegetated sediments were generally around zero, with the exception of a spike in oxic sediments in autumn ($\sim 100 \mu\text{mol g}^{-1}$ dry sediment) and winter ($\sim 50 \mu\text{mol g}^{-1}$ dry sediment) (**Fig. 3.2A**), whereas in the presence of seagrass, they are slightly higher at between $75\text{-}150 \mu\text{mol g}^{-1}$ dry sediment. Autumn and spring both follow the same patterns for non-vegetated and vegetated sediments, with autumn having slightly higher nitrate levels in oxic sediments than anoxic sediments, and the opposite being the case for spring. However, there is a larger variance in the presence of seagrass; the mean nitrate concentration in anoxic sediment $\sim 200 \mu\text{mol g}^{-1}$ dry sediment, whereas it is much lower in the oxic sediment at $\sim 50 \mu\text{mol g}^{-1}$ dry sediment. Nitrate concentrations were found to be significantly higher in spring than the autumn ($\sim 100 \mu\text{mol g}^{-1}$ dry sediment), and in oxic sediments in comparison to anoxic sediments ($\sim 150 \mu\text{mol g}^{-1}$ dry sediment) (GLMM: Spring; z-value= 4.146, p-value= <0.001; Oxic; z-value= 3.073, p-value= <0.01). Nitrate was significantly lower in oxic sediments in spring (GLMM: z-value= -3.620, p-value= <0.001). A separate simplified model found that nitrate concentrations were significantly lower when ammonium levels were higher (GLM: z-value= -2.608, p-value= <0.01), while high phosphate and sulphate concentrations were significantly associated with higher nitrate concentration (GLM: Phosphate; z-value= 3.033, p-value= <0.01; Sulphate; z-value= 6.560, p-value= <0.001)

Nitrite concentration was generally low within the season and treatment, $\sim 0.5\text{-}10 \mu\text{mol g}^{-1}$ dry sediment (**Fig 3.2B**), with spikes in oxic sediment in both treatments in autumn ($\sim 20\text{-}30 \mu\text{mol g}^{-1}$ dry sediment), and then a large spike in anoxic sediment in winter in the seagrass treatment ($\sim 40 \mu\text{mol g}^{-1}$ dry sediment). Nitrite concentrations were significantly lower in spring ($\sim 0.5 \mu\text{mol g}^{-1}$ dry sediment) (GLMM: z-value= -10.167, p-value= <0.001), with no other significant results (p-value= > 0.1)

An increase in mean phosphate concentration was found in oxic sediments compared to anoxic sediments in both vegetated and non-vegetated sites (**Fig 3.2C**). The mean phosphate concentrations in oxic sediments decreased from autumn (~ 150 $\mu\text{mol g}^{-1}$ dry sediment) to winter and spring (~ 50 $\mu\text{mol g}^{-1}$ dry sediment). The opposite pattern can be observed in the mean phosphate concentration in the anoxic seagrass sediments. The range of phosphate concentration appears to remain largely unchanged throughout the year in the non-vegetated treatment, with a mean at 10-50 $\mu\text{mol g}^{-1}$ dry sediment regardless. However, phosphate concentrations were significantly lower in seagrass compared to non-vegetated sediments, and significantly lower in winter than in autumn (GLM: Seagrass; z-value= -3.525, p-value= <0.001; Winter; z-value= -2.065, p-value= <0.05). There was a significantly higher phosphate concentration in both the seagrass treatment in winter, and in oxic sediments within the seagrass meadows (GLM: Winter:Seagrass; z-value= 4.316, p-value= <0.001; Seagrass:Oxic; z-value= 4.604, p-value= <0.001). However, in oxic sediments in the presence of seagrass in winter, there was significantly lower phosphate (GLM: z-value= -4.199, p-value= <0.001). Higher phosphate concentrations were significantly associated with high nitrate and ammonium concentrations (GLM: Nitrate; z-value= 5.659, p-value= <0.001; Ammonium; z-value= 4.757, p-value= <0.001). Phosphate concentrations were significantly lower in association with increased sulphate concentrations (GLM: z-value= -2.804, p-value= <0.01). There were no other significant results, with all results bar Winter:Seagrass having p-value > 0.1.

In autumn, regardless of treatment type, anoxic sediments appear to have a higher mean sulphate concentration than oxic sediment (**Fig 3.2D**), whereas the opposite can be seen for winter and spring. The mean concentration for non-vegetated

treatments has a range of about $\sim 2500\text{-}5000 \mu\text{mol g}^{-1}$ dry sediment regardless of season in both oxic and anoxic sediments, except for a spike in oxic sediments in autumn to $\sim 7500 \mu\text{mol g}^{-1}$ dry sediment. In the presence of seagrass, mean sulphate concentration also has a range of $\sim 2500\text{-}5000 \mu\text{mol g}^{-1}$ dry sediment regardless of season and sediment type, however, two spikes are observed: the first being a spike in oxic sediment in autumn to a mean concentration of $\sim 8000 \mu\text{mol g}^{-1}$ dry sediment, and the second spike observed in winter also being $\sim 8000 \mu\text{mol g}^{-1}$ dry sediment. Sulphate concentration was significantly lower in seagrass (LME: t-value= -2.077, p-value= < 0.05) and winter (t-value= -4.061, p-value= < 0.001). In terms of nutrient availability, high sulphate concentrations were significantly associated with higher nitrate and nitrite concentrations (GLM: Nitrate; z-value= 6.522, p-value= <0.001; Nitrite; z-value= 17.952, p-value= <0.001), but significantly lower when associated with high phosphate concentrations (GLM: z-value= -3.642, p-value= <0.001).

Ammonium levels were lower in spring than in autumn or winter, regardless of the presence of seagrass (**Fig. 3.2E**). In autumn and winter, for both vegetated and non-vegetated treatment, oxic sediments appear to have higher ammonium levels than anoxic sediments. In the presence of seagrass, ammonium concentrations in oxic sediments in autumn were $\sim 1.2 \times 10^4 \mu\text{mol g}^{-1}$ dry sediment with a mean of $\sim 6.0 \times 10^3 \mu\text{mol g}^{-1}$ dry sediment, which was about $4.5 \times 10^3 \mu\text{mol g}^{-1}$ dry sediment higher than in the anoxic sediment in the same treatment. Ammonium concentration was significantly lower in spring (GLMM: z-value= -24.564, p-value= <0.001) and winter (GLMM: z-value= -7864, p-value= <0.001). Ammonium concentration was significantly higher in oxic sediments and in the seagrass treatment (GLMM: Oxic; z-value= 22.388, p-value= <0.001; Seagrass; z-value= 3.1.1, p-value= <0.01). Ammonium concentration was significantly higher in oxic treatments in spring, and significantly lower in oxic

sediments in winter (GLMM: Oxic:Spring; z-value= 5.680, p-value= <0.001; Oxic:Winter; z-value= -5.032, p-value= < 0.001). Ammonium was also significantly higher in oxic sediment in the seagrass treatment (GLMM: z-value= 8.958, p-value= < 0.001). There was no significant effect of nutrient availability on ammonium concentration.

3.3. N₂O Production

The N₂O production was almost negligible in winter, regardless of site or presence of seagrass (**Fig. 3.4**). However, in the spring there is a significant increase in N₂O concentration (compared to the winter) in both vegetated and non-vegetated treatments (i.e. from 0ppm N₂O in Winter to maximum ~95 ppm N₂O in Spring). The rate of N₂O removal in the non-vegetated treatment (~4.1ppm min⁻¹) was higher than when seagrass was present (~3.3 ppm min⁻¹).

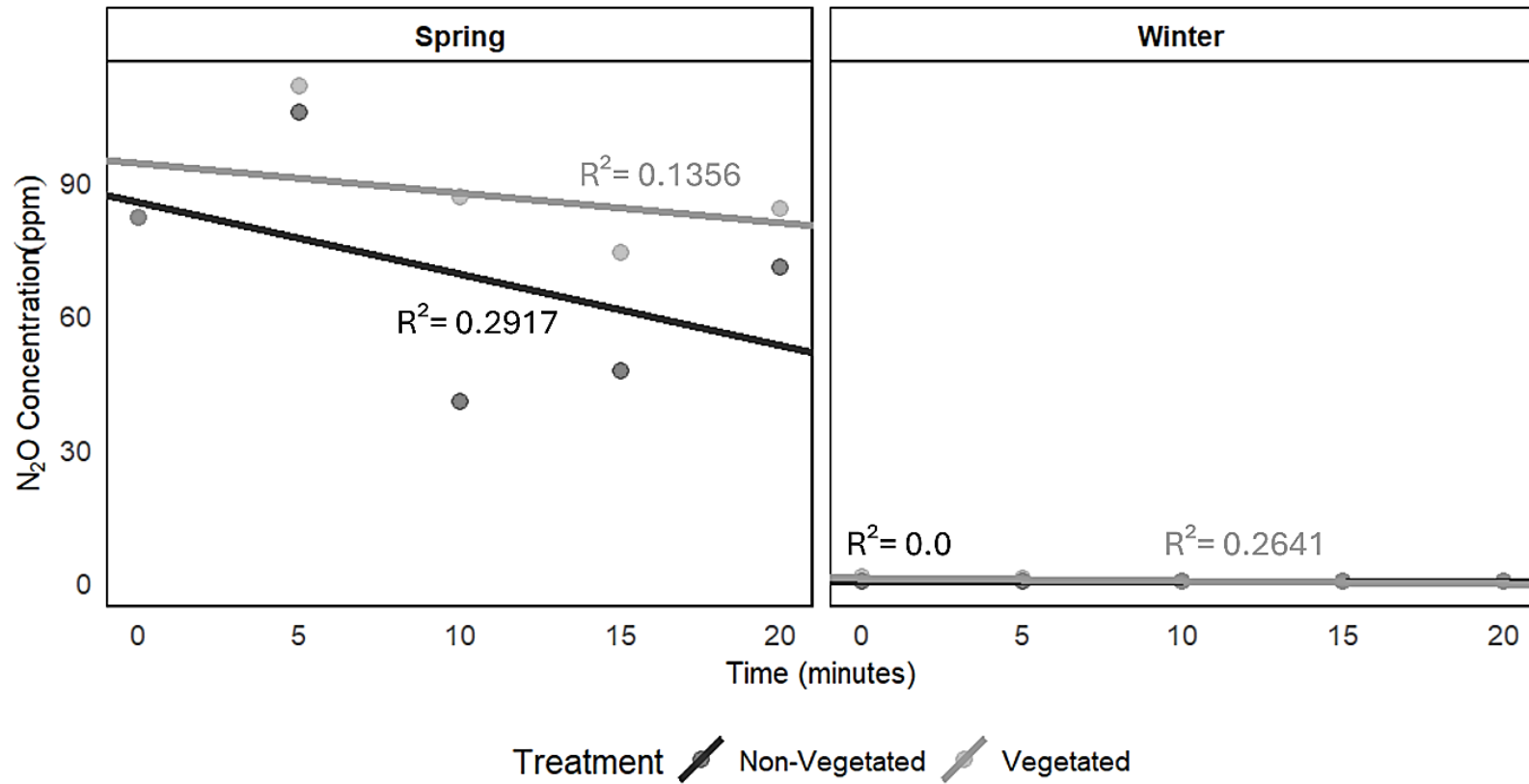


Figure 3.4. Spring and Winter N₂O gas flux data showing the linear regression per treatment per season measured over 20 mins fitted to the raw data for all replicates. Only the average of the replicates is shown above, with the average N₂O concentration at 0 minutes in spring being the same for non-vegetated and vegetated treatments.

There are significantly lower N₂O concentrations observed in winter than in spring (GLM: z-value= -991.46, p-value= <0.001) and significantly higher concentrations of N₂O in the vegetated treatment than in the non-vegetated treatment regardless of season (GLM: z-value= 12.66, p-value= <0.001) but also significantly higher N₂O concentrations in seagrass treatment in winter (GLM: z-value= 769.47, p-value <0.001). Again, this is likely skewed due to there being no N₂O detected in the non-vegetated samples while to vegetated samples had detectable amounts of N₂O; these two samples could be defined as outliers as they have a disproportionately large effect on the results. However, they also possibly encompass natural variation in N₂O production; they have been included in the study because of the assumption that this is true and has not been picked up due to small sample size.

3.4. qPCR Analysis of Bacterial and Archaeal 16S rRNA Gene Abundance

Bacterial 16S rRNA gene abundance was approximately three orders of magnitude higher than archaeal 16S rRNA gene abundance across all measured seasons (**Fig 3.5**).

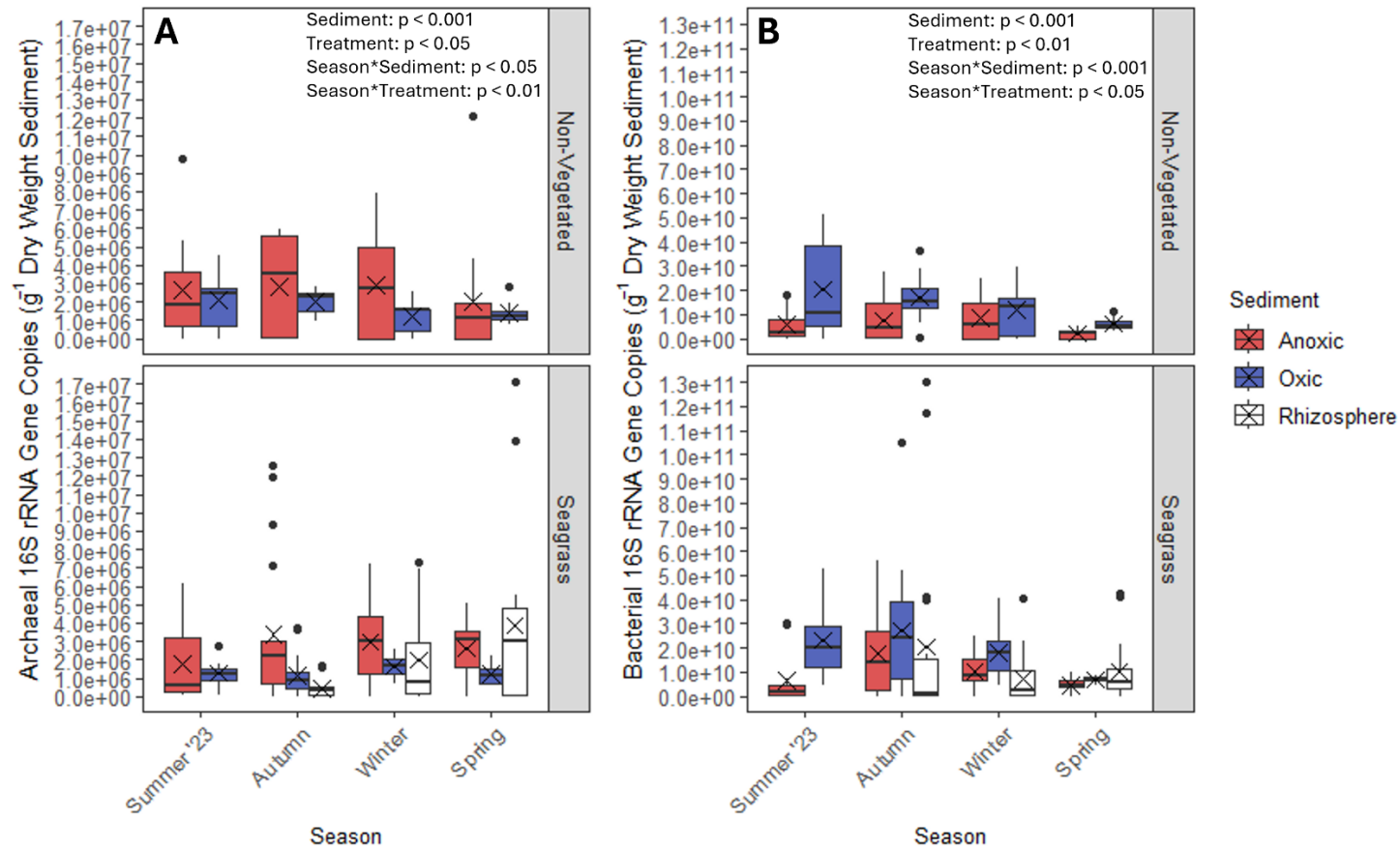


Fig 3.5. 16S rRNA genes abundance for Archaeal (A) and Bacterial (B) in anoxic, oxic, and rhizosphere sediment samples from vegetated and unvegetated sediment across four seasons. The edges of the boxes represent the upper and lower quartiles, while the thick black line represents the median and the X marks the mean. The ends of the whiskers represent the range, with outliers represented by black dots.

In both vegetated and non-vegetated treatments, the mean Archaeal 16S rRNA gene abundance was higher in anoxic sediment ($\sim 2\text{-}3 \times 10^6$ gene copies g^{-1} dry weight sediment) compared to oxic sediments ($1\text{-}2 \times 10^6$ gene copies g^{-1} dry weight sediment) (**Fig 3.5A**). In the autumn the lowest mean archaeal 16S rRNA gene abundance was found in the rhizosphere (0.5×10^6 gene copies g^{-1} dry weight sediment) which then increased in winter (2.0×10^6 gene copies g^{-1} dry weight sediment) and spring (4.0×10^6 gene copies g^{-1} dry weight sediment). It was found that archaeal 16S rRNA gene abundance was significantly lower in the rhizosphere than in anoxic sediment (LME: DF= 1.940×10^7 , t-value= -3.849 , p-value= <0.001). Archaeal 16S rRNA gene abundance was significantly higher in the seagrass treatment than the non-vegetated treatment (LME: DF= 2.100×10^5 , t-value= 2.417 , p-value= <0.05) and significantly higher when bacterial 16S rRNA gene abundance was also high (LME: DF= 1.053×10^5 , t-value= 3.967 , p-value= <0.001).

There were no significant differences when only season was tested (p-value > 0.1). In spring, archaeal 16S rRNA gene abundance was significantly higher in the rhizosphere (LME: Spring:Rhizosphere; DF= 1.480×10^7 , t-value= 4.235 , p-value= <0.001) and significantly lower in oxic sediments (LME: Spring:Oxic; DF= 1.065×10^6 , t-value= -2.343 , p-value= <0.05). The seagrass treatment in spring had significantly lower archaeal 16S rRNA gene abundance (LME: Spring:Seagrass; DF= 1.566×10^8 , t-value= -2.226 , p-value= <0.05). When bacterial 16S rRNA gene abundance was high in oxic sediments, as well as in the seagrass treatment, archaeal 16S rRNA gene abundances were significantly lower (LME: Oxic:16SBacteria; DF= 2.022×10^5 , t-value= -3.063 , p-value= <0.01 ; Seagrass:16SBacteria; DF= 5.546×10^4 , t-value= -3.538 , p-value= <0.01). However, when bacterial 16S rRNA gene abundance were high in oxic sediments in spring, archaeal 16S rRNA gene abundance was also

significantly higher (LME: Oxic:Seagrass:16SBacteria; DF= 1.792e+05, t-value= 2.905, p-value= <0.01). There were no other significant differences (p-value > 0.1) with Summer:Seagrass being the only marginal different (p-value= <0.1).

In contrast to the archaea, the mean bacterial 16S rRNA gene abundance was lower in anoxic sediment than oxic sediment in both non-vegetated and vegetated sediments (0-1.5x10¹⁰ gene copies g⁻¹ dry weight anoxic sediment, 0-2.5x10¹⁰ gene copies g⁻¹ dry weight oxic sediment) (**Fig 3.5B**). In all four seasons, the mean gene abundance was between ~0.5 and 2.5x10¹⁰ gene copies g⁻¹ dry weight sediment regardless of oxic/anoxic sediment. Rhizosphere samples in autumn and winter also had a lower mean abundance than oxic samples, with a lower median than anoxic samples (~0.5x10¹⁰ mean gene copies g⁻¹ dry weight rhizosphere sediment, 2-2.5x10¹⁰ mean gene copies g⁻¹ dry weight oxic sediment, 1.5x10¹⁰ median gene copies g⁻¹ dry weight anoxic sediment, 0.5x10¹⁰ median gene copies g⁻¹ dry weight rhizosphere sediment).

Bacterial 16S rRNA gene abundance was significantly lower in the rhizosphere than in anoxic sediment (LME: DF= 278, t-value= -6.898, p-value= <0.001). However, bacterial abundance was significantly higher in the seagrass treatment than in the non-vegetated treatment (LME: DF= 278, t-value= 4.230, p-value= <0.001) and when archaeal abundance increased (LME: DF= 278, t-value= 3.114, p-value= <0.01). In winter and spring, bacterial abundance was significantly higher in the rhizosphere (LME: Spring:Rhizosphere; DF= 278, t-value= 4.233, p-value= <0.001; Winter:Rhizosphere; DF= 278, t-value= 3.346, p-value= <0.001). In the seagrass treatment in spring, summer and winter, bacterial abundance was significantly lower (LME: Spring:Seagrass; DF= 278, t-value= -2.408, p-value= <0.05; Summer:Seagrass; DF= 278, t-value= -3.087, p-value= <0.01; Winter:Seagrass; DF=

278, t-value= -2.164, p-value= <0.05). In spring, when archaeal abundance was higher, bacterial gene abundance was significantly lower (LME: Spring:16SArchaea; DF= 278, t-value= -2.175, p-value= <0.05) and the same was true when 16S archaeal abundance was high when seagrass was present (LME: Seagrass:16SArchaea; DF= 278, t-value= -2.724, p-value= <0.001). In the rhizosphere, when high archaeal 16S rRNA gene abundance was observed, bacterial abundance was significantly higher (LME: Rhizosphere:Archaea; DF= 278, t-value= 15.941, p-value= <0.001). However, when archaeal abundance was higher in the rhizosphere in spring and winter, bacterial abundance was significantly lower (LME: Spring:Rhizosphere:16SArchaea; DF= 278, t-value= -14.912, p-value= <0.001; Winter:Rhizosphere:16SArchaea; DF= 278, t-value= -14.612, p-value= <0.001). Bacterial abundance significantly increased when associated with seagrass presence in summer when archaeal abundance was high (LME: Summer:Seagrass:16SArchaea; DF= 278, t-value= 2.724, p-value= <0.01). There were no other significant results (p-value > 0.1) with one marginal result (Summer:Oxic:16SArchaea; p-value= <0.1).

Simplified linear mixed effect models were used to test for relationships between archaeal and bacterial 16S rRNA gene copies and nutrient concentration. It was found that archaeal 16S rRNA gene copy number was significantly higher when associated with increased nitrite and ammonium concentrations (LME: Nitrite; DF= 1.022e+12, t-value= 2.307, p-value= 0.021041; Ammonium; DF= 2.556e+05, t-value= 3.297, p-value= <0.001), but was significantly lower when phosphate concentrations were increased (LME: DF= 1.705, t-value= -3.602, p-value= <0.001). Bacterial 16S rRNA gene copy number was found to be significantly higher when nitrite, sulphate, and ammonium concentrations were higher (LME: Nitrite; DF= 194, t-value= 2.857, p-value= <0.01; Sulphate; DF= 194, t-value= 3.702, p-value= <0.001; Ammonium; DF=

194, t-value= 8.074, p-value= <0.001). There were no other significant associations with nutrient concentration (p-value > 0.1).

3.5. qPCR Analysis of Ammonia-Oxidising Bacteria (AOB) and Archaea (AOA) *amoA* Gene Abundance

AOB *amoA* gene abundance was about two-fold greater than AOA (**Fig. 3.6**). The mean AOA *amoA* gene abundance in oxic sediments was greater than anoxic sediments regardless of vegetation presence or season, (i.e. between $\sim 1.0\text{-}5.0 \times 10^5$ gene copies g^{-1} dry weight sediment). The rhizosphere had lower AOA *amoA* gene abundances in oxic and anoxic sediments in autumn and winter but increased drastically in the spring to have the highest mean abundance of any sediment in any season in the seagrass treatment ($\sim 7.5 \times 10^5$ gene copies g^{-1} dry weight sediment). It also has the highest range, from 0 up to $\sim 1.25 \times 10^5$ gene copies g^{-1} dry weight sediment.

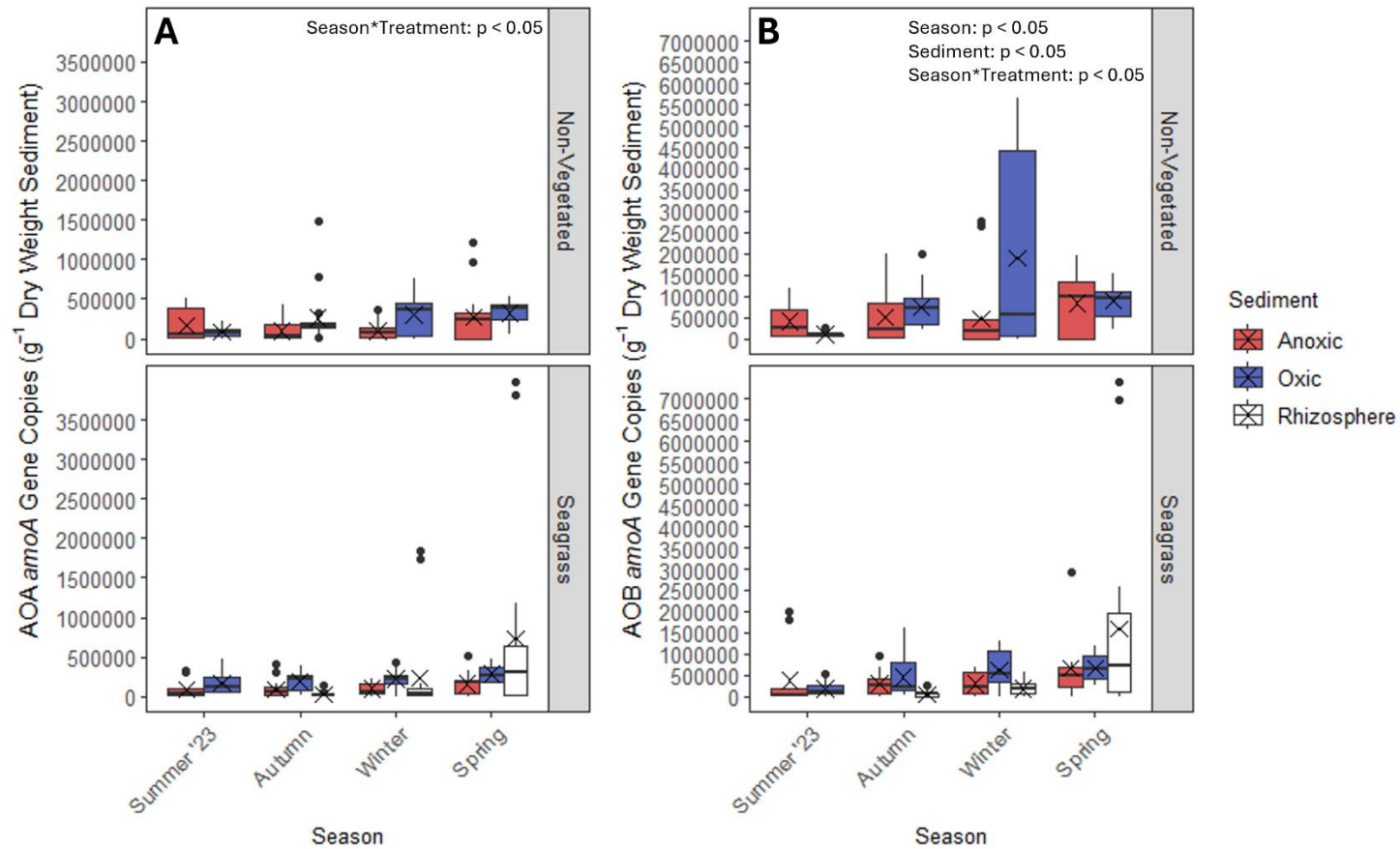


Fig 3.6. Ammonia oxidiser *amoA* gene abundance in oxic, anoxic, and rhizosphere samples from vegetated and non-vegetated sediments across four seasons; Ammonia Oxidising Archaea (AOA) (**A**) and Ammonia Oxidising Bacteria (AOB) (**B**). The edges of the boxes represent the upper and lower quartiles, while the thick black line represents the median and the X marks the mean. The ends of the whiskers represent the range, with outliers represented by black dots.

Fully maximised LMERs were used to understand the relationships between AOA/AOB *amoA* gene abundance, season, vegetation/non-vegetated, oxic/anoxic sediments, and simplified LMERs were used for nutrient associations, all with site as a random factor. In spring, **Fig. 3.6B** shows non-vegetated treatment to have a slightly higher mean AOB *amoA* gene abundance for anoxic and oxic sediments than the vegetated treatment, $\sim 1 \times 10^6$ gene copies g^{-1} dry weight sediment as opposed to 0.5×10^6 gene copies g^{-1} dry weight sediment. AOA *amoA* gene abundance was significantly higher when AOB *amoA* gene abundance was high (LME: DF= 2.797e+02, t-value= 2.615, p-value= <0.01). AOB *amoA* gene copy number was significantly lower in the rhizosphere in spring (LME: Spring:Rhizosphere; DF= .795e+02, t-value= -2.127, p-value= <0.05) as well as when AOB *amoA* gene abundance was high in the presence of seagrass in spring (LME: Spring:Seagrass:AOB; DF= 2.650e+02, t-value= -2.276, p-value= <0.05) and summer (LME: Summer:Seagrass:AOB; DF= 2.788e+02, t-value= -2.180, p-value= <0.05). AOA *amoA* gene copy number was significantly higher in oxic sediment in the seagrass treatment in summer when in association with higher AOB *amoA* gene abundance (LME: Spring:Oxic:Seagrass:AOB; DF= 2.800e+02, t-value= 2.076, p-value= <0.05).

As in **Fig. 3.6A**, AOA *amoA* also showed a much higher mean abundance in the rhizosphere in spring than in any other vegetated sediment type, at about 2×10^6 gene copies g^{-1} dry weight sediment. The highest mean AOB *amoA* gene abundance is observed in oxic sediments in winter, within the non-vegetated sediments. The range is up to almost 6×10^6 gene copies g^{-1} dry weight sediment, with the mean sitting just above 2×10^6 gene copies g^{-1} dry weight sediment. Oxic sediments appear to have slightly higher AOB *amoA* gene abundance than anoxic sediments regardless of

treatment for autumn, winter, and spring, but the opposite being true in summer. Elevated concentrations of ammonium was correlated with significantly higher AOA *amoA* gene abundance (LME: DF= 193.56, t-value= 2.396, p-value= <0.05). There were no other significant results between AOA *amoA* gene copy number and nutrient concentration, with all except sulphate having a p-value > 0.1.

There was a far greater number of significant results regarding AOB *amoA* gene abundance. AOB *amoA* gene abundance was significantly higher in spring, in oxic sediment, and when AOA *amoA* gene abundance was also high (LME: Spring; DF= 7.444e+08, t-value= 1.995, p-value= <0.05; Oxic; DF= 2.560e+06, t-value= 2.443, p-value= <0.05; AOA; DF= 1.890e+06, t-value= 4.808, p-value= <0.001). AOB *amoA* gene abundance was significantly lower in oxic sediment in both spring and winter (LME: Spring:Oxic; DF= 1.179e+06, t-value= -2.179, p-value= <0.05; Winter:Oxic; DF= 1.574e+07, t-value= -2.031, p-value= <0.05). In spring and summer, when AOA *amoA* gene abundance was high, AOB *amoA* gene abundance was significantly lower (LME: Spring:AOA; DF= 5.911e+06, t-value= -3.207, p-value= 0.001340; Summer:AOA; DF= 3.169e+06, t-value= -2.247, p-value= <0.05). AOB *amoA* gene abundance was also significantly lower when AOA *amoA* gene abundance was high in oxic sediment and in the seagrass treatment (LME: Oxic:AOA; DF= 6.366e+05, t-value= -3.867, p-value= <0.001; Seagrass:AOA; DF= 5.982e+05, t-value= -2.461, p-value= <0.05). When AOA *amoA* gene abundance was higher in oxic sediment in spring and winter, however, AOB *amoA* gene abundance was also significantly higher (LME: Spring:Oxic:AOA; DF= 1.914e+06, t-value= 3.679, p-value= <0.001; Winter:Oxic:AOA; DF= 4.160e+07, t-value= 3.182, p-value= <0.01). In the seagrass treatment for both spring and summer, when AOA *amoA* gene abundance was high, AOB *amoA* gene abundance was also significantly higher (LME:

Spring:Seagrass:AOA; DF= 7.595e+07, t-value= 2.751, p-value= <0.01; Summer:Seagrass:AOA; DF= 1.032e+07, t-value= 3.733, p-value= <0.001), as well when AOA *amoA* gene copy number was higher in oxic sediments in the seagrass treatment (LME: Oxic:Seagrass:AOA; DF= 2.371e+07, t-value= 2.153, p-value= <0.05). In spring and summer when AOA *amoA* gene abundance was higher in the oxic sediment within the seagrass treatment, AOB *amoA* gene copy number was significantly lower (LME: Spring:Oxic:Seagrass:AOA; DF= 1.367e+07, t-value= -2.213, p-value= <0.05; Summer:Oxic:Seagrass:AOA; DF= 3.250e+07, t-value= -2.173, p-value= <0.05). There were no other significant results (p-value > 0.1).

3.6. qPCR Analysis of Denitrifier Gene Abundance

The abundance of the denitrifier genes (*nirS/nirK*) are presented in **Fig 3.7**. The *nirK* gene abundance was around two orders of magnitude lower than *nirS* gene abundance; the highest mean *nirK* gene abundance was at around 6.0×10^5 gene copies g^{-1} dry weight sediment, whereas the lowest mean *nirS* gene abundance was $\sim 1 \times 10^7$ gene copies g^{-1} dry weight sediment.

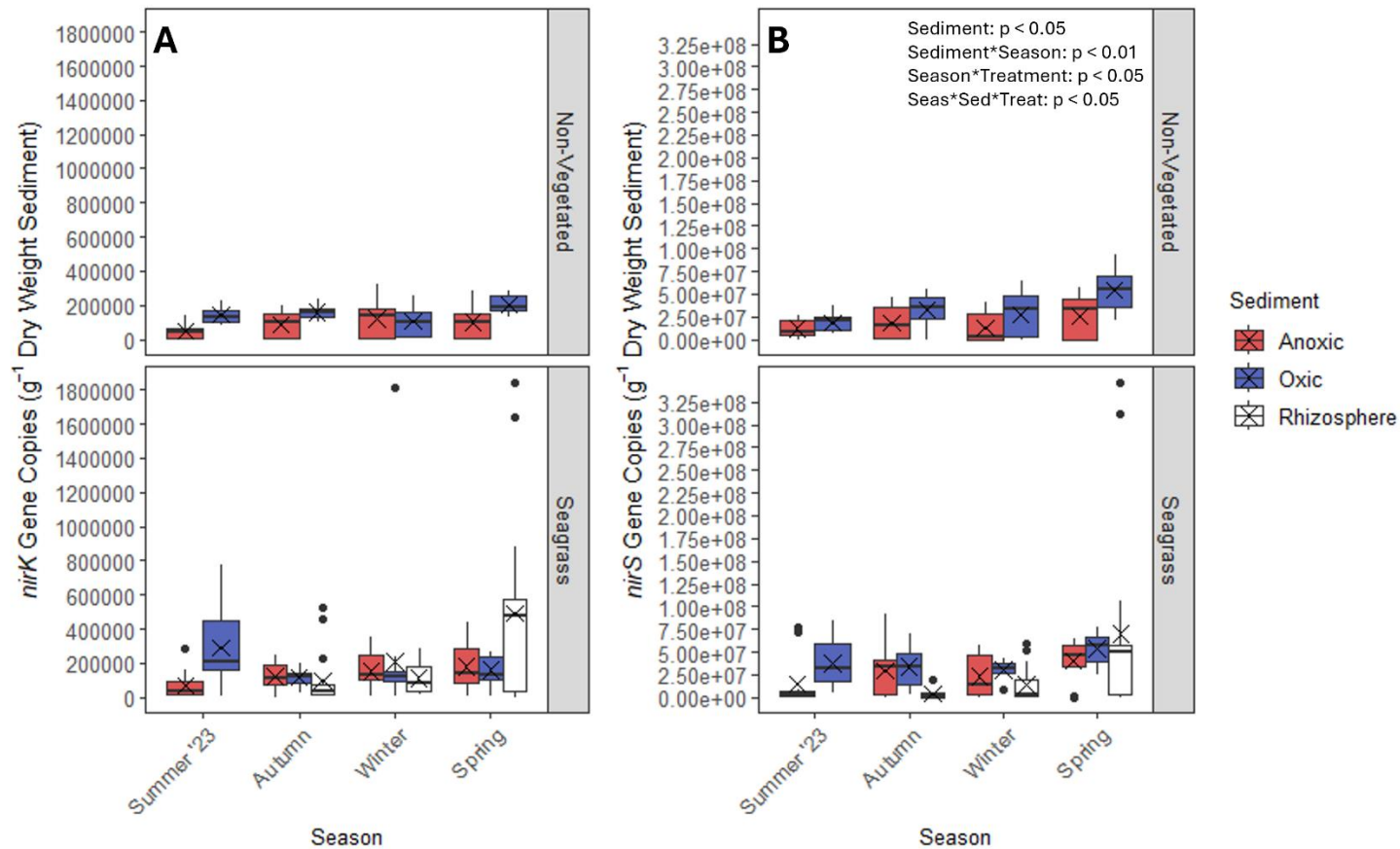


Fig 3.7. Denitrifier gene abundance; *nirK* (A), and *nirS* (B), from anoxic, oxic and rhizosphere samples taken from vegetated and non-vegetated sediment across four seasons. The edges of the boxes represent the upper and lower quartiles, while the thick black line represents the median and the X marks the mean. The ends of the whiskers represent the range, with outliers represented by black dots.

Non-vegetated sediments had lower *nirK* gene abundances compared to sediments with seagrass, with the highest mean falling at about 2.0×10^5 gene copies g^{-1} dry weight sediment, about half that of the abundances observed with seagrass (**Fig. 3.7A**). Anoxic and oxic sediment types within the seagrass sediments in autumn, winter and spring have very similar means ($\sim 1.0 \times 10^3$ difference), while in summer, the mean *nirK* abundance is about 2.0×10^5 gene copies g^{-1} dry weight sediment higher in the oxic sediment than the anoxic sediment. In autumn and winter, the rhizosphere *nirK* gene abundance was lower than the oxic and anoxic sediments, falling at about 1.0×10^5 gene copies g^{-1} dry weight sediment, before increasing suddenly in spring to about 5.0×10^5 gene copies g^{-1} dry weight sediment. The *nirK* gene abundance was found to be significantly higher when *nirS* abundance increased (LME: DF= 2.799e+02, t-value= 2.037, p-value= <0.05). *nirK* gene abundance was also significantly higher in the rhizosphere when *nirS* gene abundance was high (LME: Rhizosphere:*nirS*; DF= 2.792e+02, t-value= 4.189, p-value= <0.001). In the rhizosphere in spring and winter, when *nirS* abundance was high, *nirK* gene abundance was significantly lower (LME: Spring:Rhizosphere:*nirS*; DF= 2.793e+02, t-value= -3.834, p-value= <0.001; Winter:Rhizosphere:*nirS*; DF= 2.794e+02, t-value= -3.954, p-value= <0.001). There were no other significant results (p-value > 0.1) with two marginal results: Spring:Oxic:Seagrass:*nirS* (p-value= <0.1), and Spring:Rhizosphere (p-value= <0.1). Higher levels of ammonium were associated with significantly increased *nirK* gene abundance (LME: DF= 191.45, t-value= 1.974, p-value= <0.05), though there were no other significant results regarding nutrient concentration (p-value > 0.1).

It was found that *nirS* gene abundance significantly increased in oxic sediments, and when *nirK* abundance was higher (LME: Oxic; DF= 2.855e+06, t-

value= 2.017, p-value= <0.05; *nirK*; DF= 2.320e+05, t-value= 4.635, p-value= <0.001). In the rhizosphere in spring, *nirS* gene abundance was significantly lower (LME: Spring:Rhizosphere; DF= 1.376e+07, t-value= -3.013, p-value= <0.01), as well as in oxic sediment in the seagrass treatment (LME: Oxic:Seagrass; DF= 7.828e+06, t-value= -2.204, p-value= <0.05). When *nirK* gene abundance was increased in oxic sediments and the rhizosphere, *nirS* gene abundance was significantly lower (LME: Oxic:*nirK*; DF= 1.377e+07, t-value= -2.032, p-value= <0.05; Rhizosphere:*nirK*; DF= 1.086e+05, t-value= -3.652, p-value= <0.001). *nirS* gene abundance was also significantly lower when *nirK* gene abundance was high in winter (LME: Winter:*nirK*; DF= 1.196e+07, t-value= -2.340, p-value= <0.05).

The *nirS* gene abundance between non-vegetated and vegetated sediments was similar within each season (**Fig. 3.7B**), with the mean increasing slightly from summer through to spring for both anoxic and oxic sediments. The mean *nirS* abundance for both vegetated and non-vegetated treatment types appear to be higher in oxic sediments (up to 5.0×10^7) than in anoxic sediments (up to 2.5×10^7). In the autumn, the mean *nirS* abundance is $\sim 2 \times 10^7$ gene copies g^{-1} dry weight sediment. The *nirS* gene abundance increases in winter to $\sim 2.5 \times 10^7$ gene copies g^{-1} dry weight sediment, with a range up to 5×10^7 gene copies g^{-1} dry weight sediment. *nirS* abundance increases further in spring in the rhizosphere to have the highest mean ($\sim 7.5 \times 10^7$ gene copies g^{-1} dry weight sediment) and range (up to 1×10^8 gene copies g^{-1} dry weight sediment). In oxic sediment within the seagrass treatment, *nirS* gene abundance was significantly higher in spring, summer, and winter (LME: Spring:Oxic:Seagrass; DF= 7.851e+05, t-value= 3.183, p-value= <0.01; Summer:Oxic:Seagrass; DF= 2.007e+07, t-value= 2.067, p-value= <0.05; Winter:Oxic:Seagrass; DF= 1.277e+07, t-value= 3.028, p-value= <0.01). In spring,

when *nirK* abundance was increased in oxic and rhizosphere sediments, *nirS* abundance was significantly higher (LME: Spring:Rhizosphere:*nirK*; DF= 4.302e+05, t-value= 2.262, p-value= <0.05; Spring:Rhizosphere:*nirK*; DF= 3.575e+06, t-value= 4.371, p-value= <0.001). In winter, when *nirK* abundance is higher in the rhizosphere and in oxic sediments, *nirS* abundance is significantly higher (LME: Winter:Rhizosphere:*nirK*; DF= 1.306e+08, t-value= 2.729, p-value= <0.01; Winter:Oxic:*nirK*; DF= 3.28f, t-value= 2.561, p-value= <0.05). In the autumn, when *nirK* abundance was higher in oxic sediments within the seagrass treatment, *nirS* abundance was significantly higher, though the opposite is true in spring, summer, and winter (LME: Oxic:Seagrass:*nirK*; DF= 8.027, t-value= 2.603, p-value= <0.01; Spring:Oxic:Seagrass:*nirK*; DF= 1.571e+06, t-value= -3.356, p-value= <0.001; Summer:Oxic:Seagrass:*nirK*; DF= 8.110e+06, t-value= -2.480, p-value= <0.05; Winter:Oxic:Seagrass:*nirK*; DF= 9.148e+06, t-value= -3.946, p-value= <0.001). There were no other significant results (p-value > 0.1).

Both seagrass and non-vegetated sediments showed greater *nosZ* gene abundance in oxic compared to anoxic sediments, regardless of season (**Fig. 3.8**).

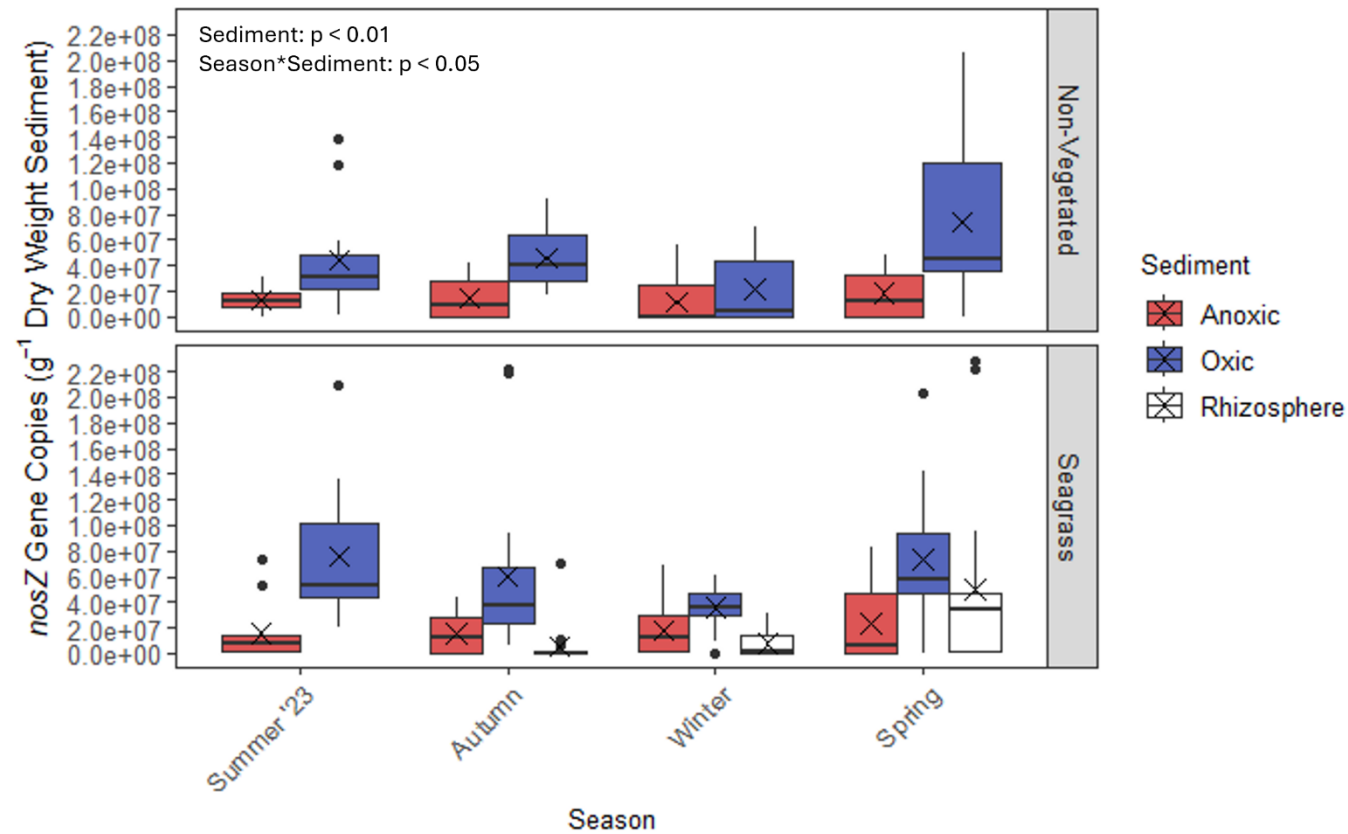


Fig 3.8. *nosZ* gene abundance from anoxic, oxic and rhizosphere samples taken from vegetated and non-vegetated sediment across four seasons. The edges of the boxes represent the upper and lower quartiles, while the thick black line represents the median and the X marks the mean. The ends of the whiskers represent the range, with outliers represented by black dots.

An increase in *nosZ* gene abundance was found in the rhizosphere from autumn, through winter, to be highest in the spring; an increase of about 2.0×10^7 gene copies g^{-1} dry weight sediment. The highest *nosZ* abundances for all sediment types for both treatments was in spring. For example, the highest range in the spring for non-vegetated was found in anoxic sediment, up to 2×10^8 gene copies g^{-1} dry weight sediment, and in the seagrass treatment, the largest range was up to 1.4×10^8 gene copies g^{-1} dry weight sediment, which was also found in the anoxic sediment. The *nosZ* gene abundance was significantly higher in oxic sediments (LME: DF= $5.829e+19$, t-value= 2.913, p-value= <0.01) as well as in rhizosphere sediments in the spring (LME: Spring:Rhizosphere; DF= $3.121e+21$, t-value= 2.394, p-value= <0.05). A simplified LME showed that *nosZ* was significantly higher than *nirS* and *nirK* (LME: *nirS*; DF= $2.325e+04$, t-value= 12.749, p-value= <0.001 ; *nirK*; DF= $5.438e+05$, t-value= 2.562, p-value= <0.05). When both *nirS* and *nirK* gene abundances were high, however, *nosZ* was significantly lower (LME: DF= $3.679e+04$, t-value= -5.603, p-value= <0.001).

3.7. Relationship Between N₂O Production, Leaf Biomass, Nutrient Availability, and Microbial Abundance

The relationship between nutrient concentrations and mean N₂O concentration is presented (**Fig. 3.9**). In winter, there are no observed interactions as the mean N₂O concentrations were largely 0ppm all R² values for winter were 0.0. Increased nitrite levels show an increase in mean N₂O concentration in both non-vegetated and vegetated sediments, even though observed nitrite levels were incredibly low in comparison to other nutrients.

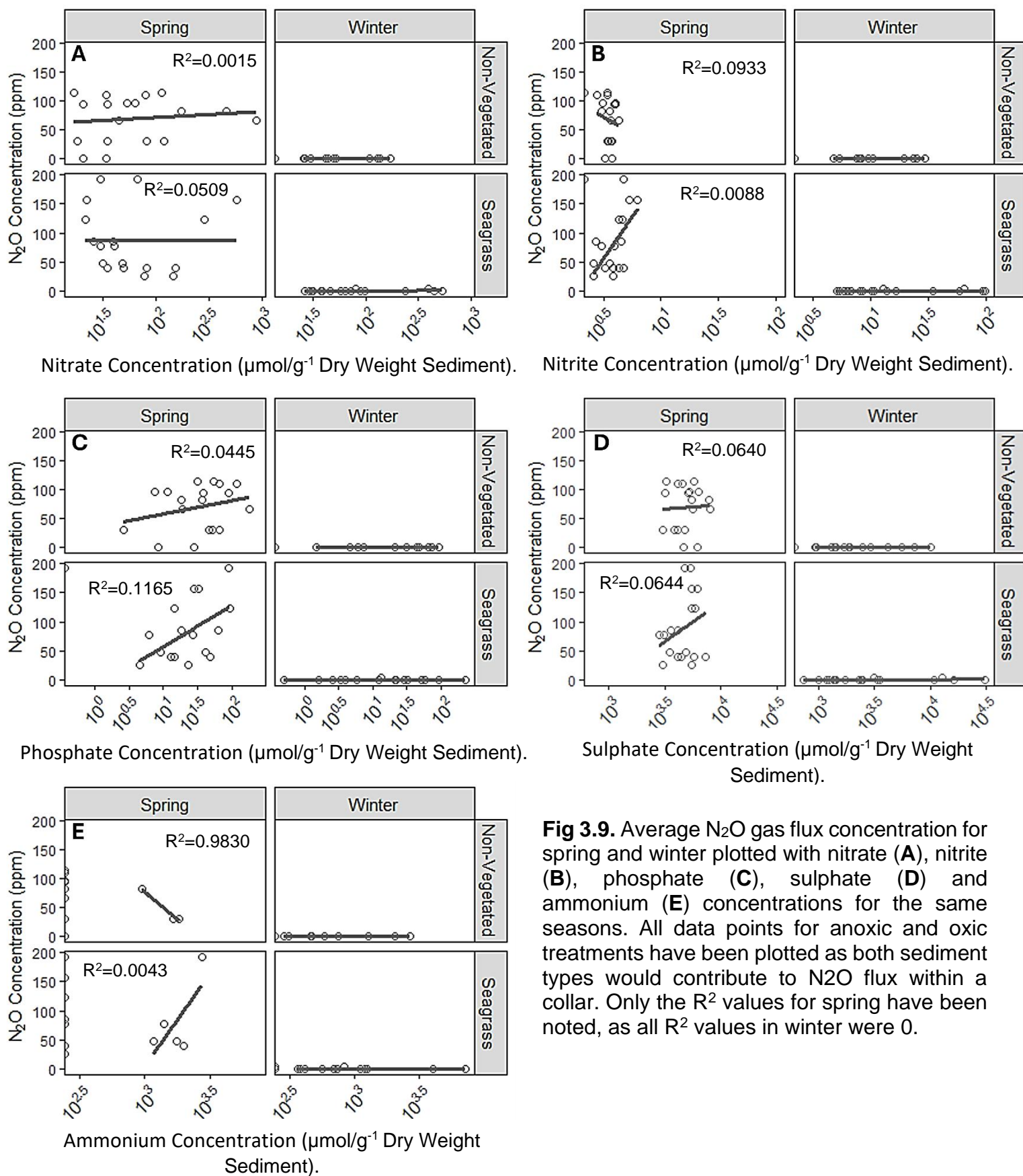


Fig 3.9. Average N_2O gas flux concentration for spring and winter plotted with nitrate (A), nitrite (B), phosphate (C), sulphate (D) and ammonium (E) concentrations for the same seasons. All data points for anoxic and oxic treatments have been plotted as both sediment types would contribute to N_2O flux within a collar. Only the R^2 values for spring have been noted, as all R^2 values in winter were 0.

The R^2 value for nitrite (**Fig. 3.9B**) is higher in non-vegetated with a negative correlation (0.0933) with N_2O concentration than vegetated, which has a positive correlation with N_2O concentration (0.0088), with N_2O concentrations reaching up to 150ppm when nitrite concentration is at its highest ($\sim 1 \times 10^1 \mu\text{mol g}^{-1}$ dry sediment). Phosphate (**Fig. 3.9C**) appears to have a positive effect on N_2O concentration regardless of treatment, though slightly less positive in non-vegetated sediments, with an R^2 value for non-vegetated treatment being 0.0445 and 0.1165 in vegetated treatment. Higher nitrate (**Fig. 3.9A**) concentration appears to increase N_2O in non-vegetated treatment ($R^2= 0.0015$) with very little effect in the seagrass treatment ($R^2= 0.0509$). Ammonium (**Fig. 3.9E**), however, appears to have a negative correlation with mean N_2O concentration in the non-vegetated treatment, with an R^2 value of 0.9830, while it has a slightly positive correlation in the seagrass treatment ($R^2= 0.0043$). Sulphate (**Fig. 3.9D**) is found in much higher amounts than the other nutrients and appears to have a positive correlation with mean N_2O concentration regardless of treatment, though less positive in non-vegetated ($R^2=0.0640$) than in vegetated ($R^2= 0.0644$).

Due to a small sample size, there was not enough data to explore a fully maximised model with all interactions, so only one-way interactions between N_2O and nutrient concentration were calculated. The model found that higher concentrations of nitrite was associated with significantly decreased N_2O production (GLM: z-value= -8.747, p-value= <0.001) and sulphate was associated with significantly increased mean N_2O concentration (GLM: z-value= 6.659, p-value= <0.001). No other nutrients had a significant effect on N_2O concentration.

Fig. 3.10. shows the mean N_2O concentration in relation to *nirK*, *nirS*, and *nosZ* gene abundance. In the presence of seagrass in the winter, both *nirK* and *nirS* gene

abundance show a slightly positive correlation with N₂O concentration, with the R² value for *nirK* being 0.03667212 and for *nirS* being 0.1441567, while *nosZ* shows a slightly negative correlation with N₂O concentration (R²= 0.09140311). These effects may be over- or under-exaggerated due to the single collar with any N₂O registered in the samples.

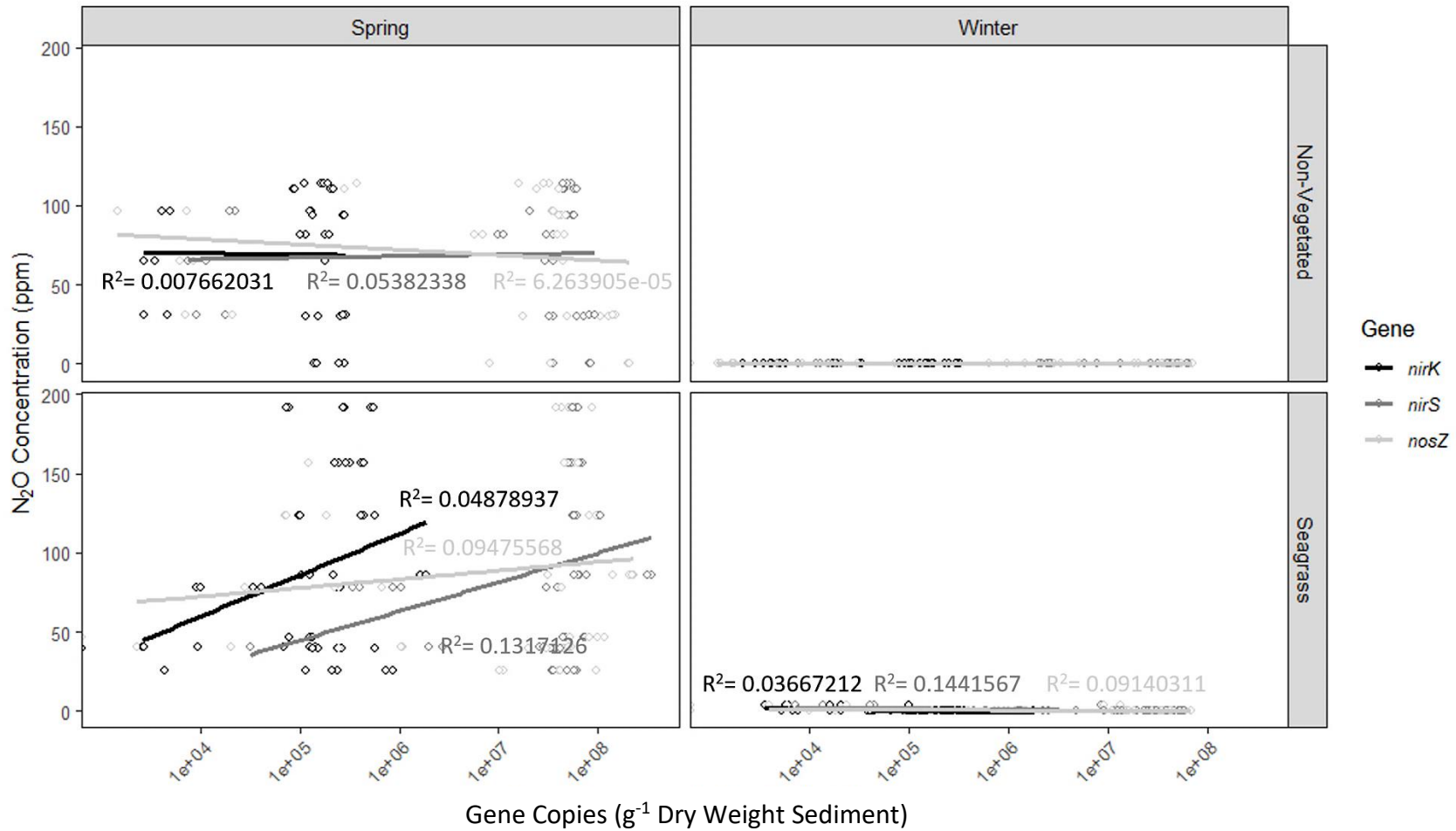


Fig 3.10. Spring and winter N_2O gas flux data plotted with gene abundance per 1g dry weight of sediment for the same seasons. All data points for anoxic and oxic treatments have been plotted as both sediment types would affect N_2O flux. All R^2 values for the non-vegetated treatment in winter were 0.0.

The relationships between *nirS*, *nirK*, and *nosZ* genes and N₂O concentration appear to be stronger in the presence of seagrass as opposed to bare sediment (**Fig. 3.10**). In the non-vegetated sediments, higher *nosZ* gene abundance related to slightly reduced N₂O concentration ($R^2= 6.263905e-05$), while higher *nirS* gene abundance related to increased N₂O concentration ($R^2= 0.05382338$). Conversely, *nirK* gene abundance had a slight negative correlation with N₂O concentration ($R^2= 0.007662031$). In the vegetated sediments, *nirK* ($R^2= 0.04878937$), *nirS* ($R^2= 0.1317126$) and *nosZ* ($R^2= 0.09475568$) gene abundance all show a positive correlation with N₂O concentration.

GLM was used to test for significance between gene abundance and N₂O concentration. Neither *nosZ* nor *nirK* had an effect (GLM: p-value > 0.1), while there were significantly higher N₂O concentrations associated with higher *nirS* gene abundance (GLM: DF= 1.725e+02, t-value= 2.164, p-value= <0.05). In winter, there was no relationship between root biomass ($R^2= 0.00208096$) or leaf biomass ($R^2= 0.0178241$) with N₂O concentration (**Fig. 3.11**). In spring, however, increased leaf biomass shows a positive correlation with N₂O concentration ($R^2= 0.5654409$) (**Fig. 3.11A**), while increased root biomass shows the opposite ($R^2= 0.01982893$) (**Fig. 3.11B**).

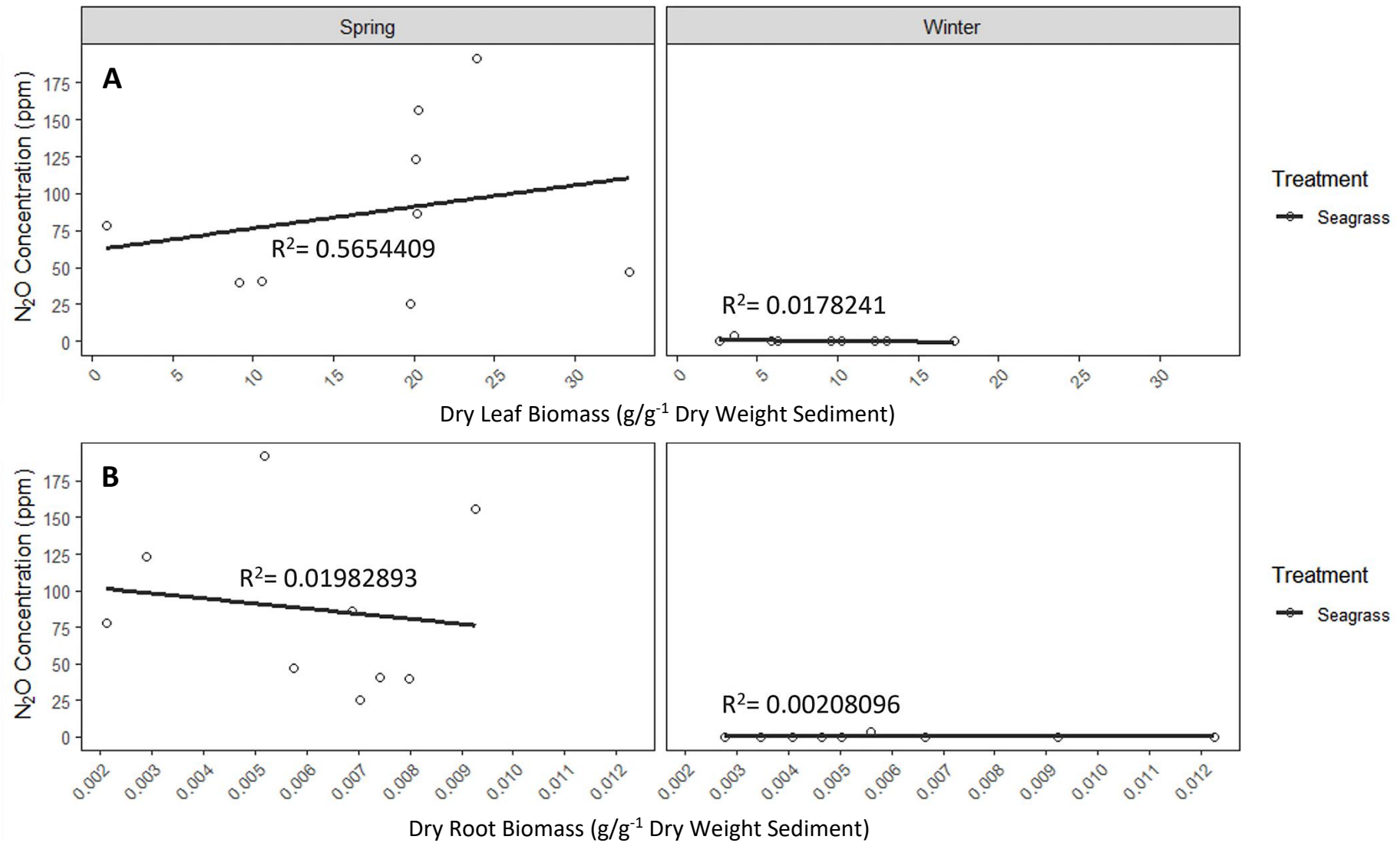


Fig 3.11. Mean N₂O gas flux data plotted with leaf (**A**) and root (**B**) biomass data collected in spring and winter.

Increased root biomass was significantly negatively associated with N₂O concentrations in spring (GLM: z-value= -4.299, p-value= <0.001), but significantly positively associated with N₂O concentrations in the winter (GLM: z-value= 27.842, p-value= <0.001). Increased leaf biomass had no significant association with N₂O concentration in spring (GLM: p-value > 0.1), but increased leaf biomass was significantly associated with increased N₂O concentration in winter (GLM: z-value= 3.820, p-value= <0.001). When both leaf biomass and root biomass increased, N₂O concentration was significantly increased in spring (GLM: z-value= 3.217, p-value= <0.01). However, increased leaf and root biomass was associated with significantly decreased N₂O concentration in winter (GLM: z-value= -7.883, p-value<0.001).

Simplified models were used to compare root and leaf biomass with nutrient concentrations, so only one-way associations were noted. It was determined that root biomass was significantly higher when nitrite levels were increased (GLM: z-value= 4.433, p-value= <0.001), but significantly lower when ammonia levels were high (GLM: z-value= -2.171, p-value= <0.05). However, leaf biomass significantly increased with higher ammonium levels (GLM: z-value= 3.352, p-value= <0.001) and significantly decreased with higher phosphate levels (GLM: z-value= -2.647, p-value= <0.01).

A simplified LME determined that high leaf biomass was associated with higher bacterial 16S rRNA gene copies (LME: DF= 3.085e+02, t-value 5.214, p-value= <0.001) but lower AOB *amoA* gene copies and archaeal 16S rRNA gene abundance (LME: AOB; DF= 2.921e+02, t-value= -2.999, p-value= <0.01; 16SArchaea; DF= 3.100e+02, t-value= -2.344, p-value= <0.05). High root biomass was associated with significantly lower bacterial 16S rRNA gene copies (LME: DF= 2.785e+02, t-value= -3.286, p-value= <0.01).

To compare archaeal/bacterial 16S rRNA gene abundance with nutrient concentration, a simplified LMER model was used. There was the same issue with not having enough power to run a negative binomial distribution due to the gene dataset size, however, site was still used as a random factor. Archaeal 16S gene abundance significantly increased when nitrate and ammonium concentrations were high (LME: Nitrate; DF= 4.151e+04, t-value= 3.531, p-value= <0.001; Ammonium; DF= 2.491e+04, t-value= 3.279, p-value= <0.01) but significantly decrease when phosphate was highly concentrated (LME: DF= 1.135e+04, t-value= -5.055, p-value= <0.001).

Bacterial 16S rRNA gene abundance increased when nitrite concentrations were high (LME: DF= 1.866e+07, t-value= 4.938, p-value= <0.001), but decreased when sulphate concentrations were increased (LME: DF= 6.711e+03, t-value= -5.465, p-value= <0.001). The only significant result regarding AOA *amoA* gene abundance and nutrient concentration was when nitrite levels increased, AOA *amoA* gene abundance significantly decreased (LME: DF= 128.060, t-value= -8.820, p-value= <0.01). AOB *amoA* gene abundance was significantly lower in high ammonium and nitrate concentrations (LME: Ammonium; DF= 4.047e+03, t-value= -2.658, p-value= <0.01; Nitrate; DF= 6.922e+03, t-value= -2.704, p-value= <0.01). However, when phosphate concentrations were increased, AOB *amoA* gene abundance was significantly higher (LME: DF= 1.867e+03, t-value= 4.453, p-value= <0.001). All other results were non-significant with a p-value > 0.1.

When nitrate and nitrite concentrations were increased, *nirS* gene abundance was significantly lower (LME: Nitrate; DF= 1.474e+05, t-value= -2.418, p-value= <0.05; Nitrite; DF= 2.396e+08, t-value= -5.567, p-value= <0.001), while *nirS* gene abundance was significantly higher when sulphate concentrations were increased

(LME: DF= 9.078e+06, t-value= 4.418, p-value= <0.001). There were no significant changes in *nirK* gene abundance with nutrient concentration. When ammonium concentration was higher, there was a significant increase in *nosZ* gene abundance (LME: Ammonium; DF= 1.079e+04, t-value= 1.988, p-value= <0.01; Sulphate; DF= 1.096+06, t-value= 2.994, p-value= <0.01). *nosZ* gene abundance was significantly decreased when nitrite concentrations were raised (LME: DF= 3.004e+07, t-value= -4.093, t-value= <0.001).

Chapter 4.0: Discussion

The recent interest in coastal vegetated habitats as greenhouse gas (GHG) sinks has led to an influx in carbon dioxide (CO₂) flux-based studies in these habitats. There has, however, been a noticeable lack of studies focused on nitrous oxide (N₂O) flux (especially in seagrass ecosystems), despite N₂O, being 298 times more potent than CO₂ (Gebremichael *et al.* 2022). There is also a lack of knowledge on the microbial communities associated with N transformation processes in seagrass environments. For example, if seagrasses like *Zostera noltei* produce enough N₂O to counteract the reduction in GHG emissions from the amount of CO₂ sunk, then this would still result in a higher GHG effect. For example, for every 1 mol of N₂O produced, ~ 300 mol of CO₂ would need to be removed for no net change in GHG emissions. If this is the case, promoting seagrasses as a nature-based solution to climate change would be detrimental in terms of the GHG effect. However, if seagrasses sink more N₂O than they produce, they could still contribute to a slowing down of climate change even if they do not sequester CO₂. It is therefore crucial to better understand N₂O flux in vegetated seagrass meadows.

In this study, the largest change in N₂O flux was not between vegetated/ non-vegetated state, but between seasons. In the winter, N₂O concentrations were negligible, which may be due to reduced microbial activity with lower winter temperatures compared to spring. Furthermore, there were statistically higher N₂O concentrations in the presence of seagrass, while higher removal rates of N₂O were observed in the non-vegetated sediments. However, both vegetated and non-vegetated sediments exhibited a net decrease in N₂O concentration over time.

In this study, bacteria were more predominant than archaea across sites. Similar findings were found in estuaries elsewhere. For example, Zhou *et al.* (2017) found bacterial 16S rRNA gene abundance were up to 5.0×10^{10} gene copies g⁻¹ dry weight and archaeal 16S rRNA gene abundances reached a maximum of 4.0×10^5 gene copies g⁻¹ dry weight. Seasonal changes were also observed, with lower abundances of archaea in the winter (primarily in the rhizosphere) increasing in abundance in the spring which may be linked to an increase in seagrass biomass in the spring and summer months, whereas bacterial 16S rRNA gene abundance was relatively stable throughout all seasons, though appear slightly lower in the spring. Previous studies have found that excessive nutrient concentrations, such as nitrogen and phosphorus, inhibit seagrass growth via the promotion of macroalgae growth leading to smothering, light reduction, and increased rates of biomass decomposition (Liu *et al.* 2023). This could potentially explain the lower bacterial 16S rRNA gene abundance in spring, though algal biomass was not measured in this study.

Specifically, archaeal communities were more abundant in oxic sediments compared to anoxic sediments, whilst the bacterial communities were more abundant in anoxic sediments. However, there was significantly lower archaeal 16S rRNA abundance in the rhizosphere compared to anoxic sediments. Whereas similar

bacterial 16S rRNA gene abundances were found in the rhizosphere, anoxic and oxic sediments. Zhou *et al.* (2017) also found bacterial communities were associated with deeper anoxic sediments while the archaeal communities were found in surface oxic sediments. Previous studies found that *Bathyarchaeota* were associated with anoxic sediments as opposed to rhizosphere or oxic sediments (Zou *et al.* 2020; Zhou *et al.* 2018). In this study, the archaeal community diversity was not analysed and so whether *Bathyarchaeota* were present in the anoxic sediments remains unknown.

Archaeal 16S rRNA gene abundance was also higher in anoxic sediment in the presence of seagrass compared to non-vegetated sediments, which may be linked to seagrass biomass, (or more specifically, biomass die-off) and an increase in organic matter input being utilised by archaea. Other studies also showed an increase in archaeal 16S rRNA gene abundance in vegetated sediments compared to non-vegetated sediments (Zheng *et al.* 2019). Seagrass leaf biomass was significantly lower in winter than the autumn, which supports the idea that biomass dieback is being utilised by the archaea. However, leaf biomass was also significantly lower in the spring than the autumn; it may not necessarily be seagrass dieback promoting archaeal 16S rRNA abundance, but instead, possible competition with the bacteria limiting the archaea. Therefore, rather than archaea being seagrass-dependent, bacteria could instead be linked with high seagrass biomass. Seagrass leaf and root biomass were significantly higher in the summer than in the autumn, which is when bacterial 16S rRNA abundance increases. Seagrass leaf biomass is also higher in the autumn than in the winter and in the spring; bacterial 16S rRNA gene abundance follows the same pattern. When leaf biomass was higher, so was bacterial 16S rRNA gene abundance. There is also evidence of a link between seagrass (*Posidonia oceanica*) meadow regression and a decline in bacterial community; this may also be

true in the case of *Zostera noltei*, as bacterial 16S rRNA gene abundance was significantly higher in the seagrass treatment than in the non-vegetated treatment (Garcia-Martinez *et al.* 2009).

In this study, there AOB were more predominant than AOA regardless of vegetation presence or season, suggesting that AOB were the likely drivers of ammonia oxidation in these ecosystems. Li *et al.* (2015) also found that AOB were the dominant ammonia-oxidisers in estuarine sediments. Other studies have found that the ratio of AOB:AOA is not dependent on habitat, but heavy metal (such as copper) and ammonium concentration, and therefore the dominating group varies (Urakawa *et al.* 2014). In contrast, in the Yellow River estuary AOA were more predominant than AOB in both sediment and water habitats (Li *et al.* 2018). However, there was significantly lower AOB *amoA* gene abundance when ammonium concentrations were high, which was surprising since many studies have found a high AOB abundance when ammonium concentrations were high (Urakawa *et al.* 2014; Rütting *et al.* 2021). There were also significantly higher ammonium concentrations in non-vegetated sediments in winter, which likely contributed to the observed increase in AOB *amoA* gene abundance in non-vegetated oxic sediments in winter. Anoxic micro-niches within the oxic sediment allowing N₂-fixation to occur and produce these increased ammonium concentrations (Underwood *et al.* 2022). A significant association between increased nitrite concentration (though this was still low in comparison to nitrate) and higher AOB *amoA* gene abundance could suggest a higher rate of ammonia oxidation than denitrification, though rate measurements would need to confirm this. Both AOB and AOA *amoA* gene abundances increased in the rhizosphere from winter to spring in the presence of seagrass which may be due to an influx of ammonium via run-off in the autumn and winter and resulted in elevated nitrate levels in the spring.

Every nutrient measured (nitrate, nitrite, phosphate, sulphate, ammonium) was present in significantly higher concentrations in the seagrass meadows compared to bare sediment, which may be due to higher nutrient trapping by the vegetation in these habitats. Isotope studies could be applied to confirm this, but if *Zostera noltei* can be linked to the trapping of eutrophication nutrients (N and phosphorous (P) in particular, but also sulphur (S)), it could be utilised in reducing nutrient run-off and subsequent nutrient stress within British estuaries (Nedwell *et al.* 2016). The seasonal changes in nitrite, nitrate, and ammonium could also suggest that these nutrients are likely being oxidised and reduced at the same rates and coupled nitrification: denitrification is occurring within the estuary, but there is likely a seasonal change in their relative proportions. However, one limitation of this study was that nitrification and denitrification process rates were not measured and so the relative contributions of nitrification and denitrification processes within the estuary remains unknown.

In this study, there was around 10-fold fewer copies of *nirK* observed across all sites than *nirS*. Similar results have been found previously in Laizhou Bay which is highly nutrified estuary due to agricultural run-off, comparable to estuaries in the east of the UK (Zhang *et al.* 2014; Nedwell *et al.* 2002). This could either be due to *nirS*-containing communities being less responsive to environmental factors compared to *nirK*-containing communities (Li *et al.* 2017). This could also be due to the proportion of organisms with one, the other, or both *nirS* and *nirK* genes present within their genome (Wittorf *et al.* 2018). Seasonally, *nirS* was significantly higher in oxic sediment within the seagrass treatment in spring, summer, and winter, than in anoxic sediment in the non-vegetated treatment in the autumn. Other studies have found no link between *nirS* gene abundance and season (Zheng *et al.* 2015); therefore, these differences are more likely linked to the association of lower *nirS* gene abundance with

increased depth (where the sediment is more anoxic) (Marshall *et al.* 2023). The main results were that *nirK* and *nirS* gene abundances were clearly highly influenced by each other, which was also found to be the case in San Francisco Bay (Lee and Francis, 2017).

Some studies have found *nosZ* gene abundance to be significantly associated with seagrass presence, such as He *et al.* (2024) and Nakagawa *et al.* (2019). These findings have also been reflected in this study with significantly higher *nosZ* gene abundance in the rhizosphere in spring. When either *nirK* or *nirS* gene abundance increased, *nosZ* gene abundance also significantly increased, suggesting that complete denitrification may be occurring and the nitrite was being reduced to nitric and nitrous oxide, and then to N₂. However, many studies found the opposite to be true (e.g. Zhang *et al.* 2014; Ming *et al.* 2021). The higher abundance of *nosZ* in oxic sediments autumn was surprising; and it may be due to the presence of anoxic micro-niches allowing these organisms to thrive within the larger oxic environment (Underwood *et al.* 2022).

Interestingly the abundance of *nosZ* and *nirS* was similar across season, sediment type, and vegetated state. However, *nosZ* gene abundance was found to be significantly lower than *nirS* and *nirK* gene abundance combined; this could potentially lead to higher rates of N₂O production compared to N₂O sunk, though this cannot be said for certain as gene abundance does not equate to gene activity. However, *nirS* gene abundance was several orders of magnitude lower than *nosZ* gene abundance; rate measurements would need to be taken to confirm whether this has an impact on N₂O production. There was not a large seasonal change in *nirK*, *nirS* or *nosZ* gene abundance, though there were significantly higher abundances of *nosZ*, in spring. This has been found elsewhere, as the denitrifiers are known to be more tolerant of

changes in temperature, light, and pH (Saleh-Lakha *et al.* 2009). The increased activity in spring could be due to spikes in nitrate and nitrite concentrations due to increased abundance of ammonia-oxidisers (which are sensitive to temperature, light, and pH changes) activity in the warmer weather (Scarlett *et al.*, 2021).

What is interesting is the observed relationship between N₂O production and denitrifier gene abundance (i.e. *nirS*, *nirK*, and *nosZ* gene). Although there was no significant net increase or decrease in N₂O concentration when *nosZ* or *nirK* gene abundance increased, there was a significant increase in N₂O concentration when *nirS* gene abundance increased. This suggests that *nirS*-containing communities are likely the dominant N₂O producers, but the *nosZ*-containing communities are not reducing N₂O at the same rate as it is being produced; rate experiments would be necessary to confirm this.

Another important factor to note is that higher root biomass is associated with lower N₂O concentration, possibly due to increased root surface area for N₂-fixation associated with the rhizosphere, while higher leaf biomass is associated with a higher N₂O concentration, which may be due to a preference of N uptake in the form of ammonium as opposed to nitrate (Welsh, 2000; Nayar *et al.* 2018) In non-vegetated habitats, the production of N₂O is much slower than that in vegetated habitats; there is a much slower increase in N₂O production despite an increase in *nirK* and *nirS* gene abundance in these areas, (although not surprisingly a decrease in N₂O concentration was associated with higher *nosZ* gene abundance). In the presence of seagrass, N₂O levels increased, suggesting that in seagrass habitats, complete denitrification to N₂ may not be occurring. There is also a higher mean abundance, (though not statistically significant), of *nirS* and *nirK* genes in vegetated habitats compared to non-vegetated habitats in spring, suggesting an increase in nitrite-reducing communities contributing

factor to the higher levels of N₂O in the vegetated treatment. Nitrite concentrations being significantly lower in spring support the theory of higher rates of denitrification, as it could be getting reduced to N₂O as soon as it becomes available. This could also be a contributing factor to the lower rates of N₂O sinking observed in the seagrass meadow than the adjacent bare mud.

In summary, these estuarine habitats are very understudied, especially in terms of the microbes driving the N-cycle processes. Depending on season, sediment, and vegetation cover (specifically seagrass), the microbial gene abundances changed. For example, archaeal 16S rRNA gene copies increased in anoxic sediment and in the seagrass treatment, while bacterial 16S rRNA gene copies were higher in the presence of seagrass but lower in anoxic sediments. The functional genes such as AOB and AOA *amoA*, *nirS*, *nirK* and *nosZ* had more complex relationships with the environmental parameters. Though the rate of N₂O sink in the presence of seagrass was lower than in the non-vegetated sediment due to an overall higher abundance of denitrifiers, the important factor to note is that the net N₂O concentration decreased temporally. Not only is there evidence that seagrasses sink CO₂, but there is also now supporting evidence that they may sink the far more potent GHG, N₂O. Therefore, the protection of seagrasses (such as *Z. noltei*) is likely a worthwhile investment for the future of our planet in terms of slowing climate change. Not only would the protection of *Z. noltei* be beneficial to reduce GHG emissions, but the evidence is also now there to suggest that *Z. noltei* traps more eutrophication nutrients (N, P, S) than bare mudflats; *Z. noltei* could potentially be a nature-based solution to reduce estuarine pollution and subsequent eutrophication.

5.0: Future Work

This study provided important information on microbial gene abundances in relation to nutrient concentrations and N₂O flux. However, microbial biodiversity and process rates were not measured herein and more research in this area is required in order to better assess whether these habitats should be restored; for example, rate experiments partnered with qPCR can broach the gap of activity versus abundance that was not measured in this study. There are also issues such as incomplete denitrification that could not be directly measured, as well as other processes (e.g. comammox, DNRA etc.) that were not measured. Moreover, more research is necessary to analyse other seagrass sites as well as over further seasonal cycles. However, due to time constraints this was not possible herein. To determine whether nutrients came from elsewhere or were produced by the seagrass, isotope experiments could also be carried out, along with biodiversity assessments to better determine the cost-benefits of seagrass restoration. Though these experiments have not yet been carried out, what we now know about *Zostera noltei*, its role in N₂O flux, and its potential as a nutrient trap is incredibly promising.

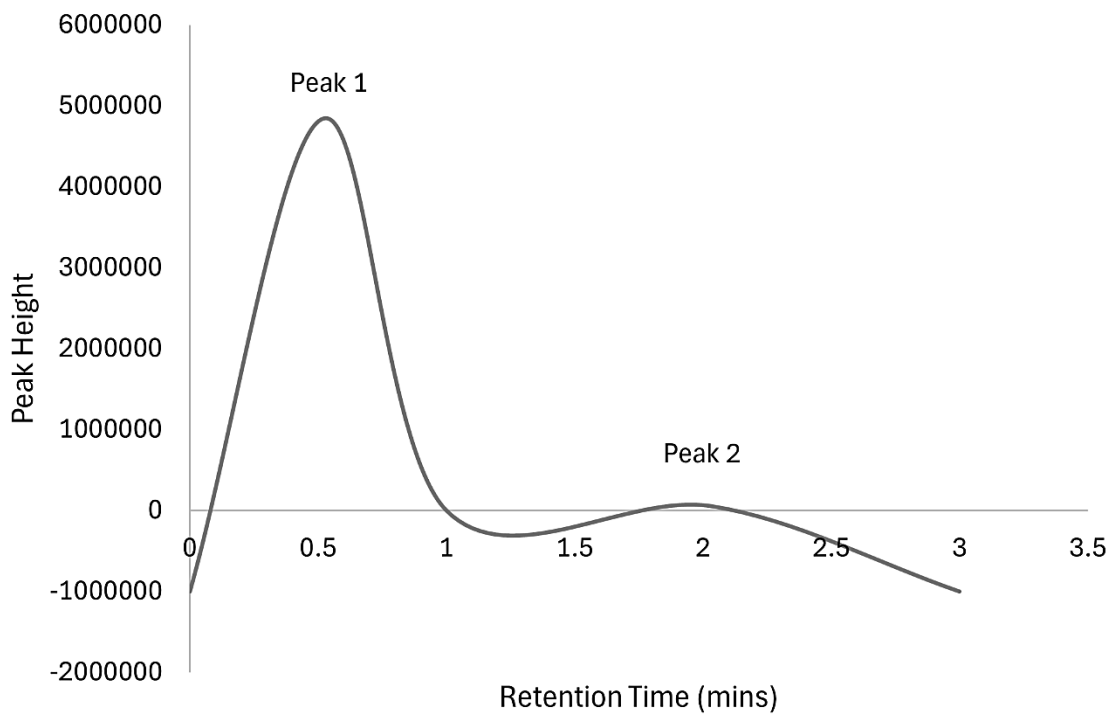
6.0: Appendix

Figure A1. Standard curve showing how the N_2 (peak 1) and N_2O (peak 2) peaks using 1000ppm N_2O synthetic air.

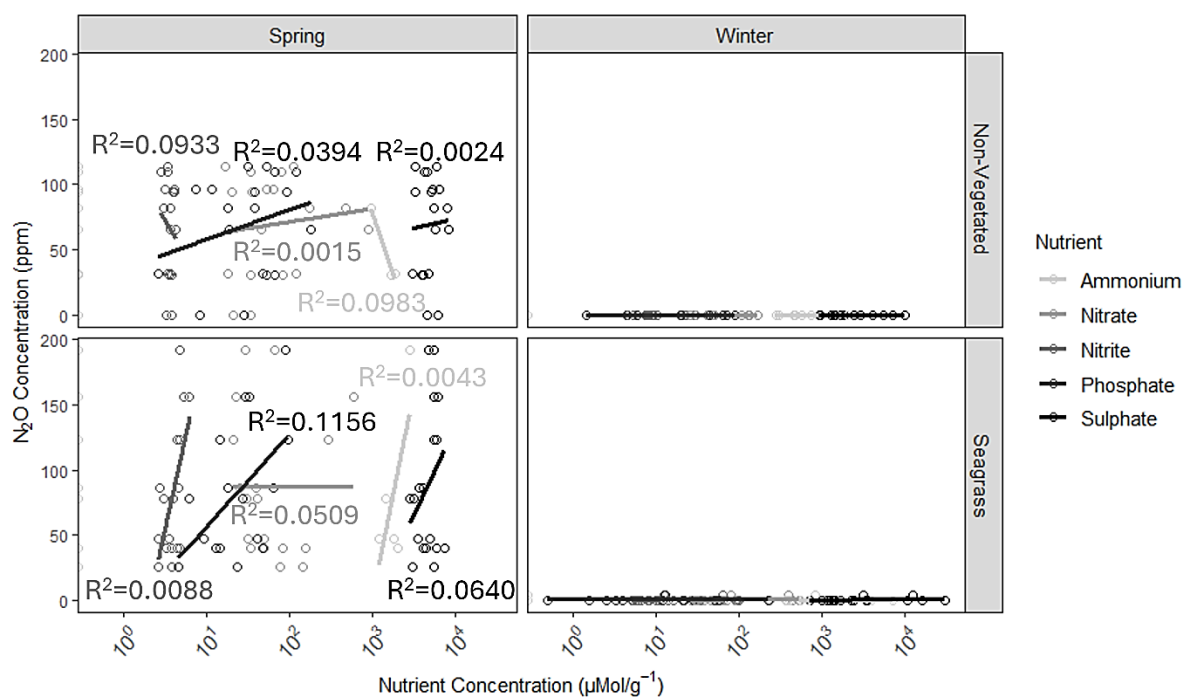


Figure A2. All nutrient concentrations in comparison with N_2O concentration on one plot.

Table A1. qPCR data analysis standard curve details.

Gene target	% Efficiency	R^2	Slope	y-intercept
Bacterial 16S rRNA gene	98.39	0.996	-3.361	38.337
Archaeal 16S rRNA gene	101.98	0.989	-3.275	32.444
Archaeal <i>amoA</i>	81.84	0.993	-3.851	37.950
Bacterial <i>amoA</i>	83.66	0.981	-3.788	36.567
<i>nirK</i>	93.69	0.986	-3.483	33.920
<i>nirS</i>	84.29	0.990	-3.767	38.888
<i>nosZ</i>	84.78	0.986	-3.750	40.637

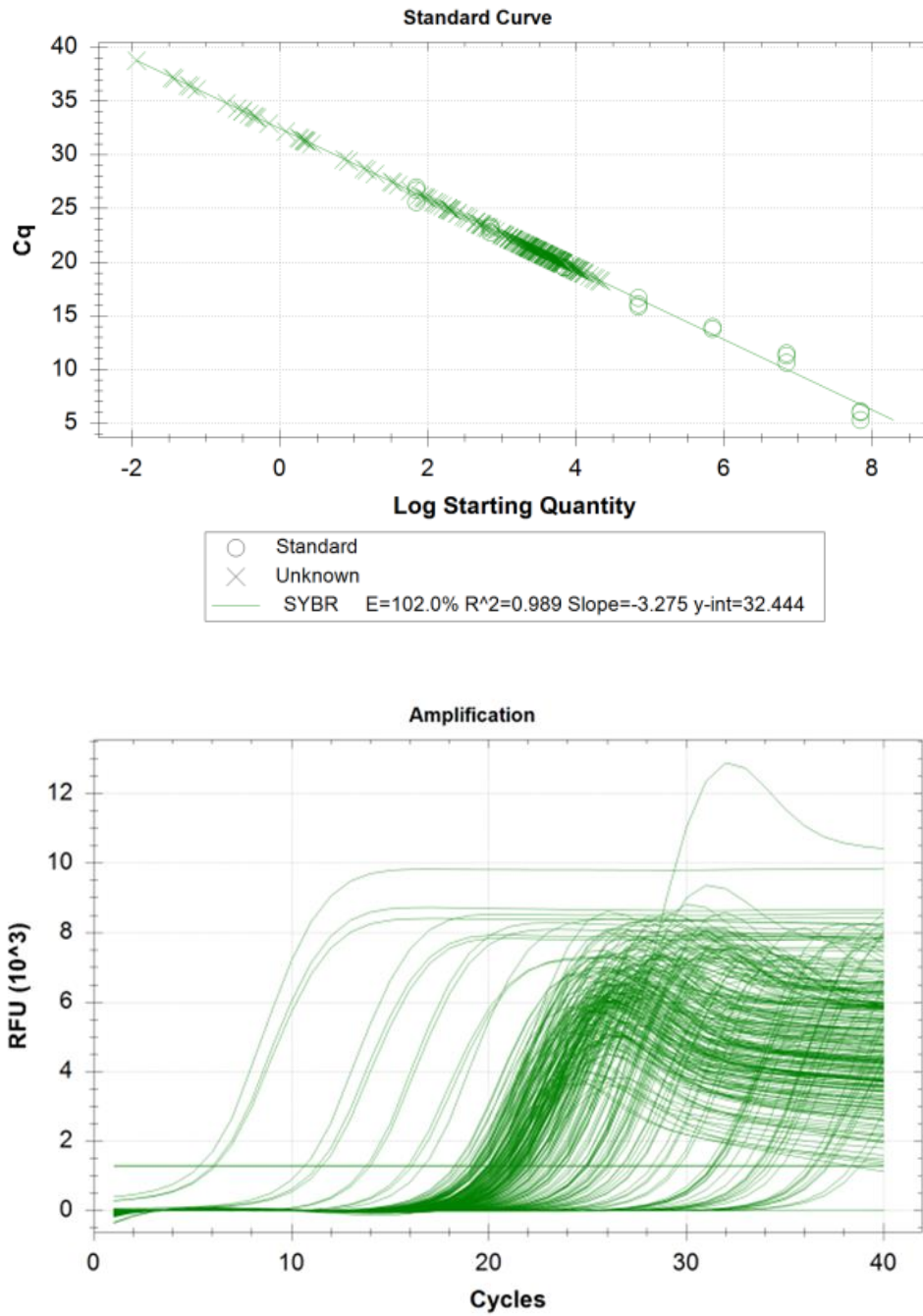


Figure A3. Standard curve and amplification curve from the BioRad qPCR files for Archaeal 16S rRNA gene.

Table A2. Primers used in this study for qPCR analysis.

Gene target	Primer name	Primer sequence	Primer length	Product size (bp)	Gene copy number	Process	Primer reference
Bacterial 16S rRNA gene	341F/ 805R	CCTACGGGNGGCWGCAG/ GACTACHVGGGTATCTAATCC	17/ 21	464	1-21	N/A*	Klindworth <i>et al.</i> 2013
Archaeal 16S rRNA gene	344f / 915r	ACGGGGYGCAGCAGGCGCGA/ GTGCTCCCCCGCCAATTCCT	20/ 20	571	1-5	N/A*	Lane <i>et al.</i> 1985
Archaeal <i>amoA</i>	CrenamoA- 23F/ CrenamoA- 616R	ATGGTCTGGCTWAGACG/ GCCATCCATCTGTATGTCCA	17/ 20	593	1	Ammonia oxidation	Tourna <i>et al.</i> 2008
Bacterial <i>amoA</i>	amoA-1F/ amoA-2R	GGGGTTTCTACTGGTGGT/ CCCCTCKGSAAAGCCTTCTTC	18/ 21	491	1-10	Ammonia oxidation	Rotthauwe <i>et al.</i> 1997
<i>nirS</i> (<i>nirS</i> F, <i>nirS</i> R)	<i>nirS</i> - Cd3aF/ <i>nirS</i> -R3cd	AACGYSAAGGARACSGG/ GASTTCGGRTGSGTCTTSAYGAA	17/ 23	425	1-2	Nitrite reduction	Throbäck <i>et al.</i> 2004
<i>nirK</i> (<i>nirK</i> F, <i>nirK</i> R)	<i>nirK</i> -1F/ <i>nirK</i> 5R	GGMATGGTKCCSTGGCA/ GCCTCGATCAGRTRRTGG	17/ 18	514	1	Nitrite reduction	Braker <i>et al.</i> 1998
<i>nosZ</i> (<i>nosZ</i> 267)	<i>nosZ</i> 2F/ <i>nosZ</i> 2R	CGCRACGGCAASAAGGTSMSSGT/ CAKRTGCAKSGCRTGGCAGAA	23/ 21	267	1-2	Nitrous oxide reduction	Henry <i>et al.</i> 2006

*Taxonomic gene

Table A3. Mean Archaeal 16S rRNA gene copies per site.

Site	Treatment	Sediment	Season	16S Archaea
CPB	Seagrass	Oxic	Autumn	503879.7512
		Anoxic		403875.1756
		Rhizosphere		200017.9886
	Non-Vegetated	Oxic		2110516.595
		Anoxic		1447657.127
NS	Seagrass	Oxic	822201.1214	
		Anoxic	1887404.553	
		Rhizosphere	765253.3431	
	Non-Vegetated	Oxic	1562597.274	
		Anoxic	1425446.952	
LOS	Seagrass	Oxic	2072060.428	
		Anoxic	7793264.196	
		Rhizosphere	254878.7232	
	Non-Vegetated	Oxic	2329104.876	
		Anoxic	5561814.141	
CPB	Seagrass	Oxic	Winter	1861095.895
		Anoxic		1323582.831
		Rhizosphere		3849093.703
	Non-Vegetated	Oxic		297945.4831
		Anoxic		788330.0637
NS	Seagrass	Oxic	1404612.927	
		Anoxic	3016127.045	
		Rhizosphere	662399.8301	
	Non-Vegetated	Oxic	1864268.885	
		Anoxic	3439545.501	
LOS	Seagrass	Oxic	1622903.823	
		Anoxic	4625678.345	
		Rhizosphere	1398205.765	
	Non-Vegetated	Oxic	1435687.92	
		Anoxic	4497673.341	
CPB	Seagrass	Oxic	Spring	1192315.624
		Anoxic		1151479.51
		Rhizosphere		1774546.074
	Non-Vegetated	Oxic		1613416.246
		Anoxic		2734567.743
NS	Seagrass	Oxic	758284.7654	
		Anoxic	3084932.672	
		Rhizosphere	6440607.707	
	Non-Vegetated	Oxic	1058064.679	
		Anoxic	1702811.548	
LOS	Seagrass	Oxic	1662873.396	
		Anoxic	3570703.294	
		Rhizosphere	3354725.532	

	Non-Vegetated	Oxic	Summer '23	1464047.362
		Anoxic		1595980.503
CPB	Seagrass	Oxic		949843.6959
		Anoxic		368102.7323
	Non-Vegetated	Oxic		1145917.641
		Anoxic		1443768.044
NS	Seagrass	Oxic		1626861.942
		Anoxic		3176095.065
	Non-Vegetated	Oxic	3027961.613	
		Anoxic	3842736.505	

Table A4. Mean Bacterial 16S rRNA gene copies per site.

Site	Treatment	Sediment	Season	Bac.copies
CPB	Seagrass	Oxic	Autumn	14583874573
		Anoxic		9565999154
		Rhizosphere		4987620811
	Non-Vegetated	Oxic		10251942959
		Anoxic		6180753862
NS	Seagrass	Oxic	48175177429	
		Anoxic	30401414798	
		Rhizosphere	56111585244	
	Non-Vegetated	Oxic	20908404716	
		Anoxic	2359159040	
LOS	Seagrass	Oxic	19356874877	
		Anoxic	13838855589	
		Rhizosphere	398164103.7	
	Non-Vegetated	Oxic	20066257828	
		Anoxic	14036787037	
CPB	Seagrass	Oxic	Winter	16686547041
		Anoxic		3027038747
		Rhizosphere		15115228105
	Non-Vegetated	Oxic		534038460.5
		Anoxic		384300079.5
NS	Seagrass	Oxic	15895550201	
		Anoxic	9150287644	
		Rhizosphere	2564734752	
	Non-Vegetated	Oxic	18283578522	
		Anoxic	10726446655	
LOS	Seagrass	Oxic	22154260327	
		Anoxic	18700689265	
		Rhizosphere	4580681905	
	Non-Vegetated	Oxic	16465783768	
		Anoxic	14524526129	
CPB	Seagrass	Oxic	Spring	33790.47474
		Anoxic		13471.10288

	Non-Vegetated	Rhizosphere		511.6731132
		Oxic		24458.52314
		Anoxic		1410.512023
NS	Seagrass	Oxic		46158.2645
		Anoxic		32901.90512
		Rhizosphere		1083.97702
	Non-Vegetated	Oxic		46650.26281
		Anoxic		9827.624914
LOS	Seagrass	Oxic		33128.83042
		Anoxic		29882.22122
		Rhizosphere		10537.04783
	Non-Vegetated	Oxic	28699.87039	
		Anoxic	22735.28389	
CPB	Seagrass	Oxic	Summer '23	12324042331
		Anoxic		1331017435
	Non-Vegetated	Oxic		4649400443
		Anoxic		2703830716
NS	Seagrass	Oxic		34015687244
		Anoxic		11879696014
	Non-Vegetated	Oxic		35858191021
		Anoxic		8940142174

Table A5. Mean Archaeal *amoA* gene copies per site.

Site	Treatment	Sediment	Season	Archaeal <i>amoA</i>
CPB	Seagrass	Oxic	Autumn	54019.9401
		Anoxic		7097.308446
		Rhizosphere		12986.69968
	Non-Vegetated	Oxic		120663.1377
		Anoxic		130616.1155
NS	Seagrass	Oxic	306518.8804	
		Anoxic	64264.95195	
		Rhizosphere	41855.7913	
	Non-Vegetated	Oxic	531880.4239	
		Anoxic	14211.47576	
LOS	Seagrass	Oxic	198928.7094	
		Anoxic	207297.6158	
		Rhizosphere	8718.585623	
	Non-Vegetated	Oxic	131452.9733	
		Anoxic	150397.4469	
CPB	Seagrass	Oxic	Winter	136764.2249
		Anoxic		44637.51679
		Rhizosphere		645100.19
	Non-Vegetated	Oxic		22390.5263
		Anoxic		30154.51467
NS	Seagrass	Oxic		311981.7381

LOS	Non-Vegetated	Anoxic	Spring	51911.80927	
		Rhizosphere		24141.02684	
		Oxic		361451.8439	
	Seagrass	Anoxic		49140.16106	
		Oxic		212106.4584	
		Anoxic		183841.6131	
Non-Vegetated	Rhizosphere	34612.50424			
	Oxic	525009.4164			
	Anoxic	214308.204			
CPB	Seagrass	Oxic	Summer '23	184561.7425	
		Anoxic		59905.78898	
		Rhizosphere		370726.5843	
	Non-Vegetated	Oxic		147693.2863	
		Anoxic		362439.0789	
		Oxic		313374.4967	
NS	Seagrass	Anoxic	175723.6988		
		Rhizosphere	1464763.94		
		Oxic	461272.254		
	Non-Vegetated	Anoxic	130940.6409		
		Oxic	344306.8623		
		Anoxic	238241.9784		
LOS	Seagrass	Rhizosphere	369688.8309		
		Oxic	352098.3162		
		Anoxic	312051.2776		
	CPB	Seagrass	Oxic	Summer '23	55218.83552
			Anoxic		33039.14289
			Oxic		61834.55807
Non-Vegetated		Anoxic	148469.2033		
		Oxic	277811.0726		
		Anoxic	142000.9655		
NS	Seagrass	Oxic	115855.9588		
		Anoxic	183270.5437		
	Non-Vegetated	Oxic			
		Anoxic			

Table A6. Mean Bacterial *amoA* gene copies per site.

Site	Treatment	Sediment	Season	Bacterial <i>amoA</i>
CPB	Seagrass	Oxic	Autumn	94686.18657
		Anoxic		21798.26312
		Rhizosphere		21933.95456
	Non-Vegetated	Oxic		416304.0022
		Anoxic		614902.0448
		Oxic		219862.5264
NS	Seagrass	Anoxic	262588.3694	
		Rhizosphere	100533.1046	
		Oxic	656814.4877	
	Non-Vegetated	Anoxic	120955.6592	
		Oxic		
		Anoxic		

LOS	Seagrass	Oxic	Winter	1056065.993
		Anoxic		597884.4823
		Rhizosphere		45817.42915
	Non-Vegetated	Oxic		1137354.162
		Anoxic		796243.5693
CPB	Seagrass	Oxic		472182.773
		Anoxic		42157.77187
		Rhizosphere		128914.8406
	Non-Vegetated	Oxic		59542.16696
		Anoxic		70985.45281
NS	Seagrass	Oxic		705649.5806
		Anoxic		316514.2644
		Rhizosphere		222041.7755
	Non-Vegetated	Oxic		651907.4467
		Anoxic		109802.0744
LOS	Seagrass	Oxic	720710.5638	
		Anoxic	537215.5019	
		Rhizosphere	223102.1932	
	Non-Vegetated	Oxic	4968131.147	
		Anoxic	1219345.971	
CPB	Seagrass	Oxic	442356.4736	
		Anoxic	177436.5648	
		Rhizosphere	882786.1887	
	Non-Vegetated	Oxic	396197.2076	
		Anoxic	438083.9968	
NS	Seagrass	Oxic	784542.0528	
		Anoxic	1242933.268	
		Rhizosphere	2996346.633	
	Non-Vegetated	Oxic	1132428.625	
		Anoxic	588791.4744	
LOS	Seagrass	Oxic	787989.5871	
		Anoxic	595260.9248	
		Rhizosphere	906467.5647	
	Non-Vegetated	Oxic	1157636.708	
		Anoxic	1473157.642	
CPB	Seagrass	Oxic	62320.93414	
		Anoxic	41345.12077	
	Non-Vegetated	Oxic	116265.5961	
		Anoxic	269639.8447	
NS	Seagrass	Oxic	299070.6541	
		Anoxic	700435.8367	
	Non-Vegetated	Oxic	95129.29796	
		Anoxic	548436.1998	

Table A7. Mean *nirK* gene copies per site.

Site	Treatment	Sediment	Season	<i>nirK</i>
CPB	Seagrass	Oxic	Autumn	56219.0114
		Anoxic		29738.17549
		Rhizosphere		42677.02279
	Non-Vegetated	Oxic		146813.3753
		Anoxic		65589.9862
NS	Seagrass	Oxic	140423.0703	
		Anoxic	144465.3664	
		Rhizosphere	185668.9219	
	Non-Vegetated	Oxic	147718.5915	
		Anoxic	43646.56462	
LOS	Seagrass	Oxic	148628.4463	
		Anoxic	186122.8626	
		Rhizosphere	66383.30438	
	Non-Vegetated	Oxic	178564.049	
		Anoxic	153086.141	
CPB	Seagrass	Oxic	Winter	68789.27116
		Anoxic		43524.36885
		Rhizosphere		153242.6872
	Non-Vegetated	Oxic		13907.2169
		Anoxic		13538.61546
NS	Seagrass	Oxic	118039.9435	
		Anoxic	123707.7442	
		Rhizosphere	58273.02162	
	Non-Vegetated	Oxic	176673.3907	
		Anoxic	108598.8033	
LOS	Seagrass	Oxic	441778.6995	
		Anoxic	290255.8725	
		Rhizosphere	129390.7877	
	Non-Vegetated	Oxic	121609.5159	
		Anoxic	243476.0064	
CPB	Seagrass	Oxic	Spring	211623.9541
		Anoxic		51994.17253
		Rhizosphere		120767.841
	Non-Vegetated	Oxic		166647.9355
		Anoxic		38622.36573
NS	Seagrass	Oxic	135320.1558	
		Anoxic	148593.6257	
		Rhizosphere	849566.5999	
	Non-Vegetated	Oxic	268037.7399	
		Anoxic	94141.7294	
LOS	Seagrass	Oxic	136776.7951	
		Anoxic	338540.2572	
		Rhizosphere	511004.2309	
	Non-Vegetated	Oxic	170480.7404	
		Anoxic	172812.5815	

CPB	Seagrass	Oxic	Summer '23	112387.3707
		Anoxic		27526.59929
	Non-Vegetated	Oxic		142506.6573
		Anoxic		62836.75367
NS	Seagrass	Oxic		466264.4096
		Anoxic		111413.4148
	Non-Vegetated	Oxic		147029.726
		Anoxic		33932.26256

Table A8. Mean *nirS* gene copies per site.

Site	Treatment	Sediment	Season	<i>nirS</i>	
CPB	Seagrass	Oxic	Autumn	8015136.824	
		Anoxic		3023815.699	
		Rhizosphere		1649460.04	
	Non-Vegetated	Oxic		22997814.28	
		Anoxic		11500982.01	
		Rhizosphere		42570189.61	
NS	Seagrass	Oxic	Autumn	46326814.11	
		Anoxic		8454271.71	
		Rhizosphere		47321074.29	
	Non-Vegetated	Oxic		11704369.8	
		Anoxic		49899865.26	
		Rhizosphere		37295818.1	
LOS	Seagrass	Oxic	Autumn	2002941.121	
		Anoxic		27504140.6	
		Rhizosphere		31861860.07	
	Non-Vegetated	Oxic		Winter	22917251.43
		Anoxic			2339443.601
		Rhizosphere			19389377.84
CPB	Seagrass	Oxic	Winter		1743184.264
		Anoxic			714340.3233
		Rhizosphere			33416983.84
	Non-Vegetated	Oxic		Winter	17246656.72
		Anoxic			8126626.365
		Rhizosphere			47981359.53
NS	Seagrass	Oxic	Winter		12017618.85
		Anoxic			34598941.92
		Rhizosphere			49875165.15
	Non-Vegetated	Oxic		Winter	13009144.66
		Anoxic			31129744.13
		Rhizosphere			26396963.87
LOS	Seagrass	Oxic	Spring		32854338.16
		Anoxic			13955431.37
		Rhizosphere			11829607.24
	Non-Vegetated	Oxic		Spring	28442027.89
		Anoxic			
		Rhizosphere			

		Anoxic		3519620.032
NS	Seagrass	Oxic		67654457.11
		Anoxic		47137839.42
		Rhizosphere		127457092.6
	Non-Vegetated	Oxic		78755169.88
		Anoxic		23001246.64
LOS	Seagrass	Oxic		60336342.49
		Anoxic		57999615.98
		Rhizosphere		69809310.28
	Non-Vegetated	Oxic		55645291.63
		Anoxic		49413510.95
CPB	Seagrass	Oxic	Summer '23	15405573.37
		Anoxic		3207954.835
	Non-Vegetated	Oxic		13023855.42
		Anoxic		7441778.093
	NS	Seagrass		Oxic
Anoxic			27329323	
Non-Vegetated		Oxic	24218947.15	
		Anoxic	16110345.27	

Table A9. Mean *nosZ* gene copies per site.

Site	Treatment	Sediment	Season	<i>nosZ</i>
CPB	Seagrass	Oxic	Autumn	22680695.79
		Anoxic		4484678.685
		Rhizosphere		2604084.142
	Non-Vegetated	Oxic		31782546.92
		Anoxic		10373022.47
NS	Seagrass	Oxic	113413239.8	
		Anoxic	18577923.76	
		Rhizosphere	13998562.96	
	Non-Vegetated	Oxic	72403474.77	
		Anoxic	11507567.36	
LOS	Seagrass	Oxic	45206196.11	
		Anoxic	23352730.09	
		Rhizosphere	681559.992	
	Non-Vegetated	Oxic	34432074.89	
		Anoxic	21978656.24	
CPB	Seagrass	Oxic	Winter	32010088.8
		Anoxic		2208034.638
		Rhizosphere		14219414.97
	Non-Vegetated	Oxic		2077364.434
		Anoxic		5010.479794
NS	Seagrass	Oxic	38794689.59	
		Anoxic	18561704.03	
		Rhizosphere	6131554.01	

	Non-Vegetated	Oxic	Spring	53298861.78
		Anoxic		12718679.1
LOS	Seagrass	Oxic		36013686.51
		Anoxic		33666795.75
		Rhizosphere		2552588.427
	Non-Vegetated	Oxic		9233254.05
		Anoxic		21595479.3
CPB	Seagrass	Oxic		46170083.22
		Anoxic		5215703.454
		Rhizosphere		8820817.832
	Non-Vegetated	Oxic	40541155.3	
		Anoxic	2087379.274	
NS	Seagrass	Oxic	118949164.2	
		Anoxic	36634738.01	
		Rhizosphere	83698505.62	
	Non-Vegetated	Oxic	154176273.1	
		Anoxic	17841315.49	
LOS	Seagrass	Oxic	55142289.78	
		Anoxic	27823156.14	
		Rhizosphere	58152072.39	
	Non-Vegetated	Oxic	27271529.57	
		Anoxic	35274128.36	

CPB	Seagrass	Oxic	Summer '23	37865225.36
		Anoxic		5470305.026
	Non-Vegetated	Oxic		32498762.38
		Anoxic		12624580.41
NS	Seagrass	Oxic		114209315
		Anoxic		25857316.95
	Non-Vegetated	Oxic		56548890.09
		Anoxic		13062079.56



Figure A4. Example of collar set up in bare sediment prior to attaching the gas chamber.



Figure A5. Example of a full sampling set up- this exact set up (using a Li-Cor) was used for sampling CO_2 . When sampling N_2O , rather than tubes coming from the top of the chamber, the entrances were sealed with silica.



Figure A6. Example of *Zostera noltei* (and *Zostera marina*) at low tide.

NS- SG2 OX Win	5.16	0.869	4.073	100.319	1.73	99.966
NS- SG2 AN Win	n.a.	n.a.	n.a.	n.a.	n.a.	99.966
NS - SG3 OX Aut	5.127	1.328	6.133	153.68	2.35	99.966
NS - SG3 AN Aut	5.133	0.651	3.041	74.94	2	99.966
NS - SG3 OX Win	5.167	0.756	3.935	87.155	1.17	99.966
NS - SG3 AN Win	n.a.	n.a.	n.a.	n.a.	n.a.	99.966
NS - UV1 OX Aut	5.163	0.949	4.371	109.63	1.9	99.966
NS - UV1 AN Aut	n.a.	n.a.	n.a.	n.a.	n.a.	99.966
NS - UV1 OX Win	5.13	1.386	6.475	160.404	2.32	99.966
NS - UV1 AN Win	5.14	0.548	2.718	63.032	1.37	99.966
NS - UV2 OX Aut	5.203	0.987	5.492	114.067	0.98	99.966
NS - UV2 AN Aut	5.157	0.673	3.56	77.472	1.09	99.966
NS - UV2 OX Win	5.163	0.691	3.63	79.569	1.07	99.966
NS - UV2 AN Win	n.a.	n.a.	n.a.	n.a.	n.a.	99.966
NS - UV3 OX Aut	5.177	1.011	4.821	116.813	1.49	99.966
NS - UV3 AN Aut	n.a.	n.a.	n.a.	n.a.	n.a.	99.966
NS - UV3 OX Win	5.16	0.889	4.225	102.593	1.55	99.966
NS - UV3 AN Win	5.12	0.729	3.37	84.027	1.59	99.966
LOS- SG1 OX Aut	5.137	0.611	3.433	70.324	0.95	99.966
LOS- SG1 AN Aut	5.16	1.04	5.259	120.214	1.27	99.966
LOS- SG1 OX Win	5.123	0.64	3.04	73.664	1.31	99.966
LOS- SG1 AN Win	5.133	0.599	3.174	68.94	1.08	99.966
LOS- SG2 OX Aut	5.123	0.652	3.084	75.13	1.55	99.966
LOS- SG2 AN Aut	n.a.	n.a.	n.a.	n.a.	n.a.	99.966
LOS- SG2 OX Win	5.14	0.646	3.299	74.349	1.12	99.966
LOS- SG2 AN Win	n.a.	n.a.	n.a.	n.a.	n.a.	99.966
LOS- SG3 OX Aut	5.143	0.584	3.198	67.192	1	99.966
LOS- SG3 AN Aut	5.14	0.596	3.08	68.549	1.15	99.966
LOS- SG3 OX Win	5.133	0.626	3.131	72.108	1.22	99.966
LOS- SG3 AN Win	5.13	0.505	2.731	57.987	1.03	99.966
LOS- UV1 OX Aut	5.137	0.574	3.029	65.96	1.04	99.966
LOS- UV1 AN Aut	n.a.	n.a.	n.a.	n.a.	n.a.	99.966
LOS- UV1 OX Win	5.12	0.473	2.337	54.287	1.18	99.966
LOS- UV1 AN Win	5.12	0.472	2.348	54.129	1.2	99.966
LOS- UV2 OX Aut	5.13	0.637	3.079	73.332	1.35	99.966
LOS- UV2 AN Aut	5.137	0.634	3.128	72.986	1.26	99.966
LOS- UV2 OX Win	5.127	0.505	2.504	58.001	1.14	99.966
LOS- UV2 AN Win	5.127	0.499	2.528	57.301	1.13	99.966
LOS- UV3 OX Aut	5.147	0.613	3.204	70.561	1.05	99.966
LOS- UV3 AN Aut	5.13	0.471	2.461	53.998	1	99.966
LOS- UV3 OX Win	n.a.	n.a.	n.a.	n.a.	n.a.	99.966
LOS- UV3 AN Win	n.a.	n.a.	n.a.	n.a.	n.a.	99.966
CPB - SG1 OX Spr	5.15	0.542	2.795	77.075	1.57	99.985
CPB - SG1 AN Spr	n.a.	n.a.	n.a.	n.a.	n.a.	99.985
CPB - SG2 OX Spr	5.18	0.753	3.87	109.086	1.37	99.985
CPB - SG2 AN Spr	n.a.	n.a.	n.a.	n.a.	n.a.	99.985

CPB - SG3 OX Spr	n.a.	n.a.	n.a.	n.a.	n.a.	99.985
CPB - SG3 AN Spr	n.a.	n.a.	n.a.	n.a.	n.a.	99.985
CPB - UV1 OX Spr	n.a.	n.a.	n.a.	n.a.	n.a.	99.985
CPB - UV1 AN Spr	n.a.	n.a.	n.a.	n.a.	n.a.	99.985
CPB - UV2 OX Spr	n.a.	n.a.	n.a.	n.a.	n.a.	99.985
CPB - UV2 AN Spr	5.41	0.37	1.352	50.866	0.39	99.985
CPB - UV3 OX Spr	n.a.	n.a.	n.a.	n.a.	n.a.	99.985
CPB - UV3 AN Spr	n.a.	n.a.	n.a.	n.a.	n.a.	99.985
NS- SG1 OX Spr	5.157	0.717	3.129	103.612	1.4	99.985
NS- SG1 AN Spr	n.a.	n.a.	n.a.	n.a.	n.a.	99.985
NS- SG2 OX Spr	5.18	0.681	3.842	98.17	1.07	99.985
NS- SG2 AN Spr	5.157	0.496	3.011	70.126	1	99.985
NS- SG3 OX Spr	n.a.	n.a.	n.a.	n.a.	n.a.	99.985
NS- SG3 AN Spr	n.a.	n.a.	n.a.	n.a.	n.a.	99.985
NS- UV1 OX Spr	5.16	0.643	3.314	92.495	1.35	99.985
NS - UV1 AN Spr	n.a.	n.a.	n.a.	n.a.	n.a.	99.985
NS - UV2 OX Spr	5.157	0.706	3.3	102.071	1.97	99.985
NS - UV2 AN Spr	n.a.	n.a.	n.a.	n.a.	n.a.	99.985
NS - UV3 OX Spr	n.a.	n.a.	n.a.	n.a.	n.a.	99.985
NS - UV3 AN Spr	n.a.	n.a.	n.a.	n.a.	n.a.	99.985
LOS- SG1 OX Spr	5.197	1.043	5.264	153.208	1.37	99.985
LOS- SG1 AN Spr	n.a.	n.a.	n.a.	n.a.	n.a.	99.985
LOS- SG2 OX Spr	n.a.	n.a.	n.a.	n.a.	n.a.	99.985
LOS- SG2 AN Spr	n.a.	n.a.	n.a.	n.a.	n.a.	99.985
LOS- SG3 OX Spr	n.a.	n.a.	n.a.	n.a.	n.a.	99.985
LOS- SG3 AN Spr	n.a.	n.a.	n.a.	n.a.	n.a.	99.985
LOS- UV1 OX Spr	n.a.	n.a.	n.a.	n.a.	n.a.	99.985
LOS - UV1 AN Spr	n.a.	n.a.	n.a.	n.a.	n.a.	99.985
LOS - UV2 OX Spr	n.a.	n.a.	n.a.	n.a.	n.a.	99.985
LOS - UV2 AN Spr	n.a.	n.a.	n.a.	n.a.	n.a.	99.985
LOS - UV3 OX Spr	n.a.	n.a.	n.a.	n.a.	n.a.	99.985
LOS - UV3 AN Spr	n.a.	n.a.	n.a.	n.a.	n.a.	99.985
CPB SG1 AN AUT 1	n.a.	n.a.	n.a.	n.a.	n.a.	99.985
CPB SG2 AN AUT 2	n.a.	n.a.	n.a.	n.a.	n.a.	99.985
CPB UV2 AN AUT 3	n.a.	n.a.	n.a.	n.a.	n.a.	99.985
NS UV3 AN AUT 4	n.a.	n.a.	n.a.	n.a.	n.a.	99.985
NS UV2 AN WIN 5	n.a.	n.a.	n.a.	n.a.	n.a.	99.985
CPB UV1 OX WIN 6	n.a.	n.a.	n.a.	n.a.	n.a.	99.985
CPB UV1 AN WIN 7	n.a.	n.a.	n.a.	n.a.	n.a.	99.985
CPB UV3 AN WIN 8	n.a.	n.a.	n.a.	n.a.	n.a.	99.985
CPB SG3 AN SPR 9	n.a.	n.a.	n.a.	n.a.	n.a.	99.985
CPB UV1 AN SPR 10	n.a.	n.a.	n.a.	n.a.	n.a.	99.985
CPB UV3 AN SPR 11	n.a.	n.a.	n.a.	n.a.	n.a.	99.985

Table A12. Raw anion and cation data for phosphate

Injection Name	RT	Area	Height	Amount	Relative Area	Correlation Coefficient
	min	$\mu\text{S}\cdot\text{min}$	μS	$\mu\text{Mol/L}$	%	%
	CD_1_Total	CD_1_Total	CD_1_Total	CD_1_Total	CD_1_Total	CD_1_Total
	Phosphate	Phosphate	Phosphate	Phosphate	Phosphate	Phosphate
CPB - SG1 OX Aut	39.953	0.024	0.06	2.21	0.04	99.988
CPB - SG1 OX Win	39.94	0.023	0.061	2.146	0.05	99.988
CPB - SG1 AN Win	39.993	0.003	0.008	0.248	0.01	99.988
CPB - SG2 OX Aut	39.903	0.045	0.122	4.158	0.05	99.988
CPB - SG2 OX Win	39.973	0.011	0.025	0.985	0.01	99.988
CPB - SG2 AN Win	39.987	0.002	0.007	0.202	0	99.988
CPB - SG3 AN Aut	39.973	0	0.002	0.038	0	99.988
CPB - SG3 OX Aut	39.833	0.076	0.206	7.052	0.08	99.988
CPB - SG3 OX Win	39.917	0.027	0.074	2.494	0.03	99.988
CPB - SG3 AN Win	39.953	0.004	0.012	0.386	0.01	99.988
CPB - UV1 OX Aut	39.893	0.036	0.097	3.326	0.05	99.988
CPB - UV2 OX Aut	39.993	0.001	0.003	0.1	0	99.988
CPB - UV3 OX Aut	39.977	0.002	0.005	0.216	0	99.988
CPB - UV2 OX Win	39.97	0.006	0.012	0.512	0.01	99.988
CPB - UV3 OX Win	39.937	0.001	0.002	0.049	0	99.988
NS- SG1 OX Aut	39.847	0.063	0.172	5.83	0.07	99.988
NS- SG1 AN Aut	39.95	0.003	0.008	0.293	0	99.988
NS- SG1 OX Win	39.883	0.039	0.104	3.648	0.08	99.988
NS- SG1 AN Win	39.893	0.025	0.069	2.318	0.04	99.988
NS- SG2 OX Aut	39.85	0.056	0.148	5.211	0.07	99.988
NS- SG2 AN Aut	39.903	0.003	0.006	0.308	0	99.988
NS- SG2 OX Win	39.923	0.012	0.033	1.091	0.02	99.988
NS- SG2 AN Win	39.903	0	0.001	0.039	0	99.988
NS - SG3 OX Aut	39.883	0.029	0.081	2.7	0.03	99.988
NS - SG3 AN Aut	39.903	0.015	0.045	1.43	0.03	99.988
NS - SG3 OX Win	39.85	0.043	0.12	3.966	0.04	99.988
NS - SG3 AN Win	39.903	0.001	0.003	0.089	0	99.988
NS - UV1 OX Aut	39.877	0.027	0.069	2.476	0.04	99.988
NS - UV1 AN Aut	39.847	0.044	0.116	4.075	0.05	99.988
NS - UV1 OX Win	39.803	0.065	0.174	6.003	0.07	99.988
NS - UV1 AN Win	n.a.	n.a.	n.a.	n.a.	n.a.	99.988
NS - UV2 OX Aut	39.873	0.015	0.044	1.402	0.01	99.988
NS - UV2 AN Aut	39.893	0.003	0.008	0.229	0	99.988
NS - UV2 OX Win	39.893	0.007	0.021	0.635	0.01	99.988
NS - UV2 AN Win	39.88	0.016	0.042	1.481	0.02	99.988
NS - UV3 OX Aut	39.89	0.005	0.014	0.449	0	99.988
NS - UV3 AN Aut	39.873	0.013	0.037	1.223	0.01	99.988
NS - UV3 OX Win	39.85	0.027	0.07	2.509	0.03	99.988
NS - UV3 AN Win	39.88	0.003	0.011	0.307	0	99.988
LOS- SG1 OX Aut	39.84	0.001	0.002	0.055	0	99.988

LOS- SG1 AN Aut	39.86	0.007	0.021	0.683	0.01	99.988
LOS- SG1 OX Win	39.847	0.018	0.052	1.696	0.03	99.988
LOS- SG1 AN Win	39.86	0.005	0.014	0.47	0.01	99.988
LOS- SG2 OX Aut	39.697	0.11	0.277	10.176	0.18	99.988
LOS- SG2 AN Aut	39.84	0.007	0.02	0.656	0.01	99.988
LOS- SG2 OX Win	39.747	0.062	0.172	5.775	0.07	99.988
LOS- SG2 AN Win	39.85	0.007	0.02	0.632	0.01	99.988
LOS- SG3 OX Aut	39.77	0.049	0.133	4.524	0.06	99.988
LOS- SG3 AN Aut	39.77	0.048	0.133	4.431	0.07	99.988
LOS- SG3 OX Win	39.713	0.082	0.216	7.564	0.11	99.988
LOS- SG3 AN Win	39.78	0.036	0.103	3.366	0.05	99.988
LOS- UV1 OX Aut	39.73	0.073	0.198	6.798	0.09	99.988
LOS- UV1 AN Aut	39.807	0.029	0.083	2.698	0.03	99.988
LOS- UV1 OX Win	39.71	0.089	0.237	8.262	0.16	99.988
LOS- UV1 AN Win	39.777	0.043	0.119	3.947	0.08	99.988
LOS- UV2 OX Aut	39.633	0.147	0.358	13.589	0.21	99.988
LOS- UV2 AN Aut	39.637	0.13	0.331	12.066	0.18	99.988
LOS- UV2 OX Win	39.737	0.059	0.161	5.437	0.09	99.988
LOS- UV2 AN Win	39.727	0.06	0.165	5.52	0.09	99.988
LOS- UV3 OX Aut	39.633	0.125	0.316	11.559	0.14	99.988
LOS- UV3 AN Aut	39.733	0.048	0.133	4.41	0.07	99.988
LOS- UV3 OX Win	39.663	0.098	0.251	9.09	0.11	99.988
LOS- UV3 AN Win	n.a.	n.a.	n.a.	n.a.	n.a.	99.988
CPB - SG1 OX Spr	40.177	0.017	0.046	1.46	0.03	99.968
CPB - SG1 AN Spr	40.22	0.003	0.008	0.333	0	99.968
CPB - SG2 OX Spr	40.157	0.032	0.081	2.619	0.04	99.968
CPB - SG2 AN Spr	40.177	0.009	0.022	0.797	0.01	99.968
CPB - SG3 OX Spr	40.183	0.009	0.023	0.795	0.01	99.968
CPB - SG3 AN Spr	40.18	0.008	0.02	0.7	0.01	99.968
CPB - UV1 OX Spr	40.17	0.013	0.035	1.111	0.01	99.968
CPB - UV1 AN Spr	40.017	0.125	0.316	9.825	0.09	99.968
CPB - UV2 OX Spr	40.203	0.011	0.017	0.976	0.01	99.968
CPB - UV2 AN Spr	40.173	0.024	0.047	2.007	0.02	99.968
CPB - UV3 OX Spr	40.19	0.007	0.02	0.642	0.01	99.968
CPB - UV3 AN Spr	40.213	0.004	0.01	0.412	0	99.968
NS- SG1 OX Spr	40.183	0.014	0.033	1.174	0.02	99.968
NS- SG1 AN Spr	40.123	0.044	0.108	3.505	0.05	99.968
NS- SG2 OX Spr	40.15	0.028	0.061	2.259	0.03	99.968
NS- SG2 AN Spr	40.567	0.006	0.005	0.544	0.01	99.968
NS- SG3 OX Spr	40.16	0.015	0.033	1.307	0.01	99.968
NS- SG3 AN Spr	40.16	0.002	0.006	0.262	0	99.968
NS- UV1 OX Spr	40.11	0.046	0.121	3.721	0.06	99.968
NS - UV1 AN Spr	40.127	0.036	0.093	2.909	0.04	99.968
NS - UV2 OX Spr	40.133	0.032	0.086	2.628	0.06	99.968
NS - UV2 AN Spr	39.683	0	0.002	0.15	0	99.968
NS - UV3 OX Spr	40.157	0.019	0.044	1.603	0.02	99.968

NS - UV3 AN Spr	40.2	0.004	0.013	0.45	0.01	99.968
LOS- SG1 OX Spr	40.093	0.063	0.165	5.012	0.06	99.968
LOS- SG1 AN Spr	n.a.	n.a.	n.a.	n.a.	n.a.	99.968
LOS- SG2 OX Spr	40.073	0.065	0.177	5.146	0.06	99.968
LOS- SG2 AN Spr	40.17	0.009	0.019	0.791	0.01	99.968
LOS- SG3 OX Spr	40.133	0.022	0.059	1.795	0.02	99.968
LOS- SG3 AN Spr	40.127	0.019	0.05	1.574	0.02	99.968
LOS- UV1 OX Spr	40.04	0.085	0.223	6.751	0.09	99.968
LOS - UV1 AN Spr	40.103	0.046	0.123	3.674	0.06	99.968
LOS - UV2 OX Spr	40.107	0.039	0.106	3.162	0.03	99.968
LOS - UV2 AN Spr	40.14	0.023	0.054	1.916	0.03	99.968
LOS - UV3 OX Spr	40.063	0.063	0.166	5.044	0.06	99.968
LOS - UV3 AN Spr	40.127	0.025	0.069	2.094	0.04	99.968
CPB SG1 AN AUT 1	40.16	0.002	0.005	0.269	0	99.968
CPB SG2 AN AUT 2	n.a.	n.a.	n.a.	n.a.	n.a.	99.968
CPB UV2 AN AUT 3	40.137	0.007	0.02	0.69	0	99.968
NS UV3 AN AUT 4	40.147	0.009	0.027	0.839	0.01	99.968
NS UV2 AN WIN 5	40.14	0.007	0.02	0.681	0.01	99.968
CPB UV1 OX WIN 6	40.14	0.011	0.029	0.967	0.01	99.968
CPB UV1 AN WIN 7	40.14	0.007	0.021	0.689	0.01	99.968
CPB UV3 AN WIN 8	40.147	0.009	0.024	0.798	0.01	99.968
CPB SG3 AN SPR 9	40.14	0.004	0.011	0.429	0	99.968
CPB UV1 AN SPR 10	40.133	0.015	0.041	1.293	0.01	99.968
CPB UV3 AN SPR 11	40.143	0.008	0.015	0.705	0.01	99.968

Table A13. Raw anion and cation data for sulphate.

Injection Name	RT	Area	Height	Amount	Relative Area	Correlation Coefficient
	min	$\mu\text{S} \cdot \text{min}$	μS	$\mu\text{Mol/L}$	%	%
	CD_1_Total	CD_1_Total	CD_1_Total	CD_1_Total	CD_1_Total	CD_1_Total
	Sulphate	Sulphate	Sulphate	Sulphate	Sulphate	Sulphate
CPB - SG1 OX Aut	28.217	6.594	14.199	205.754	9.81	99.989
CPB - SG1 OX Win	28.323	4.319	10.796	135.004	10.01	99.989
CPB - SG1 AN Win	28.367	3.6	9.573	112.657	13.4	99.989
CPB - SG2 OX Aut	28.107	9.173	17.464	285.965	9.35	99.989
CPB - SG2 OX Win	28.17	7.581	15.401	236.449	10.32	99.989
CPB - SG2 AN Win	28.22	6.308	13.82	196.878	13.01	99.989
CPB - SG3 AN Aut	28.12	8.381	16.501	261.34	11.32	99.989
CPB - SG3 OX Aut	28.097	8.915	17.149	277.944	9.45	99.989
CPB - SG3 OX Win	28.087	9.37	17.686	292.071	10.26	99.989
CPB - SG3 AN Win	28.167	7.198	14.981	224.529	9.62	99.989
CPB - UV1 OX Aut	28.163	7.378	15.183	230.13	9.54	99.989
CPB - UV2 OX Aut	28.05	10.155	18.549	316.481	9.83	99.989
CPB - UV3 OX Aut	28.06	10.356	18.77	322.751	8.62	99.989
CPB - UV2 OX Win	28.197	6.92	14.631	215.886	9.85	99.989

CPB - UV3 OX Win	28.053	10.482	18.939	326.675	9.08	99.989
NS- SG1 OX Aut	28.11	9.119	17.374	284.289	10.8	99.989
NS- SG1 AN Aut	27.81	18.27	26.44	568.84	22.78	99.989
NS- SG1 OX Win	28.277	5.203	12.165	162.507	10.2	99.989
NS- SG1 AN Win	28.27	5.249	12.235	163.947	8.33	99.989
NS- SG2 OX Aut	28.203	6.802	14.442	212.213	8.33	99.989
NS- SG2 AN Aut	27.9	14.845	23.385	462.33	14.64	99.989
NS- SG2 OX Win	28.19	7.097	14.852	221.405	9.76	99.989
NS- SG2 AN Win	28.077	9.66	17.995	301.103	9.73	99.989
NS - SG3 OX Aut	28.153	7.756	15.704	241.904	9.25	99.989
NS - SG3 AN Aut	28.223	5.963	13.283	186.128	12.16	99.989
NS - SG3 OX Win	28.08	9.666	17.955	301.286	10.05	99.989
NS - SG3 AN Win	28.24	5.752	12.983	179.57	8.91	99.989
NS - UV1 OX Aut	28.2	6.595	14.172	205.8	9.45	99.989
NS - UV1 AN Aut	28.053	10.362	18.793	322.937	10.9	99.989
NS - UV1 OX Win	28.167	7.483	15.332	233.391	8.62	99.989
NS - UV1 AN Win	28.22	6.244	13.682	194.867	10.08	99.989
NS - UV2 OX Aut	27.927	14.065	22.604	438.081	9	99.989
NS - UV2 AN Aut	28.123	8.429	16.524	262.827	9.11	99.989
NS - UV2 OX Win	28.127	8.377	16.431	261.205	8.59	99.989
NS - UV2 AN Win	28.207	6.386	13.869	199.286	9.18	99.989
NS - UV3 OX Aut	28.103	8.968	17.17	279.57	8.98	99.989
NS - UV3 AN Aut	28.04	10.732	19.198	334.438	10.66	99.989
NS - UV3 OX Win	28.113	8.716	16.871	271.744	10.21	99.989
NS - UV3 AN Win	28.17	7.27	15.061	226.773	10.31	99.989
LOS- SG1 OX Aut	28.01	11.56	20.065	360.18	9.35	99.989
LOS- SG1 AN Aut	28.103	9.076	17.339	282.926	9.69	99.989
LOS- SG1 OX Win	28.207	6.626	14.218	206.752	9.12	99.989
LOS- SG1 AN Win	28.18	7.143	14.918	222.822	8.9	99.989
LOS- SG2 OX Aut	28.263	5.396	12.462	168.513	8.93	99.989
LOS- SG2 AN Aut	28.167	7.37	15.225	229.894	8.77	99.989
LOS- SG2 OX Win	28.14	8.081	16.088	251.994	9.26	99.989
LOS- SG2 AN Win	28.19	7.056	14.807	220.118	9.63	99.989
LOS- SG3 OX Aut	28.153	7.722	15.668	240.841	8.94	99.989
LOS- SG3 AN Aut	28.187	6.989	14.69	218.057	9.55	99.989
LOS- SG3 OX Win	28.173	7.092	14.826	221.258	9.3	99.989
LOS- SG3 AN Win	28.163	7.299	15.088	227.673	10.28	99.989
LOS- UV1 OX Aut	28.14	8.211	16.099	256.045	9.86	99.989
LOS- UV1 AN Aut	28.133	9.202	17.267	286.85	10.84	99.989
LOS- UV1 OX Win	28.333	4.739	11.235	148.067	8.35	99.989
LOS- UV1 AN Win	28.287	5.696	12.719	177.845	10.38	99.989
LOS- UV2 OX Aut	28.257	6.236	13.495	194.63	9.14	99.989
LOS- UV2 AN Aut	28.2	7.471	15.129	233.038	10.17	99.989
LOS- UV2 OX Win	28.283	5.694	12.72	177.771	8.74	99.989
LOS- UV2 AN Win	28.28	5.688	12.702	177.6	8.76	99.989
LOS- UV3 OX Aut	28.18	7.832	15.627	244.253	8.98	99.989

LOS- UV3 AN Aut	28.217	6.781	14.238	211.564	10.09	99.989
LOS- UV3 OX Win	28.117	9.294	17.393	289.735	10.52	99.989
LOS- UV3 AN Win	28.153	8.321	16.215	259.466	9.93	99.989
CPB - SG1 OX Spr	28.343	5.077	12.132	153.629	9.59	99.976
CPB - SG1 AN Spr	28.32	5.613	12.945	169.915	9.33	99.976
CPB - SG2 OX Spr	28.213	7.949	16.099	240.855	9.73	99.976
CPB - SG2 AN Spr	28.24	7.35	15.315	222.656	9.64	99.976
CPB - SG3 OX Spr	28.013	13.123	21.848	397.943	9.76	99.976
CPB - SG3 AN Spr	28.12	10.288	18.854	311.864	9.53	99.976
CPB - UV1 OX Spr	28.093	10.856	19.463	329.099	9.65	99.976
CPB - UV1 AN Spr	27.97	14.611	23.25	443.13	10.89	99.976
CPB - UV2 OX Spr	28.14	9.664	18.148	292.926	9.44	99.976
CPB - UV2 AN Spr	28.01	13.683	22.44	414.952	9.18	99.976
CPB - UV3 OX Spr	28.09	11.466	20.183	347.618	10.42	99.976
CPB - UV3 AN Spr	28.17	9.445	17.936	286.262	10.48	99.976
NS- SG1 OX Spr	28.247	7.567	15.641	229.236	9.8	99.976
NS- SG1 AN Spr	28.26	7.534	15.566	228.233	9.27	99.976
NS- SG2 OX Spr	28.203	8.772	17.105	265.831	9.22	99.976
NS- SG2 AN Spr	28.287	6.801	14.582	205.989	8.84	99.976
NS- SG3 OX Spr	28.147	10.212	18.743	309.55	9.33	99.976
NS- SG3 AN Spr	28.333	5.665	13.001	171.494	8.61	99.976
NS- UV1 OX Spr	28.277	6.997	14.858	211.921	9.74	99.976
NS - UV1 AN Spr	28.257	7.47	15.461	226.284	8.49	99.976
NS - UV2 OX Spr	28.35	5.551	12.798	168.015	11.13	99.976
NS - UV2 AN Spr	28.2	8.892	17.199	269.477	10.36	99.976
NS - UV3 OX Spr	28.11	11.354	20.011	344.235	9.63	99.976
NS - UV3 AN Spr	28.24	8.216	16.404	248.955	9.53	99.976
LOS- SG1 OX Spr	28.177	9.98	18.527	302.498	8.92	99.976
LOS- SG1 AN Spr	28.213	9.013	17.373	273.163	8.98	99.976
LOS- SG2 OX Spr	28.173	9.855	18.362	298.718	8.8	99.976
LOS- SG2 AN Spr	28.157	10.665	19.249	323.316	8.8	99.976
LOS- SG3 OX Spr	28.133	11.156	19.804	338.204	8.98	99.976
LOS- SG3 AN Spr	28.177	9.787	18.277	296.641	8.8	99.976
LOS- UV1 OX Spr	28.237	8.337	16.567	252.619	9.27	99.976
LOS - UV1 AN Spr	28.27	7.654	15.704	231.887	9.31	99.976
LOS - UV2 OX Spr	28.133	11.223	19.866	340.258	9.52	99.976
LOS - UV2 AN Spr	28.313	6.594	14.309	199.687	9.43	99.976
LOS - UV3 OX Spr	28.187	9.314	17.741	282.292	9.39	99.976
LOS - UV3 AN Spr	28.347	5.818	13.21	176.138	8.66	99.976
CPB SG1 AN AUT 1	28.027	14.552	23.214	441.337	22.61	99.976
CPB SG2 AN AUT 2	27.553	33.654	37.739	1021.35	24.8	99.976
CPB UV2 AN AUT 3	27.937	17.634	26.01	534.913	10.74	99.976
NS UV3 AN AUT 4	28.063	13.482	22.206	408.857	10.36	99.976
NS UV2 AN WIN 5	28.26	8.014	16.174	242.814	10.44	99.976
CPB UV1 OX WIN 6	28.027	14.66	23.29	444.615	10.41	99.976
CPB UV1 AN WIN 7	28.13	11.504	20.119	348.771	10.93	99.976

CPB UV3 AN WIN 8	28.257	8.372	16.589	253.692	11.47	99.976
CPB SG3 AN SPR 9	28.12	11.585	20.159	351.259	10.17	99.976
CPB UV1 AN SPR 10	28.053	13.779	22.398	417.862	10.08	99.976
CPB UV3 AN SPR 11	28.193	8.671	16.917	262.75	10.08	99.976

Table A14. Raw anion and cation data for nitrate.

Injection Name	RT	Area	Height	Amount	Relative Area	Correlation Coefficient
	min	µS*min	µS	uMol/L	%	%
	CD_1_Total	CD_1_Total	CD_1_Total	CD_1_Total	CD_1_Total	CD_1_Total
	Nitrate	Nitrate	Nitrate	Nitrate	Nitrate	Nitrate
CPB - SG1 OX Aut	21.763	0.012	0.059	1.217	0.02	99.985
CPB - SG1 OX Win	21.753	0.035	0.165	2.433	0.08	99.985
CPB - SG1 AN Win	21.763	0.019	0.088	1.562	0.07	99.985
CPB - SG2 OX Aut	21.693	0.39	1.784	21.187	0.4	99.985
CPB - SG2 OX Win	21.75	0.05	0.234	3.193	0.07	99.985
CPB - SG2 AN Win	21.713	0.283	1.303	15.519	0.58	99.985
CPB - SG3 AN Aut	21.72	0.184	0.862	10.291	0.25	99.985
CPB - SG3 OX Aut	21.75	0.018	0.086	1.515	0.02	99.985
CPB - SG3 OX Win	21.723	0.157	0.739	8.886	0.17	99.985
CPB - SG3 AN Win	21.747	0.058	0.271	3.62	0.08	99.985
CPB - UV1 OX Aut	21.72	0.137	0.641	7.783	0.18	99.985
CPB - UV2 OX Aut	21.71	0.219	1.022	12.141	0.21	99.985
CPB - UV3 OX Aut	21.733	0.084	0.393	4.985	0.07	99.985
CPB - UV2 OX Win	21.753	0.03	0.141	2.139	0.04	99.985
CPB - UV3 OX Win	21.723	0.127	0.597	7.284	0.11	99.985
NS- SG1 OX Aut	21.72	0.148	0.698	8.399	0.18	99.985
NS- SG1 AN Aut	21.743	0.012	0.056	1.185	0.01	99.985
NS- SG1 OX Win	21.743	0.053	0.249	3.383	0.1	99.985
NS- SG1 AN Win	21.677	0.438	1.969	23.685	0.69	99.985
NS- SG2 OX Aut	21.69	0.329	1.511	17.941	0.4	99.985
NS- SG2 AN Aut	21.743	0.013	0.063	1.27	0.01	99.985
NS- SG2 OX Win	21.747	0.04	0.186	2.661	0.05	99.985
NS- SG2 AN Win	21.67	0.453	2.033	24.501	0.46	99.985
NS - SG3 OX Aut	21.71	0.174	0.815	9.762	0.21	99.985
NS - SG3 AN Aut	21.74	0.016	0.073	1.392	0.03	99.985
NS - SG3 OX Win	21.74	0.026	0.12	1.922	0.03	99.985
NS - SG3 AN Win	21.743	0.015	0.069	1.344	0.02	99.985
NS - UV1 OX Aut	21.73	0.036	0.17	2.471	0.05	99.985
NS - UV1 AN Aut	21.727	0.079	0.371	4.73	0.08	99.985
NS - UV1 OX Win	21.737	0.026	0.123	1.923	0.03	99.985
NS - UV1 AN Win	21.743	0.012	0.055	1.189	0.02	99.985
NS - UV2 OX Aut	21.723	0.053	0.248	3.357	0.03	99.985
NS - UV2 AN Aut	21.73	0.039	0.184	2.634	0.04	99.985
NS - UV2 OX Win	21.727	0.032	0.152	2.259	0.03	99.985

NS - UV2 AN Win	21.723	0.083	0.391	4.975	0.12	99.985
NS - UV3 OX Aut	21.703	0.166	0.776	9.353	0.17	99.985
NS - UV3 AN Aut	21.737	0.016	0.077	1.427	0.02	99.985
NS - UV3 OX Win	21.71	0.108	0.508	6.295	0.13	99.985
NS - UV3 AN Win	21.71	0.101	0.47	5.877	0.14	99.985
LOS- SG1 OX Aut	21.7	0.121	0.565	6.972	0.1	99.985
LOS- SG1 AN Aut	21.713	0.089	0.414	5.254	0.09	99.985
LOS- SG1 OX Win	21.72	0.067	0.308	4.089	0.09	99.985
LOS- SG1 AN Win	21.733	0.015	0.069	1.335	0.02	99.985
LOS- SG2 OX Aut	21.733	0.016	0.074	1.407	0.03	99.985
LOS- SG2 AN Aut	21.727	0.013	0.062	1.261	0.02	99.985
LOS- SG2 OX Win	21.73	0.014	0.069	1.33	0.02	99.985
LOS- SG2 AN Win	21.74	0.013	0.064	1.279	0.02	99.985
LOS- SG3 OX Aut	21.727	0.02	0.094	1.616	0.02	99.985
LOS- SG3 AN Aut	21.723	0.02	0.096	1.634	0.03	99.985
LOS- SG3 OX Win	21.717	0.024	0.116	1.863	0.03	99.985
LOS- SG3 AN Win	21.717	0.018	0.084	1.51	0.03	99.985
LOS- UV1 OX Aut	21.723	0.021	0.098	1.666	0.02	99.985
LOS- UV1 AN Aut	21.727	0.017	0.079	1.47	0.02	99.985
LOS- UV1 OX Win	21.72	0.029	0.135	2.092	0.05	99.985
LOS- UV1 AN Win	21.723	0.013	0.062	1.265	0.02	99.985
LOS- UV2 OX Aut	21.713	0.037	0.172	2.509	0.05	99.985
LOS- UV2 AN Aut	21.717	0.019	0.086	1.55	0.03	99.985
LOS- UV2 OX Win	21.72	0.026	0.123	1.953	0.04	99.985
LOS- UV2 AN Win	21.72	0.025	0.118	1.914	0.04	99.985
LOS- UV3 OX Aut	21.717	0.02	0.092	1.621	0.02	99.985
LOS- UV3 AN Aut	21.71	0.018	0.085	1.515	0.03	99.985
LOS- UV3 OX Win	21.71	0.035	0.165	2.409	0.04	99.985
LOS- UV3 AN Win	21.713	0.016	0.075	1.402	0.02	99.985
CPB - SG1 OX Spr	21.84	0.027	0.125	1.641	0.05	99.981
CPB - SG1 AN Spr	21.837	0.037	0.172	2.199	0.06	99.981
CPB - SG2 OX Spr	21.837	0.045	0.211	2.663	0.06	99.981
CPB - SG2 AN Spr	21.843	0.031	0.144	1.881	0.04	99.981
CPB - SG3 OX Spr	21.823	0.077	0.356	4.389	0.06	99.981
CPB - SG3 AN Spr	21.813	0.148	0.686	8.286	0.14	99.981
CPB - UV1 OX Spr	21.83	0.045	0.208	2.643	0.04	99.981
CPB - UV1 AN Spr	21.723	0.884	3.737	48.626	0.66	99.981
CPB - UV2 OX Spr	21.813	0.165	0.767	9.225	0.16	99.981
CPB - UV2 AN Spr	21.777	0.452	2.034	24.975	0.3	99.981
CPB - UV3 OX Spr	21.837	0.06	0.281	3.478	0.05	99.981
CPB - UV3 AN Spr	21.847	0.05	0.235	2.933	0.06	99.981
NS- SG1 OX Spr	21.797	0.283	1.296	15.705	0.37	99.981
NS- SG1 AN Spr	21.8	0.304	1.388	16.865	0.37	99.981
NS- SG2 OX Spr	21.837	0.071	0.328	4.059	0.07	99.981
NS- SG2 AN Spr	21.847	0.038	0.179	2.291	0.05	99.981
NS- SG3 OX Spr	21.827	0.086	0.398	4.885	0.08	99.981

NS- SG3 AN Spr	21.847	0.039	0.182	2.322	0.06	99.981
NS- UV1 OX Spr	21.817	0.216	0.995	12.008	0.3	99.981
NS - UV1 AN Spr	21.813	0.163	0.755	9.126	0.19	99.981
NS - UV2 OX Spr	21.837	0.043	0.2	2.539	0.09	99.981
NS - UV2 AN Spr	21.757	0.602	2.63	33.153	0.7	99.981
NS - UV3 OX Spr	21.827	0.036	0.169	2.165	0.03	99.981
NS - UV3 AN Spr	21.833	0.057	0.266	3.309	0.07	99.981
LOS- SG1 OX Spr	21.827	0.065	0.303	3.725	0.06	99.981
LOS- SG1 AN Spr	21.837	0.028	0.131	1.718	0.03	99.981
LOS- SG2 OX Spr	21.78	0.288	1.316	15.947	0.26	99.981
LOS- SG2 AN Spr	21.843	0.018	0.084	1.165	0.01	99.981
LOS- SG3 OX Spr	21.84	0.019	0.088	1.212	0.02	99.981
LOS- SG3 AN Spr	21.743	0.58	2.546	31.966	0.52	99.981
LOS- UV1 OX Spr	21.82	0.079	0.368	4.526	0.09	99.981
LOS - UV1 AN Spr	21.837	0.031	0.146	1.905	0.04	99.981
LOS - UV2 OX Spr	21.817	0.118	0.545	6.63	0.1	99.981
LOS - UV2 AN Spr	21.833	0.015	0.073	1.028	0.02	99.981
LOS - UV3 OX Spr	21.82	0.031	0.147	1.911	0.03	99.981
LOS - UV3 AN Spr	21.83	0.017	0.079	1.12	0.03	99.981
CPB SG1 AN AUT 1	21.807	0.112	0.518	6.309	0.17	99.981
CPB SG2 AN AUT 2	21.79	0.158	0.728	8.834	0.12	99.981
CPB UV2 AN AUT 3	21.813	0.027	0.128	1.661	0.02	99.981
NS UV3 AN AUT 4	21.83	0.016	0.075	1.044	0.01	99.981
NS UV2 AN WIN 5	21.817	0.046	0.218	2.723	0.06	99.981
CPB UV1 OX WIN 6	21.81	0.071	0.33	4.075	0.05	99.981
CPB UV1 AN WIN 7	21.807	0.101	0.466	5.732	0.1	99.981
CPB UV3 AN WIN 8	21.837	0.028	0.132	1.735	0.04	99.981
CPB SG3 AN SPR 9	21.797	0.124	0.57	6.999	0.11	99.981
CPB UV1 AN SPR 10	21.813	0.062	0.287	3.596	0.05	99.981
CPB UV3 AN SPR 11	21.81	0.118	0.54	6.628	0.14	99.981

Table A15. Raw anion and cation data for nitrite.

Injection Name	RT	Area	Height	Amount	Relative Area	Correlation Coefficient
	min	$\mu\text{S} \cdot \text{min}$	μS	$\mu\text{Mol/L}$	%	%
	CD_1_Total	CD_1_Total	CD_1_Total	CD_1_Total	CD_1_Total	CD_1_Total
	Nitrite	Nitrite	Nitrite	Nitrite	Nitrite	Nitrite
CPB - SG1 OX Aut	17.83	0	0.004	0.954	0	99.993
CPB - SG1 OX Win	17.823	0.001	0.009	1.01	0	99.993
CPB - SG1 AN Win	17.83	0.001	0.011	1.043	0.01	99.993
CPB - SG2 OX Aut	17.833	0.001	0.005	0.966	0	99.993
CPB - SG2 OX Win	17.83	0	0.005	0.965	0	99.993
CPB - SG2 AN Win	17.83	0.001	0.008	0.998	0	99.993
CPB - SG3 AN Aut	n.a.	n.a.	n.a.	n.a.	n.a.	99.993
CPB - SG3 OX Aut	17.823	0	0.001	0.93	0	99.993
CPB - SG3 OX Win	17.833	0	0.003	0.946	0	99.993

CPB - SG3 AN Win	17.83	0.036	0.242	3.918	0.05	99.993
CPB - UV1 OX Aut	17.823	0.001	0.008	0.995	0	99.993
CPB - UV2 OX Aut	17.823	0	0.003	0.943	0	99.993
CPB - UV3 OX Aut	17.837	0.002	0.016	1.051	0	99.993
CPB - UV2 OX Win	17.83	0	0.003	0.944	0	99.993
CPB - UV3 OX Win	17.83	0.001	0.006	0.972	0	99.993
NS- SG1 OX Aut	17.833	0	0.003	0.948	0	99.993
NS- SG1 AN Aut	17.817	0	0.003	0.939	0	99.993
NS- SG1 OX Win	17.82	0.001	0.007	0.988	0	99.993
NS- SG1 AN Win	17.817	0	0.004	0.961	0	99.993
NS- SG2 OX Aut	17.827	0.001	0.01	1.013	0	99.993
NS- SG2 AN Aut	17.82	0	0.002	0.929	0	99.993
NS- SG2 OX Win	17.83	0.001	0.005	0.967	0	99.993
NS- SG2 AN Win	17.82	0.001	0.006	0.974	0	99.993
NS - SG3 OX Aut	17.82	0	0.003	0.945	0	99.993
NS - SG3 AN Aut	17.81	0.001	0.006	0.979	0	99.993
NS - SG3 OX Win	17.82	0.001	0.01	1.011	0	99.993
NS - SG3 AN Win	17.813	0	0.005	0.965	0	99.993
NS - UV1 OX Aut	17.813	0.002	0.019	1.118	0	99.993
NS - UV1 AN Aut	17.813	0	0.002	0.934	0	99.993
NS - UV1 OX Win	17.823	0.001	0.011	1.025	0	99.993
NS - UV1 AN Win	17.817	0	0.005	0.957	0	99.993
NS - UV2 OX Aut	17.823	0.001	0.009	0.993	0	99.993
NS - UV2 AN Aut	17.813	0	0.002	0.938	0	99.993
NS - UV2 OX Win	17.817	0.001	0.01	1.017	0	99.993
NS - UV2 AN Win	17.813	0	0.001	0.943	0	99.993
NS - UV3 OX Aut	17.817	0.002	0.015	1.058	0	99.993
NS - UV3 AN Aut	17.82	0	0.004	0.955	0	99.993
NS - UV3 OX Win	17.817	0.001	0.006	0.968	0	99.993
NS - UV3 AN Win	17.81	0	0.004	0.953	0	99.993
LOS- SG1 OX Aut	17.817	0.004	0.037	1.293	0	99.993
LOS- SG1 AN Aut	17.82	0.002	0.013	1.054	0	99.993
LOS- SG1 OX Win	17.823	0.001	0.005	0.972	0	99.993
LOS- SG1 AN Win	17.817	0.001	0.005	0.967	0	99.993
LOS- SG2 OX Aut	17.817	0.002	0.014	1.064	0	99.993
LOS- SG2 AN Aut	17.817	0	0.004	0.948	0	99.993
LOS- SG2 OX Win	17.817	0.002	0.015	1.061	0	99.993
LOS- SG2 AN Win	17.827	0.001	0.005	0.966	0	99.993
LOS- SG3 OX Aut	17.817	0.003	0.021	1.141	0	99.993
LOS- SG3 AN Aut	17.813	0.001	0.008	0.99	0	99.993
LOS- SG3 OX Win	17.81	0.002	0.018	1.099	0	99.993
LOS- SG3 AN Win	17.807	0.001	0.008	0.998	0	99.993
LOS- UV1 OX Aut	17.813	0.002	0.014	1.06	0	99.993
LOS- UV1 AN Aut	17.82	0	0.001	0.926	0	99.993
LOS- UV1 OX Win	17.807	0	0.005	0.965	0	99.993
LOS- UV1 AN Win	17.807	0.001	0.009	1.011	0	99.993

LOS- UV2 OX Aut	17.807	0.001	0.01	1.012	0	99.993
LOS- UV2 AN Aut	17.803	0.001	0.008	0.983	0	99.993
LOS- UV2 OX Win	17.803	0.001	0.005	0.971	0	99.993
LOS- UV2 AN Win	17.803	0	0.005	0.95	0	99.993
LOS- UV3 OX Aut	17.807	0.002	0.019	1.117	0	99.993
LOS- UV3 AN Aut	17.8	0.017	0.113	2.283	0.02	99.993
LOS- UV3 OX Win	17.807	0.001	0.012	1.037	0	99.993
LOS- UV3 AN Win	n.a.	n.a.	n.a.	n.a.	n.a.	99.993
CPB - SG1 OX Spr	17.877	0.001	0.008	0.215	0	99.976
CPB - SG1 AN Spr	17.877	0	0.003	0.167	0	99.976
CPB - SG2 OX Spr	17.883	0.002	0.013	0.257	0	99.976
CPB - SG2 AN Spr	17.887	0.001	0.008	0.208	0	99.976
CPB - SG3 OX Spr	17.887	0.001	0.012	0.236	0	99.976
CPB - SG3 AN Spr	17.887	0	0.005	0.178	0	99.976
CPB - UV1 OX Spr	17.883	0.001	0.013	0.253	0	99.976
CPB - UV1 AN Spr	17.887	0.001	0.007	0.201	0	99.976
CPB - UV2 OX Spr	17.887	0.001	0.007	0.193	0	99.976
CPB - UV2 AN Spr	17.897	0	0.003	0.163	0	99.976
CPB - UV3 OX Spr	17.89	0.001	0.013	0.223	0	99.976
CPB - UV3 AN Spr	17.903	0	0.004	0.173	0	99.976
NS- SG1 OX Spr	17.887	0	0.004	0.175	0	99.976
NS- SG1 AN Spr	17.89	0.001	0.014	0.253	0	99.976
NS- SG2 OX Spr	17.89	0.001	0.007	0.196	0	99.976
NS- SG2 AN Spr	17.887	0	0.002	0.156	0	99.976
NS- SG3 OX Spr	17.887	0.001	0.01	0.219	0	99.976
NS- SG3 AN Spr	17.883	0	0.001	0.148	0	99.976
NS- UV1 OX Spr	17.897	0.001	0.009	0.196	0	99.976
NS - UV1 AN Spr	17.89	0.001	0.009	0.208	0	99.976
NS - UV2 OX Spr	17.88	0.001	0.008	0.204	0	99.976
NS - UV2 AN Spr	17.883	0.001	0.007	0.196	0	99.976
NS - UV3 OX Spr	17.883	0.001	0.009	0.212	0	99.976
NS - UV3 AN Spr	17.89	0	0.005	0.178	0	99.976
LOS- SG1 OX Spr	17.89	0.002	0.015	0.267	0	99.976
LOS- SG1 AN Spr	n.a.	n.a.	n.a.	n.a.	n.a.	99.976
LOS- SG2 OX Spr	17.877	0.001	0.014	0.239	0	99.976
LOS- SG2 AN Spr	17.897	0.002	0.014	0.256	0	99.976
LOS- SG3 OX Spr	17.857	0.003	0.018	0.342	0	99.976
LOS- SG3 AN Spr	17.877	0.002	0.017	0.294	0	99.976
LOS- UV1 OX Spr	17.883	0.001	0.008	0.192	0	99.976
LOS - UV1 AN Spr	17.883	0	0.002	0.158	0	99.976
LOS - UV2 OX Spr	17.89	0.001	0.008	0.203	0	99.976
LOS - UV2 AN Spr	n.a.	n.a.	n.a.	n.a.	n.a.	99.976
LOS - UV3 OX Spr	17.873	0.001	0.009	0.215	0	99.976
LOS - UV3 AN Spr	17.87	0.001	0.009	0.224	0	99.976
CPB SG1 AN AUT 1	17.86	0	0.004	0.178	0	99.976
CPB SG2 AN AUT 2	17.87	0.002	0.014	0.265	0	99.976

CPB UV2 AN AUT 3	n.a.	n.a.	n.a.	n.a.	n.a.	99.976
NS UV3 AN AUT 4	n.a.	n.a.	n.a.	n.a.	n.a.	99.976
NS UV2 AN WIN 5	17.867	0	0.004	0.164	0	99.976
CPB UV1 OX WIN 6	17.873	0.001	0.011	0.232	0	99.976
CPB UV1 AN WIN 7	17.87	0	0.005	0.175	0	99.976
CPB UV3 AN WIN 8	n.a.	n.a.	n.a.	n.a.	n.a.	99.976
CPB SG3 AN SPR 9	17.87	0.001	0.009	0.21	0	99.976
CPB UV1 AN SPR 10	17.87	0	0.006	0.167	0	99.976
CPB UV3 AN SPR 11	17.883	0.002	0.015	0.27	0	99.976

Table A16. Environmental data for all sampling in Nacton Shore (NS), Copperas Bay (CPB) and Leigh-on-Sea.

date	time	season	site	rep	cloud cover (%)	air temp (°C)	water temp (°C)	salinity	notes
22/09/2023	08:08:00	summer23	NS	1	60	12.2	13.6	n.a.	n.a.
22/09/2023	08:08:00	summer23	NS	1	60	12.2	13.5	n.a.	n.a.
22/09/2023	08:08:00	summer23	NS	1	60	12.2	13.7	n.a.	n.a.
22/09/2023	09:30:00	summer23	NS	2	95	14	15.5	n.a.	n.a.
22/09/2023	09:30:00	summer23	NS	2	95	14	15.6	n.a.	n.a.
22/09/2023	09:30:00	summer23	NS	2	95	14	15.7	n.a.	n.a.
22/09/2023	10:40:00	summer23	NS	3	60	16.4	16.8	n.a.	n.a.
22/09/2023	10:40:00	summer23	NS	3	60	16.4	16.6	n.a.	n.a.
22/09/2023	10:40:00	summer23	NS	3	60	16.4	16.8	n.a.	n.a.
23/09/2023	07:56:00	summer23	CPB	1	5	10.6	11.2	n.a.	n.a.
23/09/2023	07:56:00	summer23	CPB	1	5	10.6	11.2	n.a.	n.a.
23/09/2023	07:56:00	summer23	CPB	1	5	10.6	11.3	n.a.	n.a.
23/09/2023	09:27:00	summer23	CPB	2	0	11.3	11.6	n.a.	n.a.
23/09/2023	09:27:00	summer23	CPB	2	0	11.3	11.5	n.a.	n.a.
23/09/2023	09:27:00	summer23	CPB	2	0	11.3	11.4	n.a.	n.a.
23/09/2023	10:42:00	summer23	CPB	3	0	12.7	13.1	n.a.	n.a.
23/09/2023	10:42:00	summer23	CPB	3	0	12.7	13.2	n.a.	n.a.
23/09/2023	10:42:00	summer23	CPB	3	0	12.7	13.1	n.a.	n.a.
06/11/2023	08:26:00	autumn	NS	1	10	9.1	8.9	25.6	n.a.
06/11/2023	08:26:00	autumn	NS	1	10	9.1	8.9	25.3	n.a.
06/11/2023	08:26:00	autumn	NS	1	10	9.1	8.9	25.6	n.a.
06/11/2023	09:54:00	autumn	NS	2	5	12.7	11.7	26.2	n.a.
06/11/2023	09:54:00	autumn	NS	2	5	12.7	11.7	25.5	n.a.
06/11/2023	09:54:00	autumn	NS	2	5	12.7	11.7	25.3	n.a.
06/11/2023	11:00:00	autumn	NS	3	10	15.6	12.6	25.8	n.a.
06/11/2023	11:00:00	autumn	NS	3	10	15.6	12.6	25.8	n.a.
06/11/2023	11:00:00	autumn	NS	3	10	15.6	12.6	26.1	n.a.
05/11/2023	07:30:00	autumn	CPB	1	100	9.2	9.5	19	n.a.

05/11/2023	07:30:00	autumn	CPB	1	100	9.2	9.5	22.6	n.a.
05/11/2023	07:30:00	autumn	CPB	1	100	9.2	9.5	23.2	n.a.
05/11/2023	09:07:00	autumn	CPB	2	75	9.8	9.8	23.2	n.a.
05/11/2023	09:07:00	autumn	CPB	2	75	9.8	9.8	22.5	n.a.
05/11/2023	09:07:00	autumn	CPB	2	75	9.8	9.8	18.9	n.a.
05/11/2023	10:40:00	autumn	CPB	3	30	12.8	10.3	19.9	n.a.
05/11/2023	10:40:00	autumn	CPB	3	30	12.8	10.3	20.1	n.a.
05/11/2023	10:40:00	autumn	CPB	3	30	12.8	10.3	18.7	n.a.
21/11/2023	09:29:00	autumn	LOS	1	100	10.1	10.4	24.3	n.a.
21/11/2023	09:29:00	autumn	LOS	1	100	10.1	10.4	24.8	n.a.
21/11/2023	09:29:00	autumn	LOS	1	100	10.1	10.4	24.9	n.a.
21/11/2023	10:41:00	autumn	LOS	2	100	11.6	11.4	25.4	n.a.
21/11/2023	10:41:00	autumn	LOS	2	100	11.6	11.4	24.1	n.a.
21/11/2023	10:41:00	autumn	LOS	2	100	11.6	11.4	24.8	n.a.
21/11/2023	11:50:00	autumn	LOS	3	100	11.9	11.6	21.8	n.a.
21/11/2023	11:50:00	autumn	LOS	3	100	11.9	11.6	24.8	n.a.
21/11/2023	11:50:00	autumn	LOS	3	100	11.9	11.6	24.9	n.a.
17/01/2024	09:00:00	winter	NS	1	100	2.4	2.4	28.7	n.a.
17/01/2024	09:00:00	winter	NS	1	100	2.4	2.4	28.7	n.a.
17/01/2024	09:00:00	winter	NS	1	100	2.4	2.4	27.8	n.a.
17/01/2024	10:15:00	winter	NS	2	100	2	2.5	29.1	n.a.
17/01/2024	10:15:00	winter	NS	2	100	2	2.5	28.1	n.a.
17/01/2024	10:15:00	winter	NS	2	100	2	2.5	27.9	n.a.
17/01/2024	11:20	winter	NS	3	100	3.6	3	26	n.a.
17/01/2024	11:20	winter	NS	3	100	3.6	3	28.2	n.a.
17/01/2024	11:20	winter	NS	3	100	3.6	3	26	n.a.
31/01/2024	07:50	winter	CPB	1	100	9.5	6.2	21.1	n.a.
31/01/2024	07:50	winter	CPB	1	100	9.5	6.2	20.5	n.a.
31/01/2024	07:50	winter	CPB	1	100	9.5	6.2	23.1	n.a.
31/01/2024	09:07	winter	CPB	2	100	9	6.4	21.5	n.a.
31/01/2024	09:07	winter	CPB	2	100	9	6.4	18.3	n.a.
31/01/2024	09:07	winter	CPB	2	100	9	6.4	19.8	n.a.
31/01/2024	10:20:00	winter	CPB	3	90	11	7.6	26.6	n.a.
31/01/2024	10:20:00	winter	CPB	3	90	11	7.6	25.4	n.a.
31/01/2024	10:20:00	winter	CPB	3	90	11	7.6	21.7	n.a.
02/02/2024	08:00:00	winter	LOS	1	90	8.4	6.8	25.1	n.a.
02/02/2024	08:00:00	winter	LOS	1	90	8.4	6.8	24.2	n.a.
02/02/2024	08:00:00	winter	LOS	1	90	8.4	6.8	24.2	n.a.
02/02/2024	09:49:00	winter	LOS	2	95	10.4	9.6	24.9	n.a.
02/02/2024	09:49:00	winter	LOS	2	95	10.4	9.6	24.2	n.a.
02/02/2024	09:49:00	winter	LOS	2	95	10.4	9.6	23.5	n.a.
02/02/2024	11:05:00	winter	LOS	3	85	11.7	9.9	25	much sunnier NV reps

02/02/2024	11:05:00	winter	LOS	3	85	11.7	9.9	24	n.a.
02/02/2024	11:05:00	winter	LOS	3	85	11.7	9.9	24.4	n.a.
30/04/2024	07:44:00	spring	NS	1	10	11.5	10.7	21.9	n.a.
30/04/2024	07:44:00	spring	NS	1	10	11.5	10.7	19	n.a.
30/04/2024	07:44:00	spring	NS	1	10	11.5	10.7	24.4	n.a.
30/04/2024	09:17:00	spring	NS	2	75	17.3	16.7	27	n.a.
30/04/2024	09:17:00	spring	NS	2	75	17.3	16.7	31.6	n.a.
30/04/2024	09:17:00	spring	NS	2	75	17.3	16.7	33	n.a.
30/04/2024	10:36:00	spring	NS	3	50	18.5	17.6	33.4	wispy cloud coverage but sun coming through
30/04/2024	10:36:00	spring	NS	3	50	18.5	17.6	32	100% cloud cover for NV3
30/04/2024	10:36:00	spring	NS	3	50	18.5	17.6	26.3	n.a.
11/05/2024	06:47:00	spring	CPB	1	100	12.5	13.2	21.8	n.a.
11/05/2024	06:47:00	spring	CPB	1	100	12.5	13.2	20.7	n.a.
11/05/2024	06:47:00	spring	CPB	1	100	12.5	13.2	20.9	n.a.
11/05/2024	08:10:00	spring	CPB	2	60	14	15.7	19.5	n.a.
11/05/2024	08:10:00	spring	CPB	2	60	14	15.7	20.1	n.a.
11/05/2024	08:10:00	spring	CPB	2	60	14	15.7	22.6	n.a.
11/05/2024	09:34	spring	CPB	3	40	17	18.3	19.8	n.a.
11/05/2024	09:34	spring	CPB	3	40	17	18.3	17	n.a.
11/05/2024	09:34	spring	CPB	3	40	17	18.3	21.1	n.a.
25/04/2024	06:02:00	spring	LOS	1	80	6.5	6.9	30.4	n.a.
25/04/2024	06:02:00	spring	LOS	1	80	6.5	6.9	30.5	n.a.
25/04/2024	06:02:00	spring	LOS	1	80	6.5	6.9	30.8	n.a.
25/04/2024	07:28	spring	LOS	2	90	12.1	9.2	31.4	n.a.
25/04/2024	07:28	spring	LOS	2	90	12.1	9.2	30.8	n.a.
25/04/2024	07:28	spring	LOS	2	90	12.1	9.2	31.6	n.a.
25/04/2024	08:37	spring	LOS	3	99	10.2	9.8	31.5	n.a.
25/04/2024	08:37	spring	LOS	3	99	10.2	9.8	31.6	n.a.
25/04/2024	08:37	spring	LOS	3	99	10.2	9.8	30.9	n.a.
26/06/2024	07:38:00	summer24	NS	1	0	17	17.9	28.3	n.a.
26/06/2024	07:38:00	summer24	NS	1	0	17	17.9	30.1	n.a.
26/06/2024	07:38:00	summer24	NS	1	0	17	17.9	27.4	n.a.
26/06/2024	09:09:00	summer24	NS	2	0	22.7	23.5	29	n.a.
26/06/2024	09:09:00	summer24	NS	2	0	22.7	23.5	27.4	n.a.
26/06/2024	09:09:00	summer24	NS	2	0	22.7	23.5	31.6	n.a.
26/06/2024	10:38:00	summer24	NS	3	0	28.4	27	27	extra temp data collected 11:53 (34.7°C)
26/06/2024	10:38:00	summer24	NS	3	0	28.4	27	30.3	n.a.
26/06/2024	10:38:00	summer24	NS	3	0	28.4	27	28.3	n.a.
09/07/2024	07:14:00	summer24	CPB	1	100	18	17.5	23.9	raining before sampling started
09/07/2024	07:14:00	summer24	CPB	1	100	18	17.5	24.5	n.a.

09/07/2024	07:14:00	summer24	CPB	1	100	18	17.5	23.2	n.a.
09/07/2024	08:47:00	summer24	CPB	2	100	23.6	20.5	25.5	raining during sampling
09/07/2024	08:47:00	summer24	CPB	2	100	23.6	20.5	25.3	n.a.
09/07/2024	08:47:00	summer24	CPB	2	100	23.6	20.5	23.4	n.a.
09/07/2024	10:00:00	summer24	CPB	3	100	18.7	20.5	21	n.a.
09/07/2024	10:00:00	summer24	CPB	3	100	18.7	20.5	22.5	n.a.
09/07/2024	10:00:00	summer24	CPB	3	100	18.7	20.5	23.3	n.a.
11/07/2024	07:55:00	summer24	LOS	1	5	17.4	18.6	29.2	n.a.
11/07/2024	07:55:00	summer24	LOS	1	5	17.4	18.6	29.3	n.a.
11/07/2024	07:55:00	summer24	LOS	1	5	17.4	18.6	28.9	n.a.
11/07/2024	09:23:00	summer24	LOS	2	20	20	21.3	31.2	n.a.
11/07/2024	09:23:00	summer24	LOS	2	20	20	21.3	28.8	n.a.
11/07/2024	09:23:00	summer24	LOS	2	20	20	21.3	28.9	n.a.
11/07/2024	10:55:00	summer24	LOS	3	40	25.6	24.4	32	n.a.
11/07/2024	10:55:00	summer24	LOS	3	40	25.6	24.4	33.4	n.a.
11/07/2024	10:55:00	summer24	LOS	3	40	25.6	24.4	29.8	n.a.

7.0: References

ABED, R. M., LAM, P., DE BEER, D. & STIEF, P. 2013. High rates of denitrification and nitrous oxide emission in arid biological soil crusts from the Sultanate of Oman. *Isme j*, 7, 1862-75.

ALEXANDRE, A., QUINTã, R., HILL, P. W., JONES, D. L. & SANTOS, R. 2020. Ocean warming increases the nitrogen demand and the uptake of organic nitrogen of the globally distributed seagrass *Zostera marina*. *Functional Ecology*, 34, 1325-1335.

AL-HAJ, A. N., CHIDSEY, T. & FULWEILER, R. W. 2022. Two temperate seagrass meadows are negligible sources of methane and nitrous oxide. *Limnology and Oceanography*, 67, S193-S207.

AN, S. & GARDNER, W. 2002. Dissimilatory nitrate reduction to ammonium (DNRA) as a nitrogen link, versus denitrification as a sink in a shallow estuary (Laguna Madre/Baffin Bay, Texas). *Marine Ecology Progress Series*, 237, 41-50.

ASPLUND, M. E., BONAGLIA, S., BOSTRÖM, C., DAHL, M., DEYANOVA, D., GAGNON, K., GULLSTRÖM, M., HOLMER, M. & BJÖRK, M. 2022. Methane Emissions From Nordic Seagrass Meadow Sediments. *Frontiers in Marine Science*, Volume 8 - 2021.

BARTELME, R. P., MCLELLAN, S. L. & NEWTON, R. J. 2017. Freshwater Recirculating Aquaculture System Operations Drive Biofilter Bacterial Community Shifts around a Stable Nitrifying Consortium of Ammonia-Oxidizing Archaea and Comammox Nitrospira. *Frontiers in Microbiology*, 8.

BATES D, M. M., BOLKER B, WALKER S 2015. Fitting Linear Mixed-Effects Models Using lme4.: *Journal of Statistical Software*.

BEMAN, J. M. & FRANCIS, C. A. 2006. Diversity of ammonia-oxidizing archaea and bacteria in the sediments of a hypernutrified subtropical estuary: Bahía del Tóbari, Mexico.

BILLINGSLEY, P. 1995. Probability and measure. *Wiley series in probability and mathematical statistics Show all parts in this series*.

BODELIER, P. L. E. & STEENBERGH, A. K. 2014. Interactions between methane and the nitrogen cycle in light of climate change. *Current Opinion in Environmental Sustainability*, 9-10, 26-36.

BORRERO-DE ACUÑA JOSÉ, M., ROHDE, M., WISSING, J., JÄNSCH, L., SCHOBERT, M., MOLINARI, G., TIMMIS KENNETH, N., JAHN, M. & JAHN, D. 2016. Protein Network of the Pseudomonas aeruginosa Denitrification Apparatus. *Journal of Bacteriology*, 198, 1401-1413.

BRAKER, G., FESEFELDT A FAU - WITZEL, K. P. & WITZEL, K. P. 1998. Development of PCR primer systems for amplification of nitrite reductase genes (nirK and nirS) to detect denitrifying bacteria in environmental samples.

BRAKER, G., ZHOU, J., WU, L., DEVOL, A. H. & TIEDJE, J. M. 2000. Nitrite reductase genes (nirK and nirS) as functional markers to investigate diversity of denitrifying bacteria in pacific northwest marine sediment communities. *Appl Environ Microbiol*, 66, 2096-104.

BRODERSEN KASPER, E., MOSSHAMMER, M., BITTNER MERIEL, J., HALLSTRØM, S., SANTNER, J., RIEMANN, L. & KÜHL, M. 2024. Seagrass-mediated rhizosphere redox gradients are linked with ammonium accumulation driven by diazotrophs. *Microbiology Spectrum*, 12, e03335-23.

BURDEN, A., SMEATON, C., ANGUS, S., GARBUTT, A., JONES, L., LEWIS, H. & REES, S. 2020. Impacts of climate change on coastal habitats, relevant to the coastal and marine environment around the UK. *MCCIP Science Review 2020*.

BURGIN, A. J. & HAMILTON, S. K. 2007. Have we overemphasized the role of denitrification in aquatic ecosystems? A review of nitrate removal pathways. *Frontiers in Ecology and the Environment*, 5, 89-96.

CAFFREY, J. M. & KEMP, W. M. 1990. Nitrogen cycling in sediments with estuarine populations of *Potamogeton perfoliatus* and *Zostera marina*. *Marine Ecology Progress Series*, 66, 147-160.

CHEN, J.-J., ERLER, D. V., WELLS, N. S., HUANG, J., WELSH, D. T. & EYRE, B. D. 2021. Denitrification, anammox, and dissimilatory nitrate reduction to ammonium across a mosaic of estuarine benthic habitats. *Limnology and Oceanography*, 66, 1281-1297.

CHEN, Q., FAN, J., MING, H., SU, J., WANG, Y. & WANG, B. 2020. Effects of environmental factors on denitrifying bacteria and functional genes in sediments of Bohai Sea, China. *Marine Pollution Bulletin*, 160, 111621.

CONTRERAS, E., JURADO-EZQUETA, M., PIMENTEL, R., SERRANO, L., HIDALGO, C., JIMÉNEZ, A. & POLO, M. J. 2024. Assessment of seasonal and annual patterns in phosphorus content in a monitored catchment through a partitioning

approach based on hydrometeorological data. *Environmental Research*, 242, 117501.

CÚCIO, C., ENGELEN, A. H., COSTA, R. & MUYZER, G. 2016. Rhizosphere Microbiomes of European Seagrasses Are Selected by the Plant, But Are Not Species Specific. *Frontiers in Microbiology*, 7.

DAIMS, H., LEBEDEVA, E. V., PJEVAC, P., HAN, P., HERBOLD, C., ALBERTSEN, M., JEHLICH, N., PALATINSZKY, M., VIERHEILIG, J., BULAEV, A., KIRKEGAARD, R. H., VON BERGEN, M., RATTEI, T., BENDINGER, B., NIELSEN, P. H. & WAGNER, M. 2015. Complete nitrification by *Nitrospira* bacteria. *Nature*, 528, 504-509.

D'AVACK, E.A.S., TYLER-WALTERS, H., WILDING, C.M., GARRARD, S.L., & WATSON, A., 2024. *Zostera (Zosterella) noltei* beds in littoral muddy sand. In Tyler-Walters H. and Hiscock K. (eds) *Marine Life Information Network: Biology and Sensitivity Key Information Reviews*, [on-line]. Plymouth: Marine Biological Association of the United Kingdom. [cited 25-04-2025]. Available from: <https://www.marlin.ac.uk/habitat/detail/318>

DETHAROEN, M., RATTANACHOT, E. & PRATHEP, A. 2024. *Metagenomics insights into microbial diversity shifts among seagrass sediments*.

DI BIASE, A., FLORES-OROZCO, D., PATIDAR, R., KOWALSKI, M. S., JABARI, P., KUMAR, A., DEVLIN, T. R. & OLESZKIEWICZ, J. A. 2022. Performance and recovery of nitrifying biofilm after exposure to prolonged starvation. *Chemosphere*, 290, 133323.

DONG, L. F., NEDWELL, D. B. & STOTT, A. 2006. Sources of nitrogen used for denitrification and nitrous oxide formation in sediments of the hypernutrified Colne, the

nutrified Humber, and the oligotrophic Conwy estuaries, United Kingdom. *Limnology and Oceanography*, 51, 545-557.

DUARTE, C. M., LOSADA, I. J., HENDRIKS, I. E., MAZARRASA, I. & MARBÀ, N. 2013a. The role of coastal plant communities for climate change mitigation and adaptation. *Nature Climate Change*, 3, 961-968.

DUARTE, C. M., MIDDELBURG, J. J. & CARACO, N. 2005. Major role of marine vegetation on the oceanic carbon cycle. *Biogeosciences*, 2, 1-8.

DUARTE, C. M., SINTES, T. & MARBÀ, N. 2013b. Assessing the CO₂ capture potential of seagrass restoration projects. *Journal of Applied Ecology*, 50, 1341-1349.

DUFFY, J. E. 2006. Biodiversity and the functioning of seagrass ecosystems. *Marine Ecology Progress Series*, 311, 233-250.

ERGAS, S. J. & APONTE-MORALES, V. 2014. 3.8 - Biological Nitrogen Removal. In: AHUJA, S. (ed.) *Comprehensive Water Quality and Purification*. Waltham: Elsevier.

ETTWIG, K. F., ZHU, B., SPETH, D., KELTJENS, J. T., JETTEN, M. S. M. & KARTAL, B. 2016. Archaea catalyze iron-dependent anaerobic oxidation of methane. *Proc Natl Acad Sci U S A*, 113, 12792-12796.

EVANS, J. R. 1989. Photosynthesis and nitrogen relationships in leaves of C₃ plants. *Oecologia*, 78, 9-19.

FAY, P. 1992. Oxygen relations of nitrogen fixation in cyanobacteria.

FIELDS, S. 2004. Global nitrogen: cycling out of control. *Environ Health Perspect.* United States.

FREITAG THOMAS, E. & PROSSER JAMES, I. 2003. Community Structure of Ammonia-Oxidizing Bacteria within Anoxic Marine Sediments. *Applied and Environmental Microbiology*, 69, 1359-1371.

GABY, J. C., RISHISHWAR, L., VALDERRAMA-AGUIRRE, L. C., GREEN, S. J., VALDERRAMA-AGUIRRE, A., JORDAN, I. K. & KOSTKA, J. E. 2018. Diazotroph Community Characterization via a High-Throughput nifH Amplicon Sequencing and Analysis Pipeline. *Appl Environ Microbiol*, 84.

GALLAGHER, A. J., BROWNSCOMBE, J. W., ALSUDAIRY, N. A., CASAGRANDE, A. B., FU, C., HARDING, L., HARRIS, S. D., HAMMERSCHLAG, N., HOWE, W., HUERTAS, A. D., KATTAN, S., KOUGH, A. S., MUSGROVE, A., PAYNE, N. L., PHILLIPS, A., SHEA, B. D., SHIPLEY, O. N., SUMAILA, U. R., HOSSAIN, M. S. & DUARTE, C. M. 2022. Tiger sharks support the characterization of the world's largest seagrass ecosystem.

GARCÍAS-BONET, N., EGUÍLUZ, V., DIAZ-RUA, R. & DUARTE, C. 2020. Host-association as major driver of microbiome structure and composition in Red Sea seagrass ecosystems. *Environmental Microbiology*, 23.

GARCÍA-MARTÍNEZ, M., LÓPEZ-LÓPEZ, A., CALLEJA, M. L., MARBÀ, N. & DUARTE, C. M. 2009. Bacterial Community Dynamics in a Seagrass (*Posidonia oceanica*) Meadow Sediment. *Estuaries and Coasts*, 32, 276-286.

GEBREMICHAEL, A. W., WALL, D. P., O'NEILL, R. M., KROL, D. J., BRENNAN, F., LANIGAN, G. & RICHARDS, K. G. 2022. Effect of contrasting phosphorus levels on

nitrous oxide and carbon dioxide emissions from temperate grassland soils. *Scientific Reports*, 12, 2602.

GIBLIN, AE; TOBIAS, CR; SONG, BK; WESTON, N; AND BANTA, GT, 2013. The Importance of Dissimilatory Nitrate Reduction to Ammonium (DNRA) in the Nitrogen Cycle of Coastal Ecosystems. *Oceanography*, 26(3), 124-131.

GREEN, A. E., UNSWORTH, R. K. F., CHADWICK, M. A. & JONES, P. J. S. 2021. Historical Analysis Exposes Catastrophic Seagrass Loss for the United Kingdom. *Frontiers in Plant Science*, 12.

HARDISON, A. K., ALGAR, C. K., GIBLIN, A. E. & RICH, J. J. 2015. Influence of organic carbon and nitrate loading on partitioning between dissimilatory nitrate reduction to ammonium (DNRA) and N_2 production. *Geochimica et Cosmochimica Acta*, 164, 146-160.

HAROON, M. F., HU, S., SHI, Y., IMELFORT, M., KELLER, J., HUGENHOLTZ, P., YUAN, Z. & TYSON, G. W. 2013. Anaerobic oxidation of methane coupled to nitrate reduction in a novel archaeal lineage. *Nature*, 500, 567-70.

HAYATSU, M., TAGO, K. & SAITO, M. 2008. Various players in the nitrogen cycle: Diversity and functions of the microorganisms involved in nitrification and denitrification. *Soil Science and Plant Nutrition*, 54, 33-45.

HE, Q., QIN, H., YANG, L., TAN, W., JI, D., ZHANG, J. & ZHANG, X. 2024a. N_2O emission in temperate seagrass meadows: Fluxes, pathway and molecular mechanism. *Marine Environmental Research*, 198, 106542.

HE, Q., QIN, H., YANG, L., TAN, W., JI, D., ZHANG, J. & ZHANG, X. 2024b. N₂O emission in temperate seagrass meadows: Fluxes, pathway and molecular mechanism. *Marine Environmental Research*, 198, 106542.

HELEN, D., KIM, H., TYTGAT, B. & ANNE, W. 2016. Highly diverse nirK genes comprise two major clades that harbour ammonium-producing denitrifiers. *BMC Genomics*, 17, 155.

HENRY, S., BRU D FAU - STRES, B., STRES B FAU - HALLET, S., HALLET S FAU - PHILIPPOT, L. & PHILIPPOT, L. 2006. Quantitative detection of the nosZ gene, encoding nitrous oxide reductase, and comparison of the abundances of 16S rRNA, narG, nirK, and nosZ genes in soils.

HERBERT, R. A. 1999. Nitrogen cycling in coastal marine ecosystems. *FEMS Microbiology Reviews*, 23, 563-590.

HINK, L., GUBRY-RANGIN, C., NICOL, G. W. & PROSSER, J. I. 2018. The consequences of niche and physiological differentiation of archaeal and bacterial ammonia oxidisers for nitrous oxide emissions. *The ISME Journal*, 12, 1084-1093.

HU, H.-W. & HE, J.-Z. 2017. Comammox—a newly discovered nitrification process in the terrestrial nitrogen cycle. *Journal of Soils and Sediments*, 17, 2709-2717.

HUSK, B. R., ANDERSON, B. C., WHALEN, J. K. & SANCHEZ, J. S. 2017. Reducing nitrogen contamination from agricultural subsurface drainage with denitrification bioreactors and controlled drainage. *Biosystems Engineering*, 153, 52-62.

JONES, B. L. & UNSWORTH, R. K. F. 2016. The perilous state of seagrass in the British Isles. *Royal Society Open Science*, 3, 150596.

JONES, C. M., GRAF, D. R. H., BRU, D., PHILIPPOT, L. & HALLIN, S. 2013. The unaccounted yet abundant nitrous oxide-reducing microbial community: a potential nitrous oxide sink. *The ISME Journal*, 7, 417-426.

JORDAN, T. E., CORNWELL, J. C., BOYNTON, W. R. & ANDERSON, J. T. 2008. Changes in phosphorus biogeochemistry along an estuarine salinity gradient: The iron conveyor belt. *Limnology and Oceanography*, 53, 172-184.

KNEIP, C., LOCKHART, P., VOSS, C. & MAIER, U. G. 2007. Nitrogen fixation in eukaryotes--new models for symbiosis. *BMC Evol Biol*. England.

KUYPERS, M. M., SLIEKERS AO FAU - LAVIK, G., LAVIK G FAU - SCHMID, M., SCHMID M FAU - JØRGENSEN, B. B., JØRGENSEN BB FAU - KUENEN, J. G., KUENEN JG FAU - SINNINGHE DAMSTÉ, J. S., SINNINGHE DAMSTÉ JS FAU - STROUS, M., STROUS M FAU - JETTEN, M. S. M. & JETTEN, M. S. 2003. Anaerobic ammonium oxidation by anammox bacteria in the Black Sea.

LAMMERS, P. J. & HASELKORN, R. 1983. Sequence of the nifD gene coding for the alpha subunit of dinitrogenase from the cyanobacterium *Anabaena*. *Proc Natl Acad Sci U S A*, 80, 4723-7.

LEE, J. A. & FRANCIS, C. A. 2017. Spatiotemporal Characterization of San Francisco Bay Denitrifying Communities

a Comparison of *nirK* and *nirS* Diversity and Abundance. *Microbial Ecology*, 73, 271-284.

LEHTOVIRTA-MORLEY, L. E. 2018. Ammonia oxidation: Ecology, physiology, biochemistry and why they must all come together. *FEMS Microbiology Letters*, 365.

LI, F., LI, M., SHI, W., LI, H., SUN, Z. & GAO, Z. 2017. Distinct distribution patterns of proteobacterial nirK- and nirS-type denitrifiers in the Yellow River estuary, China. *Canadian Journal of Microbiology*, 63, 708-718.

LI, M., LUNDQUIST, C. J., PILDITCH, C. A., REES, T. A. V. & ELLIS, J. 2019. Implications of nutrient enrichment for the conservation and management of seagrass *Zostera muelleri* meadows. *Aquatic Conservation: Marine and Freshwater Ecosystems*, 29, 1484-1502.

LI, J., NEDWELL DAVID, B., BEDDOW, J., DUMBRELL ALEX, J., MCKEW BOYD, A., THORPE EMMA, L. & WHITBY, C. 2015. amoA Gene Abundances and Nitrification Potential Rates Suggest that Benthic Ammonia-Oxidizing Bacteria and Not Archaea Dominate N Cycling in the Colne Estuary, United Kingdom. *Applied and Environmental Microbiology*, 81, 159-165.

LI, M., LUNDQUIST, C. J., PILDITCH, C. A., REES, T. A. V. & ELLIS, J. 2019. Implications of nutrient enrichment for the conservation and management of seagrass *Zostera muelleri* meadows. *Aquatic Conservation: Marine and Freshwater Ecosystems*, 29, 1484-1502.

LI, M., WEI, G., SHI, W., SUN, Z., LI, H., WANG, X. & GAO, Z. 2018. Distinct distribution patterns of ammonia-oxidizing archaea and bacteria in sediment and water column of the Yellow River estuary. *Scientific Reports*, 8, 1584.

LING, J., ZHOU, W., YANG, Q., YIN, J., ZHANG, J., PENG, Q., HUANG, X., ZHANG, Y. & DONG, J. 2021. Spatial and Species Variations of Bacterial Community Structure and Putative Function in Seagrass Rhizosphere Sediment. LID - 10.3390/life11080852 [doi] LID - 852.

LISA, J. A., SONG, B., TOBIAS, C. R. & HINES, D. E. 2015. Genetic and biogeochemical investigation of sedimentary nitrogen cycling communities responding to tidal and seasonal dynamics in Cape Fear River Estuary. *Estuarine, Coastal and Shelf Science*, 167, A313-A323.

LIU, P., ZOU, S., ZHANG, H., LIU, Q., SONG, Z., HUANG, Y. & HU, X. 2023a. Genome-resolved metagenomics provides insights into the microbial-mediated sulfur and nitrogen cycling in temperate seagrass meadows. *Frontiers in Marine Science*, 10.

LIU, S., JIANG, Z., DENG, Y., WU, Y., ZHANG, J., ZHAO, C., HUANG, D., HUANG, X. & TREVATHAN-TACKETT, S. M. 2018. Effects of nutrient loading on sediment bacterial and pathogen communities within seagrass meadows. *Microbiologyopen*, 7, e00600.

LIU, S., LUO, H., JIANG, Z., REN, Y., ZHANG, X., WU, Y., HUANG, X. & MACREADIE, P. I. 2023b. Nutrient loading weakens seagrass blue carbon potential by stimulating seagrass detritus carbon emission. *Ecological Indicators*, 157, 111251.

LIU, S., WANG, H., CHEN, L., WANG, J., ZHENG, M., LIU, S., CHEN, Q. & NI, J. 2020. Comammox Nitrospira within the Yangtze River continuum: community, biogeography, and ecological drivers. *The ISME Journal*, 14, 2488-2504.

MAIER, G., NIMMO-SMITH, R. J., GLEGG, G. A., TAPPIN, A. D. & WORSFOLD, P. J. 2009. Estuarine eutrophication in the UK: current incidence and future trends. *Aquatic Conservation: Marine and Freshwater Ecosystems*, 19, 43-56.

MARSHALL, A. J., PHILLIPS, L., LONGMORE, A., HAYDEN, H. L., HEIDELBERG, K. B., TANG, C. & MELE, P. 2023. Temporal profiling resolves the drivers of microbial

nitrogen cycling variability in coastal sediments. *Science of The Total Environment*, 856, 159057.

MARTÍNEZ-ESPINOSA, C., SAUVAGE, S., AL BITAR, A., GREEN, P. A., VÖRÖSMARTY, C. J. & SÁNCHEZ-PÉREZ, J. M. 2021. Denitrification in wetlands: A review towards a quantification at global scale. *Science of The Total Environment*, 754, 142398.

MCKENZIE, L. J., NORDLUND, L. M., JONES, B. L., CULLEN-UNSWORTH, L. C., ROELFSEMA, C. & UNSWORTH, R. K. F. 2020. The global distribution of seagrass meadows. *Environmental Research Letters*, 15, 074041.

MING, H., FAN, J., CHEN, Q., SU, J., SONG, J., YUAN, J., SHI, T. & LI, B. 2021. Diversity and Abundance of Denitrifying Bacteria in the Sediment of a Eutrophic Estuary. *Geomicrobiology Journal*, 38, 199-209.

MIYAJIMA, T. & HAMAGUCHI, M. 2019. Carbon Sequestration in Sediment as an Ecosystem Function of Seagrass Meadows. In: KUWAE, T. & HORI, M. (eds.) *Blue Carbon in Shallow Coastal Ecosystems: Carbon Dynamics, Policy, and Implementation*. Singapore: Springer Singapore.

MOLLIE E. BROOKS, K. K., KOEN J. VAN BENTHEM, ARNI MAGNUSSON, CASPER W. BERG, ANDERS NIELSEN, HANS J. SKAUG, MARTIN MAECHLER, BENJAMIN M. BOLKER 2017. Modeling Zero-Inflated Count Data With glmmTMB. bioRxiv preprint bioRxiv:132753.

MONTEIRO, F. M., FOLLOWS, M. J. & DUTKIEWICZ, S. 2010. Distribution of diverse nitrogen fixers in the global ocean. *Global Biogeochemical Cycles*, 24.

MULHOLLAND, M. R., BERNHARDT, P. W., WIDNER, B. N., SELDEN, C. R., CHAPPELL, P. D., CLAYTON, S., MANNINO, A. & HYDE, K. 2019. High Rates of N₂ Fixation in Temperate, Western North Atlantic Coastal Waters Expand the Realm of Marine Diazotrophy. *Global Biogeochemical Cycles*, 33, 826-840.

MUS, F., CROOK, M. B., GARCIA, K., GARCIA COSTAS, A., GEDDES, B. A., KOURI, E. D., PARAMASIVAN, P., RYU, M. H., OLDROYD, G. E. D., POOLE, P. S., UDVARDI, M. K., VOIGT, C. A., ANÉ, J. M. & PETERS, J. W. 2016. Symbiotic Nitrogen Fixation and the Challenges to Its Extension to Nonlegumes. *Appl Environ Microbiol*, 82, 3698-3710.

NAKAGAWA, T., TSUCHIYA, Y., UEDA, S., FUKUI, M. & TAKAHASHI, R. 2019. Eelgrass Sediment Microbiome as a Nitrous Oxide Sink in Brackish Lake Akkeshi, Japan. *Microbes Environ*, 34, 13-22.

NAYAR, S. A.-O., LOO, M. G. K., TANNER, J. E., LONGMORE, A. R. & JENKINS, G. P. 2018. Nitrogen acquisition and resource allocation strategies in temperate seagrass *Zostera nigricaulis*: Uptake, assimilation and translocation processes.

NEDWELL, D. B., DONG, L. F., SAGE, A. & UNDERWOOD, G. J. C. 2002. Variations of the Nutrients Loads to the Mainland U.K. Estuaries: Correlation with Catchment Areas, Urbanization and Coastal Eutrophication. *Estuarine, Coastal and Shelf Science*, 54, 951-970.

NEDWELL, D. B., UNDERWOOD, G. J. C., MCGENITY, T. J., WHITBY, C. & DUMBRELL, A. J. 2016. Chapter Five - The Colne Estuary: A Long-Term Microbial Ecology Observatory. In: DUMBRELL, A. J., KORDAS, R. L. & WOODWARD, G. (eds.) *Advances in Ecological Research*. Academic Press.

NIELSEN, L. P., RISGAARD-PETERSEN, N., FOSSING, H., CHRISTENSEN, P. B. & SAYAMA, M. 2010. Electric currents couple spatially separated biogeochemical processes in marine sediment. *Nature*, 463, 1071-4.

OHYAMA, T. 2010. Nitrogen as a major essential element of plants. *Nitrogen Assim. Plants*, 37, 1-17.

OLLIVIER, Q. R., MAHER, D. T., PITFIELD, C. & MACREADIE, P. I. 2022. Net Drawdown of Greenhouse Gases (CO₂, CH₄ and N₂O) by a Temperate Australian Seagrass Meadow. *Estuaries and Coasts*, 45, 2026-2039.

PAJARES, S. & RAMOS, R. 2019. Processes and Microorganisms Involved in the Marine Nitrogen Cycle: Knowledge and Gaps. *Frontiers in Marine Science*, 6.

PETERSE, I. F., HENDRIKS, L., WEIDEVELD, S. T. J., SMOLDERS, A. J. P., LAMERS, L. P. M., LÜCKER, S. & VERAART, A. J. 2024. Wastewater-effluent discharge and incomplete denitrification drive riverine CO₂, CH₄ and N₂O emissions. *Science of The Total Environment*, 951, 175797.

PINTO, A. J., MARCUS, D. N., IJAZ, U. Z., BAUTISTA-DE LOSE SANTOS, Q. M., DICK, G. J. & RASKIN, L. 2016. Metagenomic Evidence for the Presence of Comammox Nitrospira-Like Bacteria in a Drinking Water System. LID - 10.1128/mSphere.00054-15 [doi] LID - e00054-15.

PJEVAC, P., SCHAUBERGER, C., POGHOSYAN, L., HERBOLD, C. W., VAN KESSEL, M. A. H. J., DAEBELER, A., STEINBERGER, M., JETTEN, M. S. M., LÜCKER, S., WAGNER, M. & DAIMS, H. 2017. AmoA-Targeted Polymerase Chain Reaction Primers for the Specific Detection and Quantification of Comammox Nitrospira in the Environment. *Frontiers in Microbiology*, 8.

RAMESH, R., BANERJEE, K., PANEERSELVAM, A., RAGHURAMAN, R., PURVAJA, R. & LAKSHMI, A. 2019. Chapter 14 - Importance of Seagrass Management for Effective Mitigation of Climate Change. *In: KRISHNAMURTHY, R. R., JONATHAN, M. P., SRINIVASALU, S. & GLAESER, B. (eds.) Coastal Management. Academic Press.*

REES, A. P., GILBERT, J. A. & KELLY-GERREYN, B. A. 2009. Nitrogen fixation in the western English Channel (NE Atlantic Ocean). *Marine Ecology Progress Series, 374, 7-12.*

REES, A. P., TAIT, K., WIDDICOMBE, C. E., QUARTLY, G. D., MCEVOY, A. J. & AL-MOOSAWI, L. 2016. Metabolically active, non-nitrogen fixing, *Trichodesmium* in UK coastal waters during winter. *Journal of Plankton Research, 38, 673-678.*

ROTHAUWE, J. H., WITZEL KP FAU - LIESACK, W. & LIESACK, W. 1997. The ammonia monooxygenase structural gene *amoA* as a functional marker: molecular fine-scale analysis of natural ammonia-oxidizing populations.

RÜTTING, T., SCHLEUSNER, P., HINK, L. & PROSSER, J. I. 2021. The contribution of ammonia-oxidizing archaea and bacteria to gross nitrification under different substrate availability. *Soil Biology and Biochemistry, 160, 108353.*

SALEH-LAKHA, S., SHANNON KE FAU - HENDERSON, S. L., HENDERSON SL FAU - GOYER, C., GOYER C FAU - TREVORS, J. T., TREVORS JT FAU - ZEBARTH, B. J., ZEBARTH BJ FAU - BURTON, D. L. & BURTON, D. L. 2009. Effect of pH and temperature on denitrification gene expression and activity in *Pseudomonas mandelii*.

SCARLETT, K., DENMAN, S., CLARK, D. R., FORSTER, J., VANGUELOVA, E., BROWN, N. & WHITBY, C. 2021. Relationships between nitrogen cycling microbial

community abundance and composition reveal the indirect effect of soil pH on oak decline. *The ISME Journal*, 15, 623-635.

SCARLETT, K., TESORIERO, L., DANIEL, R. & GUEST, D. 2013. Detection and quantification of *Fusarium oxysporum* f. sp. *cucumerinum* in environmental samples using a specific quantitative PCR assay. *European Journal of Plant Pathology*, 137, 315-324.

SERRANO, O., GÓMEZ-LÓPEZ, D. I., SÁNCHEZ-VALENCIA, L., ACOSTA-CHAPARRO, A., NAVAS-CAMACHO, R., GONZÁLEZ-CORREDOR, J., SALINAS, C., MASQUE, P., BERNAL, C. A. & MARBÀ, N. 2021. Seagrass blue carbon stocks and sequestration rates in the Colombian Caribbean. *Scientific Reports*, 11, 11067.

SEYMOUR, J. R., LAVEROCK, B., NIELSEN, D. A., TREVATHAN-TACKETT, S. M. & MACREADIE, P. I. 2018. The Microbiology of Seagrasses. *In*: LARKUM, A. W. D., KENDRICK, G. A. & RALPH, P. J. (eds.) *Seagrasses of Australia: Structure, Ecology and Conservation*. Cham: Springer International Publishing.

SHAFIQUL ISLAM, M., PERVEZ, A., AMINUR RAHMAN, M. & HABIBUR RAHMAN MOLLA, M. 2021. Eco-engineering of coastal environment through saltmarsh restoration towards climate change impact mitigation and community adaptation in Bangladesh. *Regional Studies in Marine Science*, 46, 101880.

SHIBATA, H., BRANQUINHO, C., MCDOWELL, W. H., MITCHELL, M. J., MONTEITH, D. T., TANG, J., ARVOLA, L., CRUZ, C., CUSACK, D. F., HALADA, L., KOPÁČEK, J., MÁGUAS, C., SAJIDU, S., SCHUBERT, H., TOKUCHI, N. & ZÁHORA, J. 2015. Consequence of altered nitrogen cycles in the coupled human and ecological

system under changing climate: The need for long-term and site-based research. *Ambio*, 44, 178-93.

SHIEH, W. Y. & YANG, J. T. 1997. Denitrification in the rhizosphere of the two seagrasses *Thalassia hemprichii* (Ehrenb.) Aschers and *Halodule uninervis* (Forsk.) Aschers. *Journal of Experimental Marine Biology and Ecology*, 218, 229-241.

SHORT, F. & WYLLIE-ECHEVERRIA, S. 1996. Natural and human-induced disturbance of seagrasses. *Environmental Conservation*, 23, 17-27.

SPARACINO-WATKINS, C., STOLZ JF FAU - BASU, P. & BASU, P. 2014. Nitrate and periplasmic nitrate reductases.

STEIN, L. Y. & KLOTZ, M. G. 2016. The nitrogen cycle. *Current Biology*, 26, R94-R98.

TANG, W., CERDÁN-GARCÍA, E., BERTHELOT, H., POLYVIU, D., WANG, S., BAYLAY, A., WHITBY, H., PLANQUETTE, H., MOWLEM, M., ROBIDART, J. & CASSAR, N. 2020. New insights into the distributions of nitrogen fixation and diazotrophs revealed by high-resolution sensing and sampling methods. *Isme j*, 14, 2514-2526.

THREATT, S. A.-O. & REES, D. A.-O. 2022. gBiological nitrogen fixation in theory, practice, and reality: a perspective on the molybdenum nitrogenase system.

THROBÄCK, I. N., ENWALL K FAU - JARVIS, A., JARVIS A FAU - HALLIN, S. & HALLIN, S. 2004. Reassessing PCR primers targeting nirS, nirK and nosZ genes for community surveys of denitrifying bacteria with DGGE.

TIANLIN, L., WANG, Z., WANG, S., ZHAO, Y., WRIGHT, A. & JIANG, X. 2019. Responses of ammonia-oxidizers and comammox to different long-term fertilization regimes in a subtropical paddy soil. *European Journal of Soil Biology*, 93, 103087.

TIEDJE, J. 1988. Ecology of denitrification and dissimilatory nitrate reduction to ammonium.

TOURNA, M., FREITAG, T. E., NICOL, G. W. & PROSSER, J. I. 2008. Growth, activity and temperature responses of ammonia-oxidizing archaea and bacteria in soil microcosms. *Environmental Microbiology*, 10, 1357-1364.

TREUSCH, A. H., LEININGER, S., KLETZIN, A., SCHUSTER, S. C., KLENK, H. P. & SCHLEPER, C. 2005. Novel genes for nitrite reductase and Amo-related proteins indicate a role of uncultivated mesophilic crenarchaeota in nitrogen cycling. *Environ Microbiol*, 7, 1985-95.

TUBBS, C. R. & TUBBS, J. M. 1983. The distribution of *Zostera* and its exploitation by wildfowl in the solent, Southern England. *Aquatic Botany*, 15, 223-239.

TURK-KUBO, K. A., GRADOVILLE, M. R., CHEUNG, S., CORNEJO-CASTILLO, F. M., HARDING, K. J., MORANDO, M., MILLS, M. & ZEHR, J. P. 2022. Non-cyanobacterial diazotrophs: global diversity, distribution, ecophysiology, and activity in marine waters. *FEMS Microbiology Reviews*, 47.

UNDERWOOD, G. J. C., DUMBRELL, A. J., MCGENITY, T. J., MCKEW, B. A. & WHITBY, C. 2022. The Microbiome of Coastal Sediments. *In*: STAL, L. J. & CRETOIU, M. S. (eds.) *The Marine Microbiome*. Cham: Springer International Publishing.

UNSWORTH, R. K. F., MCKENZIE, L. J., COLLIER, C. J., CULLEN-UNSWORTH, L. C., DUARTE, C. M., EKLÖF, J. S., JARVIS, J. C., JONES, B. L. & NORDLUND, L. M. 2019. Global challenges for seagrass conservation. *Ambio*, 48, 801-815.

URAKAWA, H., MARTENS-HABBENA, W., HUGUET, C., DE LA TORRE, J. R., INGALLS, A. E., DEVOL, A. H. & STAHL, D. A. 2014. Ammonia availability shapes the seasonal distribution and activity of archaeal and bacterial ammonia oxidizers in the Puget Sound Estuary. *Limnology and Oceanography*, 59, 1321-1335.

VALDEZ, S. R., ZHANG, Y. S., VAN DER HEIDE, T., VANDERKLIFT, M. A., TARQUINIO, F., ORTH, R. J. & SILLIMAN, B. R. 2020. Positive Ecological Interactions and the Success of Seagrass Restoration. *Frontiers in Marine Science*, Volume 7 - 2020.

VAN CLEEMPUT, O., BOECKX, P., LINDGREN, P.-E. & TONDERSKI, K. 2007. Chapter 23 - Denitrification in Wetlands. *In: BOTHE, H., FERGUSON, S. J. & NEWTON, W. E. (eds.) Biology of the Nitrogen Cycle*. Amsterdam: Elsevier.

VAN NIFTRIK, L. A., FUERST, J. A., DAMSTÉ, J. S. S., KUENEN, J. G., JETTEN, M. S. M. & STROUS, M. 2004. The anammoxosome: an intracytoplasmic compartment in anammox bacteria. *FEMS Microbiology Letters*, 233, 7-13.

VITOUSEK, P. M., CASSMAN, K., CLEVELAND, C., CREWS, T., FIELD, C. B., GRIMM, N. B., HOWARTH, R. W., MARINO, R., MARTINELLI, L., RASTETTER, E. B. & SPRENT, J. I. Towards an ecological understanding of biological nitrogen fixation.

VON WIRÉN, N., GOJON, A., CHAILLOU, S. & RAPER, D. 2001. Mechanisms and Regulation of Ammonium Uptake in Higher Plants. *In: LEA, P. J. & MOROT-GAUDRY, J.-F. (eds.) Plant Nitrogen*. Berlin, Heidelberg: Springer Berlin Heidelberg.

WANG, X., YANG, S., MANNAERTS, C. M., GAO, Y. & GUO, J. 2009. Spatially explicit estimation of soil denitrification rates and land use effects in the riparian buffer zone of the large Guanting reservoir. *Geoderma*, 150, 240-252.

WARD, B. B. 2011. Nitrification in the Ocean. *Nitrification*.

WELSH, D. T. 2000. Nitrogen fixation in seagrass meadows: Regulation, plant–bacteria interactions and significance to primary productivity. *Ecology Letters*, 3, 58-71.

WELSH, D. T., BOURGUÉS, S., DE WIT, R. & HERBERT, R. A. 1996. Seasonal variations in nitrogen-fixation (acetylene reduction) and sulphate-reduction rates in the rhizosphere of *Zostera noltii*: nitrogen fixation by sulphate-reducing bacteria. *Marine Biology*, 125, 619-628.

WITHERS, P. J. A., NEAL, C., JARVIE, H. P. & DOODY, D. G. 2014. Agriculture and Eutrophication: Where Do We Go from Here? *Sustainability*, 6, 5853-5875.

WITTORF, L., JONES, C. M., BONILLA-ROSSO, G. & HALLIN, S. 2018. Expression of nirK and nirS genes in two strains of *Pseudomonas stutzeri* harbouring both types of NO-forming nitrite reductases. *Research in Microbiology*, 169, 343-347.

WUCHTER, C., ABBAS B FAU - COOLEN, M. J. L., COOLEN MJ FAU - HERFORT, L., HERFORT L FAU - VAN BLEIJSWIJK, J., VAN BLEIJSWIJK J FAU - TIMMERS, P., TIMMERS P FAU - STROUS, M., STROUS M FAU - TEIRA, E., TEIRA E FAU - HERNDL, G. J., HERNDL GJ FAU - MIDDELBURG, J. J., MIDDELBURG JJ FAU - SCHOUTEN, S., SCHOUTEN S FAU - SINNINGHE DAMSTÉ, J. S. & SINNINGHE DAMSTÉ, J. S. 2006. Archaeal nitrification in the ocean.

ZAEHLE, S. & DALMONECH, D. 2011. Carbon–nitrogen interactions on land at global scales: current understanding in modelling climate biosphere feedbacks. *Current Opinion in Environmental Sustainability*, 3, 311-320.

ZAKEM, E. J., AL-HAJ, A., CHURCH, M. J., VAN DIJKEN, G. L., DUTKIEWICZ, S., FOSTER, S. Q., FULWEILER, R. W., MILLS, M. M. & FOLLOWS, M. J. 2018. Ecological control of nitrite in the upper ocean. *Nature Communications*, 9, 1206.

ZEHR, J. P. & CAPONE, D. G. 2020. Changing perspectives in marine nitrogen fixation. *Science*, 368, eaay9514.

ZHANG, W., LIU, B., SUN, Z., WANG, T., TAN, S., FAN, X., ZOU, D., ZHUANG, Y., LIU, X., WANG, Y., LI, Y., MAI, K. & YE, C. 2023. Comparison of nitrogen removal characteristic and microbial community in freshwater and marine recirculating aquaculture systems. *Science of The Total Environment*, 878, 162870.

ZHANG, X., AGOGUÉ, H., DUPUY, C. & GONG, J. 2014. Relative Abundance of Ammonia Oxidizers, Denitrifiers, and Anammox Bacteria in Sediments of Hyper-Nutriented Estuarine Tidal Flats and in Relation to Environmental Conditions. *CLEAN – Soil, Air, Water*, 42, 815-823.

ZHENG, P., WANG, C., ZHANG, X. A.-O. & GONG, J. A.-O. Community Structure and Abundance of Archaea in a *Zostera marina* Meadow: A Comparison between Seagrass-Colonized and Bare Sediment Sites.

ZHENG, Y., HOU L FAU - LIU, M., LIU M FAU - GAO, J., GAO J FAU - YIN, G., YIN G FAU - LI, X., LI X FAU - DENG, F., DENG F FAU - LIN, X., LIN X FAU - JIANG, X., JIANG X FAU - CHEN, F., CHEN F FAU - ZONG, H., ZONG H FAU - ZHOU, J. &

ZHOU, J. Diversity, Abundance, and Distribution of nirS-Harboring Denitrifiers in Intertidal Sediments of the Yangtze Estuary.

ZHOU, Z., MENG, H., LIU, Y., GU, J.-D. & LI, M. 2017. Stratified Bacterial and Archaeal Community in Mangrove and Intertidal Wetland Mudflats Revealed by High Throughput 16S rRNA Gene Sequencing. *Frontiers in Microbiology*, 8.

ZHOU, Z., PAN, J., WANG, F., GU, J.-D. & LI, M. 2018. Bathyarchaeota: globally distributed metabolic generalists in anoxic environments. *FEMS Microbiology Reviews*, 42, 639-655.

ZHU-BARKER, X. & STEENWERTH, K. L. 2018. Chapter Six - Nitrous Oxide Production From Soils in the Future: Processes, Controls, and Responses to Climate Change. *In: HORWATH, W. R. & KUZYAKOV, Y. (eds.) Developments in Soil Science*. Elsevier.

ZOU, D., LIU, H. & LI, M. 2020. Community, Distribution, and Ecological Roles of Estuarine Archaea. *Frontiers in Microbiology*, 11.